Acta Universitatis Sapientiae

Alimentaria

Volume 14, 2021

Sapientia Hungarian University of Transylvania
Scientia Publishing House

***Acta Universitatis Sapientiae, Alimentaria* is indexed by the following databases:**

AGRICOLA (National Agricultural Library)
CAB Abstracts
CABI (over 50 subsections)
Chemical Abstracts Service (CAS) { SciFinder
DOAJ (Directory of Open Access Journals)
EBSCO (relevant databases)
FSTA (Food Science & Technology Abstracts)
Foodline Science
Global Health
Google Scholar
JournalTOCs
ProQuest (relevant databases)
Publons
ReadCube
Ulrich's Periodicals Directory/ulrichsweb
WorldCat (OCLC)

Contents

Acta Univ. Sapientiae, Alimentaria, **14** (2021) 1–13

DOI: 10.2478/ausal-2021-0001

Nutritional status and dietary behaviours of Northern Algeria university students

A. Aidoud[1]
e-mail: a.aidoud@univ-boumerdes.dz

O. Elahcene[2]
e-mail: elahcene_o@yahoo.fr

R. Bravo[3]
e-mail: rbravo@unex.es

L. Ugartemendia[3]
e-mail: lugartemendia@unex.es

[1] Bioinformatics, Applied Microbiology and Biomolecules Laboratory, Faculty of Sciences, Department of Agronomy, M'Hamed Bougara University, Boumerdes, Algeria
[2] Department of Agronomy, Faculty of Natural Sciences and Life, Ziane Achour University, Djelfa, Algeria
[3] Department of Biology, Faculty of Sciences, University of Extremadura, Badajoz, Spain

Abstract. The present study tries to assess the nutritional status and dietary behaviours in a group of undergraduate students in order to characterize their food habits and assess the quality of their diet. A cross-sectional study was conducted with 220 undergraduate university students (110 male and 110 female) aged between 19 and 24 years from the Food Department of Saad Dahlab Blida 1 University (Algeria). The data collection and nutritional evaluation were carried out using DIAL nutritional software. Male participants had significantly ($P < 0.005$) higher body mass index (BMI) when compared to females. Significantly higher percentages of female students ($P < 0.005$) had tried a low-fat diet ($P = 0.0075$) and a low-carbohydrate diet ($P < 0.005$). The prevalence of overweight was higher among males compared to females. In contrast, a greater percentage of underweight students were observed in the group of female subjects. Related to micronutrient intake, a significant difference by sex was observed for vitamin A, C, folic acid, iron, calcium, and sodium intakes. However, females consumed more food containing vitamins C and A, whereas males' intake of calcium, sodium, folic acid, and iron was higher than the corresponding values observed in females. To conclude, these students reported a diet characterized by a high variety of cereal products and a moderate amount of vegetables, milk and dairy products, meat, fish and eggs, dietary fats and beverages, whereas the consumption of fruits was highly infrequent.

Keywords and phrases: food intake, diet, university students, macro- and micronutrients

1. Introduction

Obesity has become a serious epidemic health problem, and it is considered the fifth leading cause of mortality at the global level (*James et al.*, 2004). Overweight and obesity are major risk factors for several of the chronic diseases, including diabetes, hypertension, cardiovascular diseases (metabolic syndrome), and cancer. Some of the major causes of obesity are those changes in people's diet, in terms of quantity and quality, which have become more "Westernized" (*Gasbarrini & Piscaglia*, 2005). Consequently, the government regularly gives healthy eating recommendations and publishes national dietary guidelines to improve healthier dietary intakes (*NCM*, 2012; *USDA*, 2015).

In the recent decades, most of these populations have rapidly changed this ancient lifestyle towards more globalized behaviours – particularly young people (*Garcia-Closas et al.*, 2006). This new lifestyle involves several risks for health, especially increased prevalence of obesity and non-communicable chronic diseases associated with obesity and diet (*Schmidhuber & Traill*, 2006). In Algeria in 2018, the death cases (% of all deaths, all ages, both sexes) are associated in a proportion of 36% with cardiovascular diseases, 13% with cancers, 4% with diabetes, and with 3% chronic respiratory diseases. The obesity of adults aged over 18 years presented a major risk factor for these diseases with a mortality rate of 27% (19% males and 34% females) (*WHO*, 2018). The dietary record (DR) is highlighted among the prospective methods (*Ortega et al.*, 2009; *Thompson & Byers*, 1994). A DR is a prospective open-ended assessment method where the subject records all the foods and beverages consumed over a specific period of time (*Ortega et al.*, 2015).

In this study, a sample of undergraduates was requested to record information about food ingredients of recipes and preparation methods of consumed foods. Then, data were collected after food consumption. In order to obtain consistent data, students were trained how to use the DIAL software before participating in this survey. Academic years are a critical period regarding unhealthy changes in eating behaviours in students because most of them live far from their family, at the university campus (*Ugartemendia et al.*, 2020).

Nutritional deficiencies are very significant to the overall health of humans at all ages and for both genders; these deficiencies can seriously affect growth and development. The present work aimed to assess the food behaviour of students in order to characterize their food habits and assess the quality of diet in a sample of Algerian university students.

2. Materials and methods

Participants

The present cross-sectional study was carried out in a group of undergraduates, which comprised a total of 220 university undergraduate students living in Blida city, which is located 50 km south of Algiers (Algeria). Volunteers were chosen randomly from the Biology Department of Blida 1 University during the fall of academic year 2016/2017. Participants were excluded if they were aged under 18 or over 25 years. Approval to perform the study was obtained from the scientific board of the Faculty of Sciences, M'Hamed Bougara University of Boumerdes. All the procedures performed in this study were in accordance with the ethical standards of the Helsinki declaration.

Data collection and dietary assessment

Students were asked to fill out a self-reported quantitative questionnaire that included questions on their eating, drinking, and physical activity. Also, their weight, height, and body mass index were measured. Body mass index (BMI) was used to assess students' weight status. BMI values were categorized according to the World Health Organization (WHO) criteria as follows: < 18.5 kg/m^2 as underweight, 18.5–24.9 kg/m^2 as normal weight, 25–29.9 kg/m^2 as overweight, and ≥ 30 kg/m^2 as obese (*WHO*, 1997). Participants were asked to record in detail the daily food and beverage intake (type, quantity, and mealtimes) throughout twenty-one consecutive days (*Aidoud et al.*, 2019). The students from the Food Department were recruited from Blida 1 University; they received training related to dietary behaviours and how to use the DIAL® software. The DIAL® software has been developed to calculate, program, and modify any kind of diet fast and easily. It contains a nutritional table with more than 800 foodstuffs and a wide variety of information about their composition (up to ~140 different components in the most frequent foodstuffs). Information about foodstuffs contains not only their most common names but also the less frequent ones. In addition, this software allows to calculate diets depending on age, body composition, and basal metabolic rate, among other variables. Therefore, this software provides a very useful environment for teaching about dietetics in higher education but also for research purposes.

Data were computer-processed for the nutritional assessment using the DIAL software (Alce Ingeniería S.L., Spain). The variables provided by the software were: body mass index (BMI), dietary content of nutrients (macro- and micronutrients), energy intake, lipid content, and percentage of energy consumed according to food groups. For each subject, BMI was calculated with the DIAL® software as weight

(kg)/height^2 (m^2). All food groups' diets are compared to recommended daily allowance (*NCM*, 2012; *USDA*, 2015) considering the self-reported weekly physical activity. The nutritional composition of the diets was analysed by students trained in the DIAL® software, which contains information about energy and nutrient content in terms of foods and recipes (*Ortega et al.*, 2010).

Statistical analysis

Data were expressed in terms of mean ± standard deviation (SD). Therefore, this was the chosen manner to express descriptive data to determine the prevalence of overweight and obesity in the sample. In order to elucidate the differences in the variables between males and females with respect to the RDA, statistical analyses were performed with one-way analysis of variance (ANOVA), followed by Tukey's post-hoc test. The degree of significance was set at $P < 0.05$. Both descriptive and inferential statistics were performed using GraphPad Prism (version 6.01, 2012; GraphPad Software, Inc; San Diego, CA, USA).

3. Results and discussions

Characteristics of the students' sample

The descriptive statistics of the students' variables assayed by the research group are presented in *Table 1*. Students participating in this study (n = 220) included 110 females and 110 males and were enrolled in Blida 1 University (age: 21.76 ± 1.39 years). Participants' average height and weight were 168 ± 8 cm and 61.76 ± 11.32 kg respectively. The mean BMI was 21.74 ± 2.77 (kg/m^2). As described in *Table 1*, this study showed that the highest percentage of the students (75.45%) were of normal weight (18.5 ≤ BMI ≤ 24.9), this value being slightly higher in the population of female students. The prevalence of overweight (25 ≤ BMI ≤ 29.9) was more frequently reported among male students compared to females (21.82% and 5.45% respectively). No case of obesity was found among the university students. However, 15.45% of the female students and 6.36% of the male students were underweight (BMI ≤ 18.5). Most studies recorded a low prevalence of obesity and overweight among Chinese and Japanese students (*Rie et al.*, 2004; *Ruka et al.*, 2005). In contrast, all participants were non-smokers and were in good health, without any medication.

Table 1. Characteristics of graduate students' sample and BMI categories (Mean ± SD)

Variables	Total n = 220	Males n = 110	Females n = 110
Age (year)	21.76 ± 1.39	22 ± 1.50	21.50 ± 1.23
Weight (kg)	61.76 ± 11.32	69.92 ± 9.54	53.59 ± 5.73
Height (cm)	168 ± 8	174 ± 6	162 ± 5
BMI (kg/m^2)*	21.74 ± 2.77	23.10 ± 2.53	20.39 ± 2.29
– Underweight (n, %)	(24), 10.91	(7), 6.36	(17), 15.45
– Normal (n, %)	(166), 75.45	(79), 71.82	(87), 79.09
– Overweight (n, %)	(30), 13.64	(24), 21.82	(6), 5.45
– Obese (n, %)	(0), 0	(0), 0	(0), 0

* Categories according to BMI (WHO): Underweight < 18.5 kg/m^2; Normal weight: 18.5–24.9 kg/m^2; Overweight: 25–29.9 kg/m^2; Obese: ≥ 30 kg/m^2.

Students' intake of the food group categories

Table 2 shows food intake in our sample, where a significant gender difference was observed. However, it was observed that the total energy intake (kJ) of female students was significantly ($P < 0.05$) lower in comparison with male students (6979 kJ/day and 9357 kJ/day respectively). Female students in average consumed 25% fewer calories than male students. The contribution of the different food groups to the total diet energy intake and macronutrients are presented in *Table 2*. This table shows the variables about students' behaviour regarding consumption in foodstuffs throughout three weeks. Generally, the most important amount of energy provided by the food group of cereals and its products (4731 ± 942 kJ/day for males and 3270 ± 1138 kJ/day for females) represents 51% and 47% of the total energy dietary intake respectively. This is in good agreement with a study conducted on Mediterranean students, which showed that Italian students consumed generally more cereals and vegetables in their diet (*Baldini et al.*, 2009).

Most students consumed moderately vegetables, milk and dairy products, meats, fish and eggs, dietary fats, and beverages – about 6–15% of the total dietary intake –, whereas the consumption of fruits was highly infrequent (3% and 2% of the diet total energy intake for male and female students respectively).

Table 2. The total energy dietary intake of the different food groups (Mean ± SD)

Food groups		Males n = 110	Females n = 110
Cereals	kJ/day	4731 ± 941.61	3270 ± 1138.35
	% energy	50.56 ± 10.06	46.85 ± 16.31
Vegetables	kJ/day	888 ± 258.03	502 ± 211.06
	% energy	9.49 ± 2.76	7.20 ± 3.02
Fruits	kJ/day	272 ± 128.12	167 ± 90.02
	% energy	2.91 ± 1.37	2.40 ± 1.29
Milk and dairy products	kJ/day	850 ± 268.16	1043 ± 314.26
	% energy	9.08 ± 2.87	14.94 ± 4.50
Meat, fish, and eggs	kJ/day	1135 ± 341.01	850 ± 297.77
	% energy	12.13 ± 3.64	12.18 ± 4.27
Oils and dietary fats	kJ/day	846 ± 237.77	716 ± 324.06
	% energy	9.04 ± 2.54	10.26 ± 4.64
Beverages	kJ/day	636 ± 196.53	431 ± 179.82
	% energy	6.80 ± 2.10	6.18 ± 2.58

Students' nutrient intake

In our study, a significant difference was observed between the sexes in terms of the frequency of macronutrient intake ($P < 0.05$). Furthermore, the authors noticed that male students consumed more macronutrients than female students (*Figures 1B–D*). Thus, the protein, carbohydrate, and fat content in male students' intake represented 15.71%, 51.15%, and 29.91% of the total energy intake respectively. However, the female students ingest an approximately equal amount of macronutrients (14.44%, 48.70%, and 28.48% respectively) as males.

As for micronutrients, a significant difference by gender was observed for vitamins A, C, folic acid, iron, calcium, and sodium intakes (*Figure 2*). However, female students consumed more foods containing vitamin C and A than male students, as demonstrated in *figures 2E–F* in the district of Blida. On the other hand, male students' intake of calcium, sodium, folic acid, and iron (*Figures 2A–D*) was more significant than female students' intake of these micronutrients. The sodium intake of both sexes was significantly ($P < 0.05$) increased compared with the RDA value of sodium.

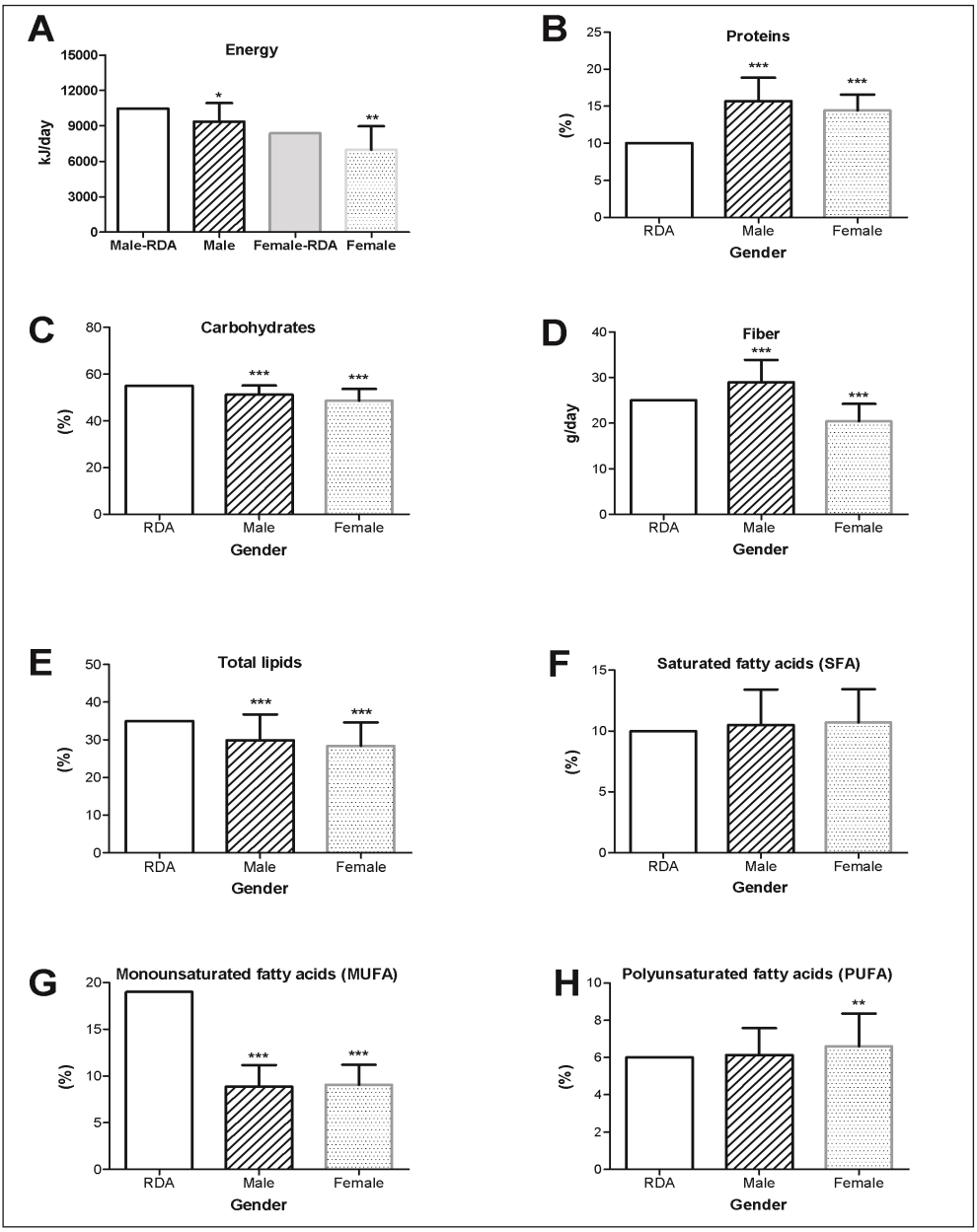

*Note: Values represent mean ± SD. *P < 0.05 between students with respect to the RDA.*

Figure 1. Macronutrient intake of university students: (A) Energy intake, (B) Protein intake, (C) Carbohydrate intake, (D) Fibre intake, (E) Total lipids intake, (F) SFA intake, (G) MUFA intake, (H) PUFA intake.

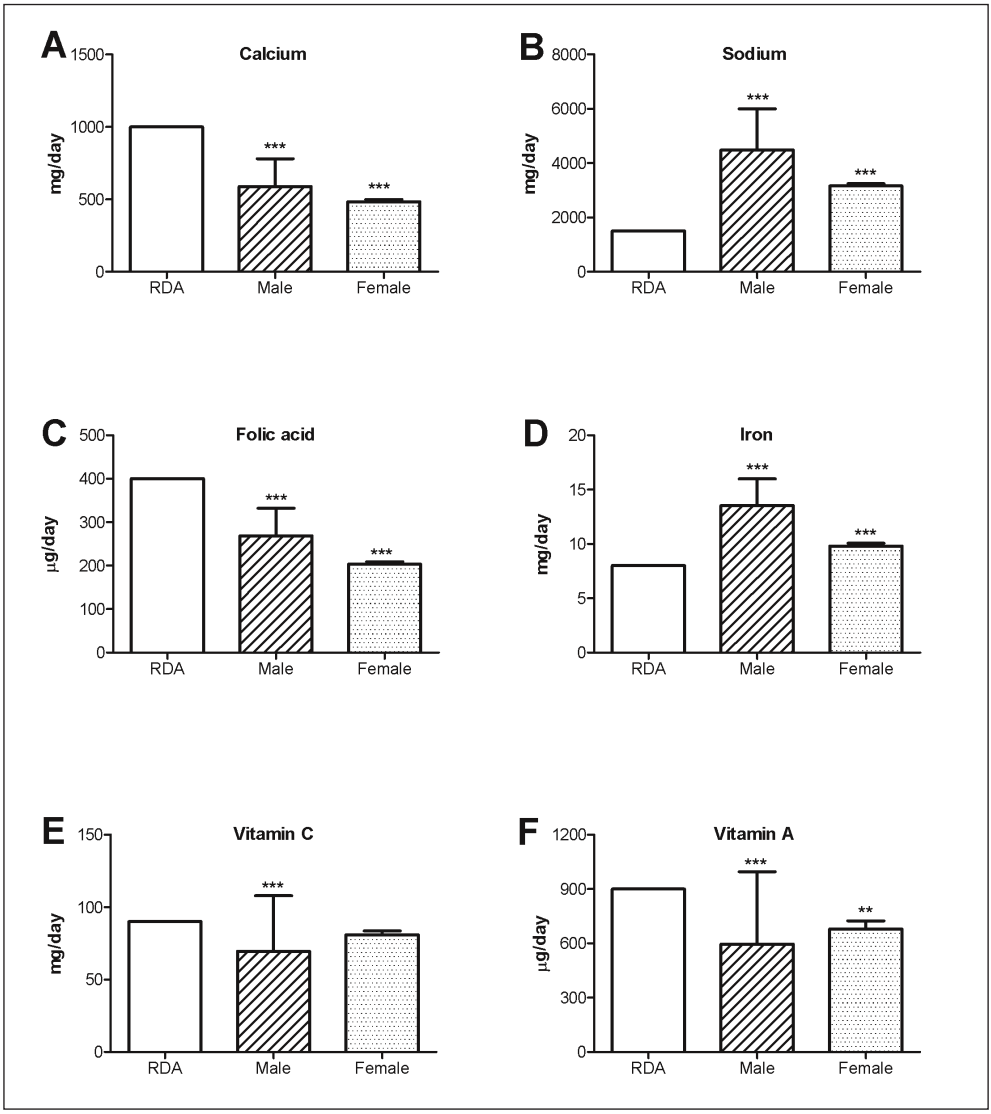

*Note: Values represent mean ± SD. *P < 0.05 between males and females with respect to RDA.*

Figure 2. Micronutrient intake of university students: (A) Calcium intake, (B) Sodium intake, (C) Folic acid intake, (D) Iron intake, (E) Vitamin C intake, (F) Vitamin A intake.

The population of the countries around the Mediterranean Sea has traditionally a characteristic dietary pattern: the Mediterranean Diet. This is a diet characterized by a high consumption of plant-based foods (i.e. whole-grain cereals, vegetables,

fruits, nuts, and seeds), a moderate intake of fish, seafood, eggs and dairy products, a moderate intake of wine and beer at meals, and, finally, by an occasional consumption of processed foods, ready-to-eat meat, and sweets. Also, olive oil is the primary oil in the diet (*Durá & Castroviejo*, 2011). In the last few decades, the Mediterranean diet has been recognized as one of the most effective dietary patterns in the prevention of several chronic diseases (*Koloverou et al.*, 2004; *Estruch et al.*, 2013; *Widmer et al.*, 2015). This may be due to the fact that this diet is rich in key nutrients and also provides an adequate balance of them. Among them, we would like to highlight the following: monounsaturated fatty acids present in olive oil, polyunsaturated fatty acids in nuts, dietary fibre in plant-based foods, and polyphenols in fruits as well as vitamins (vitamin A, vitamin D, vitamin E, folic acid, vitamin B12) and minerals (iron, calcium, magnesium, potassium).

However, the majority of these regions, which include developed, middle-income, and emerging societies, have rapidly changed this healthy lifestyle, leading to different kinds of risks for health (*Belahsen & Rguibi*, 2006). While researchers are still learning about the interplay among the combination of biological, psychological, interpersonal, and social factors, we know that eating disorders often begin in adolescence and young adulthood, a life stage associated with stressful events such as leaving home for college (*Allen et al.*, 2013; *FAO*, 2012). However, economic growth in developing countries and the globalization of the food sector is leading to 165 increasingly similar food consumption patterns worldwide. In addition, the prevalence of obesity and 166 several non-communicable chronic diseases associated with obesity and diet has increased (*FAO*, 2012; *Schmidhuber & Traill*, 2006). The period necessary for undergraduates to obtain their degrees constitutes a critical stage that may entail consequences for the quality of lifestyle and eating habits (*Lupi et al.*, 2015). Current findings also coincide with previous research suggesting that unhealthy food intake is a common coping mechanism implemented in response to stress in undergraduate students (*Wichianson et al.*, 2009). Nowadays, it is generally accepted that modern diet is energy-dense but nutrient-poor (*Nikolaou et al.*, 2015). Accordingly, we observed our sample population did not take in enough amounts of vitamin A (both sexes) or vitamin C (only male) compared with vitamin recommendations (*Troesch et al.*, 2012). The amount of energy supplied by proteins and carbohydrates was in line with the current international recommendations. In contrast, the energy provided by fats was slightly lower than the recommended value (30–35%) (*NCM*, 2012; *USDA*, 2015). A possible explanation may be that female students tend to have increased exposure to unhealthy eating habits or unbalanced diets such as low intake of fruits, vegetables, and cereals and slightly higher intake of milk and dairy products, oils, dietary fats, and beverages.

4. Conclusions

We conclude that the students of Blida 1 University reported a high variety of cereal products, which represent almost half of the energy input in their diet. Most students consumed moderately the food group of vegetables, milk and dairy products, meat, fish and eggs, dietary fats, and beverages, whereas the consumption of fruits was very limited. We recommend more nutritional education for young people, especially encouraging a higher intake of vegetables, olive oil, dairy products, fish and a lower intake of sodium so as to return to the Mediterranean diet and fight against CVD and obesity with a view to achieving an improved health in the future.

Conflict of interest

The authors declare that there are no conflicts of interest.

Acknowledgements

We wish to express our gratitude to the students from Blida 1 University for accepting to participate in this study.

References

[1] Aidoud, A., Ziane, E., Vara, L., Terrón, M. P., Garrido, M., Rodríguez, A. B., Carrasco, C., Changes in Mediterranean dietary pattern of university students: A comparative study between Spain and Algeria. *Nutrición Clínica y Dietética Hospitalaria*, 39. 2. (2019) 26–33. DOI: 10.12873/392carrasco.

[2] Allen, K. L., Byrne, S. M., Oddy, W. H., Crosby, R. D., Early onset binge eating and purging eating disorders: Course and outcome in a population-based study of adolescents. *Journal of Abnormal Child Psychology*, 41. 7. (2013) 1083–1096. DOI: 10.1007/s10802-013-9747-7.

[3] Baldini, M., Pasqui, F., Bordoni, A., Maranesi, M., Is the Mediterranean lifestyle still a reality? Evaluation of food consumption and energy expenditure in Italian and Spanish university students. *Public Health Nutrition*, 2. (2009) 148–155. DOI:10.1017/S1368980008002759.

[4] Belahsen, R., Rguibi, M., Population health and Mediterranean diet in southern Mediterranean countries. *Public Health Nutrition*, 9. 8A. (2006) 1130–1135. DOI: 10.1017/S1368980007668517.

[5] Durá, T., Castroviejo, A., Adherencia a la dieta mediterránea en la población universitaria. *Nutricion Hospitalaria*, 26. 3. (2011) 602–608.

[6] Estruch, R. et al., Primary prevention of cardiovascular disease with a Mediterranean diet. *New England Journal of Medicine*, 368. (2013) 1279–90. DOI: 10.1056/NEJMoa1200303.

[7] Food and Agricultural Organization (FAO). World Food Programme (WFP), International Fund for Agricultural Development (IFAD). Economic growth, hunger and malnutrition. Income growth and changes in food consumption. In the state of food insecurity in the world. (2012). Economic growth is necessary but not sufficient to accelerate reduction of hunger and malnutrition. Food and Agricultural Organization: Rome, Italy, 15–27.

[8] Garcia-Closas, R., Berenguer, A., González, C. A., Changes in food supply in Mediterranean countries from 1961 to 2001. *Public Health Nutrition*, 9. (2006) 53–60. DOI: 10.1079/phn2005757.

[9] Gasbarrini, A., Piscaglia, A. C., A natural diet versus modern Western diets? A new approach to prevent "well-being syndromes". *Digestive Diseases and Science*, 50. 1. (2005) 1–6. DOI: 10.1007/s10620-005-1268-y.

[10] James, W. P. T., Jackson-Leach, R., Ni Mhurchu, C., Kalamara, E., Shayeghi, M., Rigby, N. J., Overweight and obesity (high body mass index). In: Ezzati, M., Lopez, A. D., Rodgers, A., Murray, C. J. L. (eds.), *Comparative quantification of health risks: Global and regional burden of disease attributable to selected major risk factors*. Geneva, World Health Organization (2004) 497–596.

[11] Koloverou, E., Esposito, K., Giugliano, D., Panagiotakos, D., The effect of Mediterranean diet on the development of type 2 diabetes mellitus: A meta-analysis of 10 prospective studies and 136,846 participants. *Metabolism*, 63. (2004) 903–911. DOI: 10.1016/j.metabol.2014.04.010.

[12] Lupi, S., Bagordo, F., Stefanati, A., Grassi, T., Piccinni, L., Bergamini, M., De Donno, A., Assessment of lifestyle and eating habits among undergraduate students in northern Italy. *Annali dell'Istituto Superioare di Sanità*, 52. (2015) 154–161. DOI: 10.4415/ANN_15_02_14.

[13] Nikolaou, C. K., Hankey, C. R., Weight changes in young adults: A mixed-methods study. *International Journal of Obesity (London)*, 39. 3. (2015) 508–513. DOI: 10.1038/ijo.2014.16.

[14] Nordic Council of Ministers (NCM), Nordic Nutrition Recommendations 2012. Integrating nutrition and physical activity, 5th ed. Copenhagen, Nordic Council of Ministers. (2014).

[15] Ortega, R. M., López-Sobaler, A. M., Andrés, P., Requejo, A. M., Aparicio, A., Molinero, L. M., *DIAL 1.0: Programa para evaluación de dietas y gestión de datos de alimentación*. (2010).

[16] Ortega, R. M., Pérez-Rodrigo, C., López-Sobaler, A. M., Dietary assessment methods: Dietary records. *Nutrición Hospitalaria*, 31. Suppl. 3. (2015) 38–45. DOI: 10.3305/nh.2015.31.sup3.8749.

[17] Ortega, R. M., Requejo, A. M., López-Sobaler, A. M., Questionnaires for dietetic studies and the assessment of nutritional status. In: Ortega, R. M., Requejo, A. M. (eds.), *Nutriguia. Manual of clinical nutrition in primary care*. Madrid, Editura Complutense. (2009) 456–467.

[18] Rie, A., Mina, D., Kenji, T., The relationship between dietary life and indefinite complaint in female Nutrition Department students. *Seinan Jo Gakuin Bulletin*, (2004) 75–85.

[19] Ruka, S., Kenji, T., Rie, A., Chuan-Jun, L., Naotaka, S., Nutritional knowledge, food habits and health attitude of Chinese university students – A cross-sectional study. *Nutrition Journal*, 4. 4. (2005). DOI: 10.1186/1475-2891-4-4.

[20] Schmidhuber, J., Traill, W. B., The changing structure of diets in the European Union in relation to healthy eating guidelines. *Public Health Nutrition*, 9. (2006) 584–595. DOI: 10.1079/PHN2005844.

[21] Thompson, F. E., Byers, T., Dietary assessment resource manual. *Journal of Nutrition*, 124. 11 Suppl. (1994) 2245S–2317S. DOI:10.1093/jn/124.suppl_11.2245s.

[22] Troesch, B., Hoeft, B., McBurney, M., Eggersdorfer, M., Weber, P. Dietary surveys indicate vitamin intakes below recommendations are common in representative Western countries. *British Journal of Nutrition*, 108. 4. (2012) 692–698. DOI: 10.1017/S0007114512001808.

[23] Ugartemendia, L., Bravo, R., Castaño, M. Y., Cubero, J., Zamoscik, V., Kirsch, P., Rodríguez, A. B., Reuter, M., Influence of diet on mood and social cognition: A pilot study. *Food & Function*, 11. (2020) 8320–8330.

[24] USDA and US Department of Health and Human Services, Scientific Report of the 2015 Dietary Guidelines Advisory Committee. Washington (DC) (2015).

[25] Wichianson, J. R., Bughi, S. A., Unger, J. B., Spruijt-Metz, D., Nguyen-Rodriguez, S. T., Perceived stress, coping and night-eating in college students. *Stress and Health*, 25. (2009) 235–240. DOI: 10.1002/smi.1242.

[26] Widmer, R. J., Flammer, A. J., Lerman, L. O., Lerman, A., The Mediterranean diet, its components, and cardiovascular disease. *The American Journal of Medicine*, 128. 3. (2015) 229–238.

[27] World Health Organization (WHO), Non-communicable diseases (NCD) – Country profiles – Algeria (2018).

[28] World Health Organization (WHO), Obesity: Preventing and managing the global epidemic. Geneva (1997).

Acta Univ. Sapientiae, Alimentaria, **14** (2021) 14–43

DOI: 10.2478/ausal-2021-0002

The production methods of selenium nanoparticles

B. Khandsuren[1,2]
e-mail: b_khandsuren@muls.edu.mn

J. Prokisch[1,2]
e-mail: jprokisch@agr.unideb.hu

[1] Institute of Animal Science, Biotechnology and Nature Conversation, Faculty of Agricultural and Food Sciences and Environmental Management, University of Debrecen, 138 Böszörményi Street, 4032 Debrecen, Hungary
[2] Doctoral School of Animal Science, University of Debrecen, 138 Böszörményi Street, 4032 Debrecen, Hungary

Abstract. In recent years, the application of selenium nanoparticles has been increasing in medicine, agriculture, engineering, and food science. Therefore, researchers are converting inorganic selenium sources into nano form by various methods. Particularly both probiotics and pathogenic bacterial strains have the ability to synthesize selenium nanoparticles under aerobic and anaerobic conditions. Amazingly, dose-dependent selenium nanoparticles have antibacterial activity against their own pathogenic producer, even when added externally. Also, plant extracts and conventional chemical reducing agents continue to make a significant contribution to the production of selenium nanoparticles in an economic, eco-friendly, simple, and rapid way. Biological and chemical methods are suitable for the biological applications of selenium nanoparticles such as functional food or nutritional supplements and nanomedicine.

Keywords and phrases: selenium nanoparticles, bacteria, plants, fungi, reducing agents

1. Introduction

Selenium is an essential nutrient element required for the production of amino acids and enzymes, reducing cell and tissue damage caused by free radicals in the human and animal body. However, not all living organisms can produce it, so it is necessary to be obtained from the diet; and there is a narrow gap between its essential and toxic effects. Naturally, selenium is found as inorganic selenium (selenate, selenite, selenide, elemental selenium) and organic selenium

(selenocystine, Se-methylselenocysteine), with selenate and selenite showing the highest toxic effects for their high solubility and bioavailability (*Fernández-Llamosas et al.*, 2016). Actually, the toxicity effect of selenium has been reduced by synthesising its nanoparticles with various conversion methods. Recently, selenium nanoparticles have attracted even more attention in food supplements (*Garousi*, 2017; *Tóth & Csapó*, 2018) and in nanomedicine based on their higher bioavailability (*Zhang et al.*, 2008) and lower toxicity (*Wang et al.*, 2009). Compared to other general forms, nanoparticles and their applicability are dominated by several significant characteristics such as size or shape, while heat treatment has a measurable effect on the size, structure, and surface charge. Selenium nanoparticles and fortified food supplements have a positive impact on growth and antioxidant status (*Shi et al.*, 2011), rumen fermentation (*Galbraith et al.*, 2016), and fertility (*Fernandes et al.*, 2012; *Giadinis et al.*, 2016). They also exhibit anti-tumour activities both in vitro (*Ramamurthy et al.*, 2013) and in vivo (*Yazdi et al.*, 2012) by inducing mitochondria-mediated apoptosis (*Chen et al.*, 2008) and stimulating immune reaction against cancer cells (*Yazdi et al.*, 2012). In addition, their application is correlated to the protective effect against the toxicity of many toxic metals such as chromium (*Hao et al.*, 2017), mercury (*Cogun et al.*, 2012; *Wang et al.*, 2017), and arsenic (*Prasad & Selvaraj*, 2014). Actually, one of the challenges to use selenium-nanoparticle-enriched food supplements is related to find a suitable matrix, which is a floating microbubble. Therefore, the present review focused on integrating the current knowledge regarding the capability of microorganisms, plants, and chemical agents with selenite for the synthesis of selenium nanoparticles by the simple, rapid, economic, and efficient methods and on presenting it to future researchers.

2. Selenite reduction with bacteria

The biological synthesis of selenium nanoparticles was obtained with the help of secondary metabolites, which were synthesised by the plants and microbes. Metabolites contain phenols, and alkaloids help in the reduction and stability role in nanoparticle synthesis. The biosynthesis of nanoparticles using bacteria is more effective than the chemical way, which has a high purity of selenium, is a cheaper and faster process, and offers a better possibility to control the parameters (*Eszenyi et al.*, 2011). Selenium-tolerant bacterial strains can change selenite and selenate when grown in a selenium-enriched medium; this resistance action is achieved through two different processes: reduction to red elemental selenium form (*Eszenyi et al.*, 2011) or metabolic conversion to organic selenium such as selenocysteine and selenomethionine (*Andreoni et al.*, 2000).

The mechanisms of bacterial synthesis of selenium nanoparticles is explained by several stages: (1) transport of Se oxyanions into the cell; (2) the redox reactions of selenium oxyanions; (3) export of elementary Se^0 nuclei out of the cell; (4) assembly of elementary Se^0 into nanoparticles at the nuclei (*Tugarova & Kamnev*, 2017). The first step in selenium metabolism, the transport of selenate and selenite into bacterial cells (and, in particular, the intracellular reduction of these oxyanions), has been little documented. In the final stage, some authors suggested that larger-sized nanoparticles could form by the aggregation of small ones (*Kessi & Hanselmann*, 2004).

Many strains of Gram-positive (*Lactobacillus sp.*, *Bifidobacterium, Streptococcus sp.*, *Enterococcus sp.*, *Staphylococcus sp.*, *Actinobacteria sp.*, *Bacillus sp.*) and Gram-negative (*Escherichia coli*, *Ralstonia eutropha, Enterobacter cloacae*, *Pseudomonas aeruginosa*, *Pantoea agglomerans*, *Zooglea ramigera*, *Klebsiella pneumoniae*) bacteria are able to reduce selenite (Se^{+IV}) to less toxic elemental selenium (Se^0) with the formation of selenium nanoparticles. Probiotic bacterial strains are mostly used for the biosynthesis of selenium nanoparticles in the fermentation process. *Eszenyi et al.* (2011) and *Prokisch & Zommara* (2011) investigated how probiotic bacterial strains of *Lactobacillus casei*, *Lactobacillus acidophilus* LA-5, *Lactobacillus helveticus* LH-B02, *Streptococcus thermophilus*, and *Bifidobacterium* BB-12 transform the inorganic selenium compounds into an organic compound. In brief, 20 mL of 10,000 mg/L sodium hydrogen selenite stock solution was added into 980 mL of MRS broth. Then, fresh bacterial culture was added into 10 mL of mixture broth, and the culture was incubated at 37 °C for 24–36 hrs. Then nanoparticles of selenium were recovered by acidic hydrolysis with 37% (m/m) hydrochloric acid for 5 days at room temperature. In the next step, it was centrifuged at 6,000 rpm and washed with distilled water, while the final step was removing the cell fragments by filtering.

It has been found that certain bacteria defended themselves against the toxicity of selenite ion; elemental selenium was produced within the cell and stored in small, nano-sized spheres (SeNPs). During the fermentation, the transparent nutrient solution becomes red in the nano-selenium produced by the proliferating bacteria. The nanoparticles formed in the bacterium can be recovered and used after purification of the cell wall (*Figure 1*).

By the use of microorganisms belonging to the genus *Bifidobacterium*, grey selenium comprising 400–500 nm-sized nanospheres were produced. By the use of microorganisms belonging to the genus *Lactobacillus*, red selenium comprising 100–300 nm-sized nanospheres were produced. Also, red selenium is produced comprising 50–100 nm-sized nanospheres by the use of microorganisms belonging to the species *S. thermophilus*. After purification, the suspension of selenium nanoparticles contained 800 mg/kg of selenium in the form of 250 nm-sized

red elemental selenium. Studies on animals involving sheep, chicken, and fish and on humans, it was proved that this selenium form has a significantly better antioxidant effect than other selenium compounds; it cannot be overdosed and is the least toxic form of selenium. Nano-selenium contained LactoMicroSel© brand product was prepared by lactic acid bacteria in the yogurt-making process, and another product, nano-selenium was used for further nanotechnological experiments in a different type of medicinal supplement (*Eszenyi et al.*, 2011; *Prokisch & Zommara*, 2011).

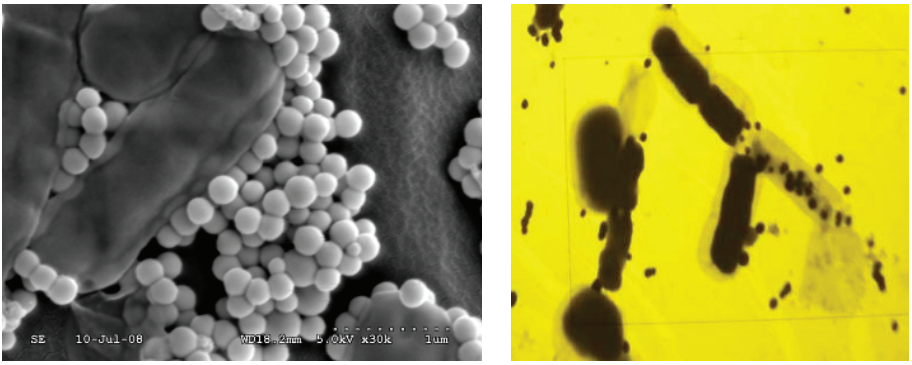

Figure 1. SEM and TEM pictures of the partially digested bacteria with selenium nanoparticles (Eszenyi et al., 2011)

Lactobacillus casei ATCC 393 (*L. casei* 393) was used for the bioconversion of selenium (*Xu et al.*, 2018). The fresh culture medium of *L. casei* 393 was cultivated with 200 mg/mL of sodium selenite at 37 °C for 24 hrs under anaerobic conditions, without shaking. At the end of the fermentation, the culture medium was centrifuged at 12,500 rpm for 10 min, and then pellets were washed twice with phosphate buffer solution. Finally, red selenium nanoparticles with a size of 50–80 nm accumulated intracellularly. As a result, *L. casei* 393 enriched with selenium nanoparticles promoted the growth and proliferation of porcine intestinal epithelial cells (IPEC-J2), human colonic epithelial cells (NCM460), and human acute monocytic leukaemia-cell (THP-1) derived macrophagocyte, and it inhibited the growth of human liver tumour cell line (HepG2).

Similarly, *Visha et al.* (2015) synthesised selenium nanoparticles with 15–50 nm by a strain of *Lactobacillus acidophilus*. The fermentation method was the same as in the previously mentioned studies. The culture medium was autoclaved at 121 °C for 20 min to disrupt the bacterial cell wall and release the selenium nanoparticles. Then the mixture centrifuged at 14,000 rpm for 15 min and washed thrice with

distilled water and finally ultrasonicated for 15 min in order to disintegrate the cohesive selenium spheres.

Enterococcus faecalis (ATCC NO.: 29212) was used as reducing bacteria for the synthesis of selenium nanoparticles (*Shoeibi & Mashreghi*, 2017). The concentrations of sodium selenite (0.19 mM–2.97 mM) were added into the culture medium (LB broth) at 37 °C on a rotary shaker (150 rpm) for 24 hrs and 48 hrs. At the end of the fermentation process, the converted nanoparticles were isolated from the culture by centrifugation at 10,000 rpm for 10 min and washed with distilled water several times. Finally, the bio-fabricated nanoparticles were spherical in shape and ranged from 29 to 195 nm in size. This study showed that low concentrations of sodium selenite (such as 0.95 mM) could produce a larger amount of selenium nanoparticles compared with higher concentrations. Also, the authors wish to point out that the extracellular synthesis of selenium nanospheres easily separated from the bacterial mass, without any physical or chemical treatment. The produced selenium nanoparticles inhibited the growth of *S. aureus*.

Some studies reported that *Staphylococcus sp.* can convert inorganic selenium into its elemental form. For example, *S. carnosus* was used for the synthesis of selenium nanoparticles with sodium selenite. The culture medium with different concentrations (1–5 mM) of sodium selenite was incubated at 37 °C for 72 hrs under constant shaking at 180 rpm. Then the reaction mixture was centrifuged for 10 min at 2,000 rpm, and the pellet was resuspended in phosphate-buffered saline. Finally, cells were lysed by sonication, employing 5 cycles of 2 min each. The solution was centrifuged for 30 min at 10,000 rpm, and the pellet was washed with ethanol and distilled water. This produced particles washed with ethanol, having an average diameter of 439 nm, and particles washed with water, having an average diameter of 525 nm. This study showed the concentration-dependent activity of the different selenium particles against *E. coli*, *S. cerevisiae*, and *Steinernema feltiae*. In addition, a high concentration of selenium nanoparticles (1,000 µM) generated biologically are also toxic against its own Gram-positive producer, even when added externally (*Estevam et al.*, 2017).

Actinobacteria (*Streptomyces minutiscleroticus* M10A62) also synthesised selenium nanoparticles (10–250 nm). Preparation method: 5 g of previously prepared wet bacterial biomass was dissolved in 100 mL of an aqueous solution of 1 mM selenite and incubated in a rotary shaker for 72 hrs. After the incubation period, the reaction mixture was centrifuged at 20,000 rpm for 1 h and filtered. The synthesised selenium nanoparticles showed good antiviral activity against *Dengue* virus (*Ramya et al.*, 2015).

Selenium-tolerant aerobic microorganisms may provide an opportunity to overcome these limitations in the biosynthetic processes. Some aquatic and soil bacterial

strains have been shown to resist selenium oxyanions and reduce them to elemental selenium or methylated selenium forms, which become this way less bioavailable and toxic. For example, the generation of selenium nanoparticles by soil bacteria *Bacillus sp.* and *Pseudomonas aeruginosa* under aerobic conditions has recently been reported; however, these studies include only the partial characterization of selenium nanospheres (*Dhanjal & Cameotra*, 2010; *Tejo Prakash et al.*, 2009).

Bacillus subtilis synthesised semiconductor monoclinic selenium nanoparticles with diameters ranging from 50 to 400 nm for the detection of H_2O_2 biosensors. In this case, 100 mL medium with 4 mM sodium selenite and 1 mL activated *B. subtilis* were incubated at 35 °C for 48 hrs on a rotary shaker (170 rpm). At the end of the growing time, it was centrifuged at 10,000 rpm for 6 min and then washed with double-distilled water and absolute ethanol several times. Also, they converted spherical monoclinic selenium nanoparticles into a highly anisotropic, one-dimensional (1D) trigonal structure after one day at room temperature (*Wang et al.*, 2010).

Bacillus mycoides SeITE01, which was isolated from the rhizosphere of the selenium hyper accumulator legume *Astragalus bisulcatus*, synthesised selenium nanoparticles with sizes ranging from 50 to 400 nm. In this procedure, 100 mL of nutrient broth with concentrations of 0.5 and 2 mM of sodium selenite was incubated at 28 °C for 48 hrs on a rotary shaker (200 rpm). After growth, the culture medium was centrifuged at 10,020 g for 10 min. Then the cell-free medium was centrifuged at 41,410 g for 30 min and washed with water, and then the two centrifugation steps were repeated. Extra- and intracellular elemental selenium production was detected in this reaction. This study showed that the size of selenium nanoparticles was dependent on the incubation times, showing a direct relationship between incubation time and the nanoparticle size. For example, the average diameter of the selenium nanoparticles was 50–100 nm and 50–400 nm after 6 hrs and 48 hrs of the incubation period respectively (*Lampis et al.*, 2014).

Cremonini et al. (2016) prepared selenium nanoparticles using *Bacillus mycoides* having a size of 160.6 ± 52.24 nm, and by using *Stenotrophomonas maltophilia* the nanoparticles' size was 170.6 ± 35.12 nm. In the method adopted for the preparation of nanoparticles, 10^5 CFU/mL *B. mycoides* and 10^7 CFU/mL *S. maltophilia* and 2 mM sodium selenite with the nutrient broth were incubated aerobically at 27 °C in a rotary shaker at 150 rpm for 6 hrs. Then the mixture medium was centrifuged at 10,000 g for 10 min, washed twice with 0.9% NaCl, suspended in Tris/HCl buffer (pH 8.2), and the cells were disrupted by ultrasonication for 5 min. Then the suspension was centrifuged at 10,000 g for 30 min. Finally, the nanoparticles were centrifuged at 40,000 g for 30 min, washed twice, and suspended in deionized sterile water. The selenium nanoparticles synthesised by both *B. mycoides* and *S. maltophilia* had high antibacterial activities with low MIC values against a clinical

strain of *Pseudomonas aeruginosa* but no biocidal effect against *Candida species* of *C. albicans* and *C. parapsilosi* (*Cremonini et al.*, 2016).

Bacillus cereus synthesised successfully red elemental selenium from a precursor selenium source that was reported by several studies. The strain AJK3 of *Bacillus cereus* isolated from a polluted lake was able to produce amorphous selenium nanoparticles of 93 nm. The medium nutrient broth complemented with various sodium selenite concentrations (0.25–1.0 mM) was inoculated at 37 °C for 24–72 hrs. Then the culture medium was separated from the bacterial cells and the nanoparticles by centrifugation at 16,750 rpm for 10 min. The particle size varied from 50 to 150 nm (*Kora*, 2018). Similarly, amorphous selenium nanospheres between 150 and 200 nm in diameter were synthesised by a strain CM100B of *Bacillus cereus* under aerobic conditions. In preparation, 100 mL of tryptic soya broth (TSB) with 2 mM of 1 M sodium selenite stock solution was inoculated at 37 °C at 200 rpm. Samples were collected at 2 h intervals and a simple centrifugation step (1,844 rpm) separated supernatants from the bacterial biomass. The authors mentioned the ability of the strain to tolerate high levels of toxic selenite ions, which was studied by challenging the microbe with different concentrations of sodium selenite (0.5–10 mM) (*Dhanjal & Cameotra*, 2010).

Bacillus megaterium (BSB6 and BSB12) isolated from the Bhitarkanika mangrove soil transformed spherical selenium nanoparticles of sizes around 200 nm. In the conversion process, 100 µl cell suspension with 2.0 mM selenite was inoculated into 100 mL nutrient broth at 37 °C for 48 hrs. Then, the mixture was medium filtered through polycarbonate micro-pore filters (0.22 µm), washed with Tris–HCl buffer three times, and fixed with 3% glutaraldehyde in 0.1 M phosphate buffer for 60 min. The suspended solution was centrifuged, washed with deionized water, and subjected to acid digestion for 5 min with 10 mL of HNO_3 and 0.5 mL of H_2SO_4 followed by the reduction of selenite with 6 M HCl at 100 °C for 30 min (*Mishra et al.*, 2011).

The selenium nanoparticles bio-transformed by *Pseudomonas aeruginosa* ATCC 27853 were spherical, polydisperse, with a size ranging from 47 to 165 nm, and the average particle size was about 95.9 nm under aerobic conditions. In brief, the nutrient broth medium supplemented with different concentrations of sodium selenite (0.25–1.0 mM) was inoculated with 100 mL of bacterial suspension containing 10^7 CFU/mL and incubated at 37 °C for 24–72 hrs under static conditions. Then the bacterial cells and the nanoparticles were separated from the culture medium by centrifugation at 10,000 rpm for 10 min (*Kora & Rastogi*, 2016).

Spherical selenium nanoparticles with diameters ranging from 50 to 500 nm were prepared by *Pseudomonas alcaliphila.* Trigonal nanorods occurred after incubating in an aqueous reaction solution for 24 hrs, as shown in *Figure 2*. In the production of nanoparticles, 1 mL freshly activated bacterial culture with 2.63 g

selenite (0.1 M) was added into the medium. After 48 hrs of the reaction, the culture was centrifuged at 10,000 rpm for 10 min and washed with double-distilled water. For the purification of nanoparticles, the solution was centrifuged at 10,000 rpm for 10 min in the complete salts solution: 0.25 M NaOH, 0.1 M NaOH, 10 mM Na_2HPO_4, and carbon-free, distilled, deionized water (*Zhang et al.*, 2011).

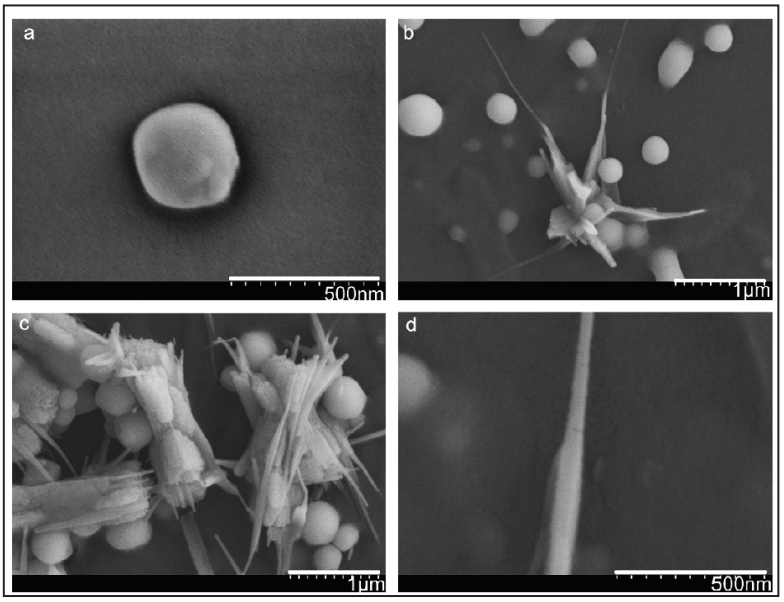

Figure 2. FESEM images of the transformation process from monoclinic selenium nanospheres to trigonal selenium nanorods.
(a) An individual selenium nanosphere, (b) the beginning of the transformation, (c) the aggregation of trigonal selenium nanorods, (d) The image of an individual selenium nanorod (*Zhang et al.*, 2011)

Under aerobic conditions at room temperature, *Pantoea agglomerans* strain UC-32 synthesised selenium nanoparticles smaller than 100 nm. In this study, UC-32 cells were grown in TSB supplemented with 1 mM sodium selenite and alkaline lysis was used for the isolation and purification of the nanoparticles from the bacterial cell mass. Then the cell suspensions were sonicated at 100 W for 2 min and centrifuged at 100,009 g for 10 min sequentially in SDS 0.1 %/1 M NaOH. Finally, pellets were resuspended in distilled water. It was also reported that stabilized selenium nanoparticles with L-cysteine (4 mM) had a high antioxidant activity compared to selenite and non-stabilized selenium nanoparticles (*Torres et al.*, 2012).

Besides, Gram-negative soil bacteria *Ralstonia eutropha* successfully synthesised extracellular, stable, uniform, and spherical selenium nanoparticles of sizes ranging from 40 to 120 nm. In this study, bacterial biomass was used for conversion. After 24 hrs of incubation, the bacterial biomass was harvested by centrifugation at a speed of 5,000 rpm at room temperature for 10 min and washed several times using sterilized Millipore water. Then 2 g of wet *R. eutropha* biomass with 100 mL aqueous $1.5x10^{-3}$ M sodium selenite solution was incubated at 30 °C for 48 hrs at 120 rpm. After the incubation time, the mixture reaction was centrifuged at 12,000 rpm for 10 min and washed several times with Millipore water and acetone. These synthesised selenium nanoparticles significantly inhibited the growth of *Pseudomonas aeruginosa*, *Staphylococcus aureus*, *Escherichia coli*, *Streptococcus pyogenes*, and *Aspergillus clavatus* (*Srivastava & Mukhopadhyay*, 2015b). However, these pathogenic bacteria have been used for the biofabrication of nano-selenium. For example, *Medina Cruz et al.* (2018) used *Escherichia coli* K-12 HB101, *Pseudomonas aeruginosa* ATCCVR 27853, Methicillin-resistant *Staphylococcus aureus* MRSA ATCC 43300, and *S. aureus* ATCC12600 as reducing agents. Fresh bacterial culture in Luria-Bertani (LB) broth was mixed with an aqueous solution of 2 mM sodium selenite and kept at 37 °C in a shaking incubator at 200 rpm for 72 hrs. At the end of the incubation time, it was centrifuged at 7,500 rpm for 15 min. The supernatant was removed, and the pellet was washed twice with a 0.9% NaCl solution and resuspended in 15 mL of Tris/HCl buffer. Finally, ultrasonication and hyperthermia-based approaches were used for the purification of selenium nanoparticles. The results showed that the average diameter of the synthesised selenium nanoparticles was 90–150 nm; 25 to 250 mg/mL concentrations of selenium nanoparticles showed antibacterial effect against *S. aureus* and *E. coli* and no significant cytotoxicity effect against human dermal fibroblasts for 24 hrs (*Medina Cruz et al.*, 2018).

Similarly, *Escherichia coli* ATCC 35218 biosynthesised red amorphous selenium nanoparticles of sizes ranging from 100 to 183 nm, and the average particle size was about 155 nm. The result showed that the bacterial strain was evident from 89.2% of selenium removal within 72 hrs at a concentration of 1 mM (*Kora & Rastogi*, 2017).

Zooglea ramigera synthesised extracellularly monoclinic crystalline selenium nanoparticles (30–150 nm). In this procedure, 1 mL of *Z. ramigera* culture and 3 mM of sodium selenite were added into 100 mL of sterilized N-broth medium and incubated at 30 °C for 48 hrs at 150 rpm. Then, the converted particles were isolated from the mixture by centrifugation at 12,000 rpm for 10 min and washed several times with distilled water and acetone (*Srivastava & Mukhopadhyay*, 2013).

3. Selenite reduction with fungi

The antifungal activity of selenium nanoparticles is well known; most fungi are sensitive to selenium compounds. However, some studies have shown that few fungi have demonstrated to have the capacity of selenium nanoparticle biosynthesis. Basically, biochemical and molecular mechanisms underlying selenium oxyanions' reduction into nanoparticles are still unclear, especially when involved in fungal transformation under aerobic conditions (*Vetchinkina et al.*, 2013).

Lentinula edodes converted sodium selenite and the organoselenium compound 1,5-diphenyl-3-selenopentanedione-1,5 (DAPS-25) into elemental form with a diameter of 180.51 ± 16.82 nm. Aqueous solutions of 10^{-6} mol sodium selenate, 10^{-2} mol sodium selenite, and 10^{-7} mol selenium-containing formulation DAPS-25 with 10^{-3} mol 50% ethanol were added to both beer wort and liquid synthetic medium of fungus separately. Results showed that red selenium nanoparticles accumulated intracellularly in the fungal *L. edodes* (*Vetchinkina et al.*, 2013).

Aspergillus terreus synthesised spherical selenium nanoparticles with an average size of 47 nm after 60 min of incubation. To complete the formation of the nanoparticles, 20 mL filtered supernatants of *Aspergillus terreus* were added to 80 mL of sodium selenite solution (100 mg/mL), and the reaction mixture was incubated at room temperature for 60 min. Then, the mixture was centrifuged at 20,000 g for 10 min and washed with distilled water three times (*Zare et al.*, 2013).

Gliocladium roseum prepared spherical selenium nanoparticles in the range of 20–80 nm. Also, a crystalline structure was observed in this study. In the preparation method, 100 mL of cell-free filtrate and a relevant amount of sodium selenite were mixed to make the overall solution of 1.5 mM sodium selenite salt, and the mixture was incubated at 30 °C for 24 hrs at 120 rpm. After 24 hrs, the mixture was centrifuged at 12,000 rpm for 15 min and washed with distilled water and acetone for the separation and purification from cell mass. All selenium nanoparticles were synthesised extracellularly (*Srivastava & Mukhopadhyay*, 2015a).

4. Selenite reduction with plant extracts

The selenium nanoparticles have been synthesised by plant extracts because metabolites produced from the plants help in the reduction of precursor molecule. This procedure has several advantages over other biological methods with bacteria and fungi because it is inexpensive, does not need any special condition, and the synthesis method is free of any toxic-reducing agents and organic solvents. In addition, the biomolecules present in the extract are assumed to provide

stabilization and to reduce the nanoparticle, also enhancing its potency as an antimicrobial and antioxidant agent.

Lemon leaf extract successfully synthesised spherical, polydispersed, and crystalline selenium nanoparticles of sizes ranging from 60 to 80 nm. In this method, 2 mL of leaf extract from the homogenisation of 0.5 g of the lemon leaf was added dropwise into 20 mL of 10 mM sodium selenite solution under magnetic stirring. Then the mixture was kept at 30 °C with a rotary shaker operating at 200 rpm for 24 hrs in dark conditions (*Prasad et al.*, 2013).

Clausena dentata is a flowering plant from the citrus family, which synthesised selenium nanoparticles ranging from 46.32 nm to 78.88 nm. In the conversion steps, 12 mL of plant extract was added to 88 mL of 1 mM aqueous selenium powder and kept until the reaction turned brown. Then the obtained extract was filtered through a paper filter (No1 Whatman). These produced selenium nanoparticles with low concentration (LC50) significantly controlled mosquito vectors at early stages, including 240.714 mg/L for *A. stephensi*, 104.13 mg/L for *A. aegypti*, and 99.602 mg/L for *C. quinquefasciatus* (*Sowndarya et al.*, 2017).

Citrus reticulata also fabricated spherical selenium nanoparticles with a size of 70 nm. In the preparation, 50 mL of orange peel extract was mixed with 5 mL of 0.1 M sodium selenite in drops until the reaction turned red. The reaction was controlled at temperatures of 30 °C, 40 °C, 50 °C, 60 °C, 70 °C , and 80 °C and at pH 2, 4, 6, 8, 10, and 12. The results showed that selenium nanoparticles were found to be efficient at 40 °C and at pH 4. The selenium nanoparticles inhibited the bloom of algae (*Sasidharan et al.*, 2015).

Garlic extract, *Allium sativum*, produced uniform, mono-dispersive, and highly stable selenium particles with the size range of 48–87 nm. Briefly, 5 mL of the garlic extract was mixed with 50 mL of 20 mM sodium selenite solution under magnetic stirrer with 150 rpm and heated at 60 °C for 24 hrs. Then, the mixture was centrifuged at 10,000 rpm for 30 min, washed with double-distilled water and ethanol three times, and finally dried at room temperature. The garlic acid-mediated selenium nanoparticles showed good feed additive material for aquaculture. Therefore, this study suggested that selenium nanoparticles can be used for feeding the larvae of any finfish and shellfish when supplementing the trace elements (*Satgurunathan et al.*, 2017). *Allium sativum* as a capping and reducing agent is used for the production of selenium nanoparticles with the size range of 40–100 nm. Briefly, 2 mL of homogenised garlic cloves extract was added dropwise into 20 mL of 10 mM sodium selenite under magnetic stirring conditions and was kept at 36 °C on the rotary shaker at 120 rpm for 5–7 days in dark condition. In this study, the cytotoxicity of this selenium nanoparticle was compared to the chemically synthesised selenium nanoparticle against Vero cells. The results showed that Vero cells treated with chemically synthesised

nanoparticles led to a CC50 of 18.8 ± 0.8 lg/mL, while Vero cells treated with green-synthesised nanoparticles produced a CC50 of 31.8 ± 0.6 lg/mL (*Anu et al.*, 2017).

Allium sativum produced 21–40 nm- and 41–50 nm-sized selenium nanoparticles at 4 hrs and 72 hrs respectively (*Sribenjarat et al.*, 2020). In the preparation process, 0.06 g of garlic extract was dissolved in 20 mL of 10 mM sodium selenite, and 80 mM of ascorbic acid solution was added dropwise until a slightly yellow colour was achieved. After colour changing, the mixture was incubated at 130 rpm for 72 hrs in the dark. The samples were collected by centrifugation at 20,000 g at 4, 24, 48, and 72 hrs of the incubation period and washed twice with distilled water. Biosynthesised selenium nanoparticles showed less cytotoxicity to normal human MRC-5 cell after 72 hrs compared to 24 hrs and inhibited the growth of *S. aureus*.

Similarly, hollow and spherical selenium nanoparticles of sizes ranging between 7 and 45 nm and between 8 and 52 nm were synthesised by *Allium sativum*. In brief, 10 drops extract of *Allium sativum* was added into 25 mL of 5 mM sodium selenite solution until the colour changed on the magnetic stirrer. The biofabricated selenium nanoparticles were stable for more than 2 months and presented high antioxidant activity. 100 µl and 25 µl concentration of selenium nanoparticles synthesised by *Allium sativum* showed the highest antimicrobial activity against *Bacillus subtilis* and the least against *Staphylococcus aureus* (*Vyas & Rana*, 2017, 2018b). In addition, these authors reported that 9–58 nm-sized selenium nanoparticles were produced by *Aloe vera* leaf extract. In the short method, 10 drops of *Aloe vera* leaf extract was added into 25 mL of 5 mM sodium selenite solution until the colour changed on the magnetic stirrer (*Vyas & Rana*, 2018a). *Aloe vera* extract synthesised spherical selenium nanoparticles of 50 nm. In this case, 4.92 mL extract was added into 13.03 mL 10 mM sodium selenite and autoclaved at 121 °C and 1.5 bar for 15 min. The synthesised selenium nanoparticles indicated high antibacterial (*E. coli* and *S. aureus*) and antifungal (*C. coccodes* and *P. digitatum*) activities (*Fardsadegh & Jafarizadeh-Malmiri,* 2019).

Zingiber officinale was used for the synthesis of selenium nanoparticles, which was confirmed by the colour change from pale yellow to red. In brief, 1% of ginger extract was added to 10 mM of sodium selenite solution in the ratio of 9:1 and kept at room temperature for 75 hrs under stirring conditions of 130 rpm. Biosynthesised selenium nanoparticles in 250 µg/mL showed antibacterial activity against *Proteus sp.* (*Menon et al.*, 2019).

Psidium guajava (guava leaves) extract transformed sodium selenite into selenium nanoparticles with diameters in the range of 8–20 nm. In the formation of nanoparticles, 100 mL of freshly prepared guava leaf extract was mixed with 900 mL of aqueous sodium selenite (25 mM) at 60 °C for 3 hours. Subsequently,

the mixture was centrifuged at 13,280 rpm for 20 min, washed thrice with distilled water, and then air-dried. The synthesised nanoparticles showed the antibacterial effect on both Gram-positive (*S. aureus* MTCC-3160) and Gram-negative (*E. coli* MTCC-405) bacteria. Also, they were non-toxic to human cell lines (CHO pro-cells) and had toxic effects against hepatic cell lines (HepG2 cells) (*Alam et al.*, 2019).

Amorphous selenium nanoparticles were synthesised using *Emblica officinalis* fruit extract of sizes ranging from 15 to 40 nm. In short, 2 mL of aqueous fruit extract of *E. officinalis* was added dropwise into 10 mL of 10 mM sodium selenite under magnetic stirring conditions, and the mixture was kept at 27 ± 2 °C for 24 hrs at 120 rpm in dark condition. The fruit-extract-mediated selenium nanoparticles showed antimicrobial and antifungal activities against several strains (*Gunti et al.*, 2019).

Selenium nanoparticles synthesised using Hawthorn (*Crataegus hupehensis* Sarg.) fruit extract are mono-dispersed and stable, with an average size of 113 nm. In the conversion method, 2 mg/mL of lyophilised extract was mixed with 0.01 M of sodium under magnetic stirring for 12 hrs, and then the mixture was dialysed (MWCO 8000–14000) in ultrapure water for 48 hrs. The prepared selenium nanoparticles indicated anti-tumour activity against HepG2 cells (*Cui et al.*, 2018).

Pelargonium zonale leaf extract synthesised 50 nm of selenium nanoparticles under microwave irradiation. 15 mL 10 mM sodium selenite solution with 1.48 mL plant extract was exposed to microwave radiation for 4 min and at constant power of 800 W. Biosynthesised selenium nanoparticles showed antibacterial and antifungal activities against *Escherichia coli*, *Staphylococcus aureus*, *Colletotrichum coccodes*, and *Penicillium digitatum* (*Fardsadegh et al.*, 2019).

Spherical selenium nanoparticles with the size of approx. 400 nm were produced with the use of parsley (*Petroselinum crispum*) leaves extract. In the steps of preparation, lyophilised leaves with distilled water were homogenised in the ratio 1:10 (w/v) and filtered. Then 10,000 ppm selenite solution was added (ratio 1:10 and 1:1 v/v) at room temperature. The mixture was centrifuged at 5,000 rpm for 10 min after the reaction had turned red. Then the supernatant was washed with distilled water, followed by repeated centrifugations (three times), filtrations, and drying (*Fritea et al.*, 2017).

Azadirachta indica leaves extract synthesised spherical and smooth-surfaced selenium nanoparticles with sizes of ~153 and ~287 nm after 5 and 10 min of reaction period, as shown in *Figure 3*. In the process, 10 mM sodium selenite solution with 100 mL of aqueous leaves extract was incubated at 37 °C on a rotary shaker at 100 rpm. After 5 and 10 min, selenium nanoparticles were centrifuged at 10,000 rpm for 10 min and washed three times with distilled water. The synthesised

selenium nanoparticles showed dose-dependent antibacterial activity against *Pseudomonas aeruginosa* (*Mulla et al.*, 2020).

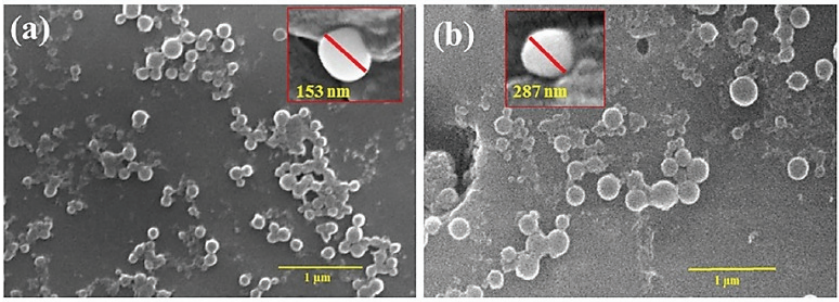

Figure 3. SEM images (FESEM images in insight) of purified spherical selenium nanoparticles at (a) 5 and (b) 10 min of the reduction reaction (*Mulla et al.*, 2020)

Selenium nanoparticles synthesised using *Ocimum tenuiflorum* leaf extract are spherical selenium nanoparticles in the size range of 15–20 nm. Briefly, 1% of leaf extract and 10 of mM selenite solution were mixed with a ratio 9:1 at room temperature under stirring conditions of 130 rpm for 72 hrs. The synthesised selenium nanoparticles inhibited the aggregation and growth of urinary stone (CaC_2O_4 monohydrate (COM) crystals) (*Liang et al.*, 2019).

5. Selenite reduction with chemical agents

Chemical transformation is the widely used technique for the production of nanoparticles, which has two types of reduction and sedimentation method. Chemical reduction method aids in maintaining a better uniformity of the particles, which can be used in the previously mentioned fields. Nanoparticle synthesis with various shapes and sizes is performed through the reduction of metal ions to neutral metal atoms by the addition of a reducing agent. Particularly in the first step of transformation, nucleation, allow atoms to form small clusters, called "seeds", of a stable structure and defined crystallinity (*Chapman et al.*, 2012; *Xiong & Xia*, 2007). The next step contains the "seeds" to form nanocrystals of different shapes and structures (*Xiong & Xia*, 2007). As aggregation occurs, the surface energy of the metal also grows, and smaller particles readily interact with each other to form larger particle sizes. A capping agent or stabilizing agent is used to prevent further aggregation by forming an electrical bilayer around the nanoparticle occurring from the adsorption of ions onto the surface of the nanoparticle.

Many biocompatible reducing agents, such as L-cysteine, D-fructose, glucose, lactose, gallic acid, some polysaccharides, ascorbic acid, etc., have been employed in the synthesis of selenium nanoparticles of various sizes and shapes. Basically, the shape of selenium nanoparticles is controlled by designing the chemical structure of the stabilizing agent through a self-assembly process.

A monodisperse and homogeneous spherical elemental selenium with an average diameter of about 100 nm was prepared by the reaction of sodium selenite with L-cysteine as a surface modifier and reducing agent in 1:4 ratios. A varied volume of 50 mM of L-cysteine solution was added dropwise into 0.25 mL of 0.1 M sodium selenite stock solution under magnetic stirring at room temperature for 30 min, and the mixture was reconstituted to a final volume of 25 mL with Milli-Q water (*Li et al.*, 2010).

Another study used dithiothreitol and gallic acid as reducing agents for the synthesis of selenium nanospheres. The gallic acid solution was used at different concentrations (3 mM–20 mM) in pH 5.7 with sodium selenite in a 1:1 ratio. The reducing agent dithiothreitol was added dropwise (~10 µL) until a brick red colour was observed, and the formation of selenium nanoparticles was monitored over a period of 24 hrs by fluorescence spectroscopy. Afterwards, the mixture solution was centrifuged and then washed with water. The results showed that alteration in the pH (pH 5–7) changed the size and shape of large-diameter nanospheres to nanofibres with diameters of 50–75 nm. Also, when grown at pH 7, nanospheres larger in diameter (> 500 nm) were obtained. At pH 5, the colour of the gallic acid turned yellowish orange, while at pH 7 the colour turned dark brown, which was indicative of the changed shape and size of the nanoparticles (*Barnaby et al.*, 2013).

A study has shown the reducing effect of monosaccharides for the conversion of selenium. For example, trigonal selenium (t-SeNPs) and amorphous selenium (a-SeNPs) were synthesised using D-fructose as reducing agent. Five mL of sodium selenite solution (1.0 mmol/L) was slowly dripped into 10.0 mL of 1.0 mmol/L aqueous solution of D-fructose. Then the mixture solution was stirred under heat at 45 °C for 15 min. This time, red amorphous selenium nanoparticles and trigonal selenium nanoparticles were obtained after 20 min. Finally, each solution was centrifuged at 13,000 rpm for 10 min and washed with deionized water, and then they were centrifuged again under the same conditions. These selenium nanoparticles were non-toxic for human healthy cells of the fibroblast cell line P4 and showed high toxicity towards the sarcoma cells (*Vieira et al.*, 2017).

Cavalu et al. (2018) also used disaccharides for the conversion and synthesised amorphous selenium nanoparticles of 20–40 nm. In the conversion method, 25 mL of sodium hydrogen selenite in the concentration of 10,000 ppm was selected as precursor selenium source mixed with 25 mL of lactose solution in a ratio of 1:8 (w/w) by vigorous stirring using a magnetic stirrer and then heated at 120 °C

for 3 min. After cooling, the mixture was centrifuged at 6,000 rpm for 10 min and washed with distilled water, followed by repeated centrifugation (4 times), filtration, and drying (*Cavalu et al.*, 2018).

Other studies reported that trigonal selenium nanowires were synthesised by chemical methods in a physical way. For example, trigonal selenium (t-Se) nanowires and microspheres were synthesised at room temperature by the chemical precipitation method using hydrazine hydrate as precipitator in the presence of 1,2,3-trimethylimidazolium-tetrafluoroborate (tmimBF4) with sodium selenite (*Ma et al.*, 2008). Similarly, trigonal selenium nanowires were successfully synthesised via low-temperature hydrothermal synthesis route. In a typical procedure, sodium selenite (0.01 mol) and thiosulfate salts ($Na_2S_2O_3$ 0.01 mol or $(NH_4)_2S_2O_3$ 0.01 mol) as reducing agents were added into 40 mL distilled water and autoclaved at 180 °C for 12 hrs. The precipitates were filtered and washed with distilled water and absolute alcohol several times after cooling down and were dried in vacuum at 50 °C for 4 hrs. Abundant nanowires with a diameter of 10–20 nm and a length up to 3–5 μm were observed in the sample with $Na_2S_2O_3$, and the mean diameter and length of these wires was 60 nm and 3 μm in the prepared sample $(NH_4)_2S_2O_3$ (*An & Wang*, 2007).

A mixed solvent of ethylene glycol assembled amorphous and trigonal selenium nanoparticles of various diameters. In a typical synthesis, 1.02 g of sodium selenite and 1, 2, 4, and 8 g of glucose were dissolved in 70 mL of ethylene glycol and 15 mL of H_2O mixed solution and incubated at 85 °C for 45 min, 1 h, and 1.5 hrs. Then the samples were washed with distilled water several times and kept in dark condition. The results showed that the size of the selenium nanoparticles increased from 320 to 480 nm in the presence of 1 and 8 g of glucose. Also, the amorphous and trigonal phase was observed with 8 g of glucose at 45 min and 1 h of the incubation period (*Chen et al.*, 2011).

Bai et al. (2017) synthesised trigonal-phase selenium nanoparticles of ~35 nm by physical method from selenium-nanoparticle-loaded chitosan microspheres. In the preparation method, 10 mL of selenite aqueous solution containing 0.4 g of sodium selenite was slowly added to the 100 mL of 1% (w/w) acetic acid containing 0.5 g of chitosan and 1.6 g of ascorbic acid and vigorously stirred at 600–800 rpm. Then the mixture solution was dialysed against 1% (w/w) of acetic acid for 6 hrs to remove the excess ascorbic acid and other by-products. After that, the colloid was well mixed with another chitosan solution, the final concentrations of selenium and chitosan being 0.09% (w/w) and 2.5% (w/w) respectively. Finally, the spray-drying process was applied to evaporate the moisture of the new mixture by the spray dryer tool. This preparation process is shown in *Figure 4*. The result showed that selenium-nanoparticle-loaded chitosan microspheres had powerful antioxidant activities, as evidenced by a dramatic increase of both selenium retention and the levels of glutathione peroxidase, superoxide dismutase, and catalase (*Bai et*

al., 2017). Basically, chitosan with low molecular weight has specific biological activities such as antibacterial activity, anticancer activity, and immune-boosting effects (*Dodane & Vilivalam,* 1998).

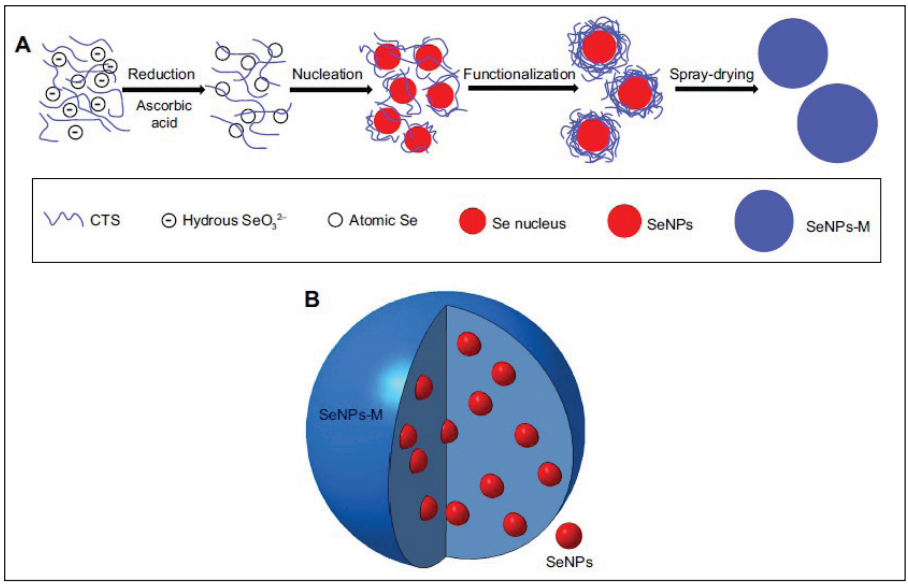

Figure 4. The preparation process (A) and the expected structure (B) of selenium-nanoparticle-loaded chitosan microspheres (SeNPs-M) (*Bai et al.*, 2017)

Actually, ascorbic acid is a widely used reducing agent for the synthesis of selenium, gold, and silver nanoparticles (*Qin et al.*, 2010; *Sun et al.*, 2009). Basically, ascorbic acid is a vitamin participating in several biochemical reactions and a naturally available antioxidant. It has high water solubility, biodegradability, and low toxicity (*Sun et al.*, 2009) compared with some chemical-reducing agents. Particularly, a spherical shape with an average diameter ranging between 15 and 18 nm of selenium nanoparticles was produced by ascorbic acid. In this study, selenium nanoparticles were prepared by the following procedure, a stock of aqueous solution of 100 mM sodium selenite and 50 mM ascorbic acid mixed in 1:4 ratios under magnetic stirring at ambient temperature for 30 min. Then the solution was centrifuged at 3,000 rpm. The authors mentioned that chemically synthesised selenium nanoparticles could be a potential antibacterial agent to treat humans affected by bacterial diseases caused by major pathogenic bacteria such as *Staphylococcus aureus*, *Escherichia coli*, and *Pseudomonas aeruginosa*.

The inhibition of synthesised nano-selenium against pathogens was similar to the effect of ampicillin (*Angamuthu et al.*, 2019). Another study used ascorbic acid

with various ratios and the stirring effect on the reduction of selenium. A stock solution of 100 mM sodium selenite and 50 mM ascorbic acid were mixed in various ratios (1:1, 1:2, 1:3, 1:4, 1:5, 1:6). Ascorbic acid was added dropwise to the sodium selenite solution under magnetic stirring at different rpms (200, 600, 1,000) at room temperature for 30 min. As a result, they suggested ratios of 1:3 and 1:4 of ascorbic acid and sodium selenite under stirring at 1,000 rpm for 30 min (*Malhotra et al.*, 2014).

With *Undaria pinnatifida*, polysaccharides and ascorbic acid produced selenium nanoparticles. In the procedure, 1 mL of 0.1% *U. pinnatifida* polysaccharide solution was mixed with 8 mL 60 mM of ascorbic acid under magnetic stirring, and then 1 mL 30 mM of sodium selenite solution was slowly added. After reaction for 5 min under sonication conditions, the solutions were purified with Milli-Q water. The produced selenium nanoparticles with IC50 values ranging from 3.0 to 14.1 μm showed the inhibition effect against human cancer cells such as A375, CNE2, Hep G2, and MCF-7 (*Chen et al.*, 2008).

Similarly, ascorbic acid and polyvinyl alcohol (PVA) or chitosan (CS) as stabilizers synthesised selenium nanoparticles with an average diameter of 66.55 ± 8.46 and 48.52 ± 2.77 nm. In the preparation process, 50 mM of sodium selenite and PVA 0.1% or CS 1% solutions were mixed under magnetic stirring conditions at room temperature for 5 min. Then, 50 mM of ascorbic acid was added dropwise to mixture solutions and mixed with a magnetic stirrer for 30 min. As a result, the synthesised selenium nanoparticles showed dose-dependent antibacterial activity, but PVA-coated selenium nanoparticles exhibited significant effects against *S. epidermidis* (MIC 125 ppm) and *S. aureus* (MIC 125 ppm). The IC50 values of the selenium nanoparticles were 26.56 and 530 ppm for PVA-coated selenium nanoparticles and CS-coated selenium nanoparticles respectively (*Boroumand et al.*, 2019).

6. Characterization techniques

In these studies, the characteristics of the selenium nanoparticles were analysed by UV-Visible Spectrophotometry, X-ray diffraction analysis (XRD), Fourier transform resonance spectroscopy (FT-IR) analysis, Dynamic Light Scattering Particle Size Analyser (DLS), Scanning Electron Microscope (SEM), Energy Dispersive X-Ray (EDS), and Transmission Electron Microscope (TEM) techniques.

UV-Vis spectrum is the most basic and important technique for the identification and characterization of nanoparticles. UV-Vis spectroscopy determines the "absorption maxima" of nanoparticles depending on the concentration of the precursor and other components of reaction mixtures. Biological-mediated selenium nanoparticles indicated an absorption peak at 226–590 nm, whereas

nanoparticles synthesised from bacterial strains of *Bacillus megaterium*, and *Bacillus cereus* exhibited maximum absorption at 200–300 nm and 590 nm respectively (*Mishra et al.*, 2011; *Dhanjal & Cameotra*, 2010). Chemically synthesised selenium nanoparticles indicated an absorption peak at 270–580 nm, whereas lactose nanoparticles showed absorption maxima at 270 nm, and a high concentration of L-cysteine-induced nanoparticles exhibited absorption maxima at 580 nm (*Cavalu et al.*, 2018; *Li et al.*, 2010).

X-ray diffraction analysis (XRD) was used to examine the composition and phase of resultant samples of selenium nanoparticles. Basically, selenium in its nanoscale form exhibits a standard XRD pattern (23, 30, 43), which confirms its nanoscale character, and it is similar to selenium nanoparticles originated from all different sources. The XRD analysis of biosynthesised selenium nanoparticles showed a clear structure. The XRD pattern was noisy and broader, with no sharp Bragg reflections. Thus, the data indicates the amorphous nature of the synthesised selenium nanoparticles (*Kora & Rastogi*, 2016). Also, the diffraction peaks at 2θ = 23.6, 29.9, 41.4, 43.8, 45.4, 51.8, 55.9, 61.8, 65.3, and 68.3 were attributed to the (100), (101), (110), (102), (111), (201), (003), (202), (210), and (211) reflections of the pure hexagonal phase of selenium crystal. The lattice parameters were as follows: a = 4.366 A° and c = 4.9536 A° (JCPDS 06-0362) (*Srivastava & Mukhopadhyay*, 2015b). For chemically synthesised selenium nanoparticles, the XRD pattern of the selenium nanoparticles indicated a broad and intense peak at about $2\theta = 23°$, which suggested that the nanoparticles were not crystalline (*Cavalu et al.*, 2018). Diffraction peaks were observed at 2θ = 23, 29, 41, 43, 45, 51, 55, 61, and 65°, corresponding to the crystalline planes (100), (101), (110), (102), (111), (201), (112), and (103). All the peaks linked with the trigonal phase of selenium nanoparticles. The lattice constants of a = 4.3662 A° and c = 4.9521 A° are consistent with the standard values for bulk selenium with a = 4.3662 A° and c = 4.9536 A°, in accordance with JCPDS file No. 73-0465 (*Vieira et al.*, 2017).

Fourier transform infrared spectroscopy (FT-IR) was used to analyse the surface interaction between synthesised nanoparticles and other molecules that took part in the synthesis and stabilization of nanoparticles. For example, in the case of FT-IR of chemically synthesised selenium nanoparticles, the spectrum has vibrational and stretching functions at wavenumbers 2919.69, 1630.51, 1380.78, and 1076.08 cm^{-1} corresponding to C–H, C=C, O–H, and C–O respectively. The band at 2,361 cm^{-1} is the C–H stretch of aryl acid. The strong band found at 1,654 cm^{-1} is characteristic of C=C stretch of an aromatic ring, N–H bending of amine, and a C=O stretch of polyphenols (*Angamuthu et al.*, 2019).

The dynamic light scattering (DLS) technique was used to measure the hydrodynamic effective diameters of produced nanoparticles. Scanning electron microscopy (SEM) and transmission electron microscopy (TEM) with energy dispersive analysis (EDS) are well-known techniques to determine the structure,

morphology, and size of prepared nanoparticles. SEM and TEM analysis showed that biosynthesised nanoparticles exhibited spherical nanospheres with a size of 100–500 nm, showing that selenium nanospheres were located intracellularly as well as extracellularly (*Eszenyi et al.*, 2011) and were also present in aggregates connected to the bacterial cell mass (*Dhanjal & Cameotra*, 2010).

7. Conclusions

The present review collected the production methods of selenium nanoparticles by biological and chemical ways as well as their properties and bioactivities. In all of the cases, selenium nanoparticles were synthesised from the reduction of sodium selenite by various types of reducing agents such as Gram-positive and Gram-negative bacterial strains, fungi, plant extracts, and pure chemical compounds. The biosynthesis usually resulted in amorphous spherical selenium nanoparticles, and chemical methods are able to synthesise selenium nanoparticles in multiple structures, depending on the reducing and stabilizer agents, their concentrations, and heat treatment. Biological sources and chemical-mediated selenium nanoparticles have shown dose-dependent antibacterial, antifungal, and anti-cancer activities.

Acknowledgements

This research was supported by the *Stipendium Hungaricum Scholarship Programme*.

References

[1] Alam, H., Khatoon, N., Raza, M., Ghosh, P. C., Sardar, M., Synthesis and characterization of nano selenium using plant biomolecules and their potential applications. *BioNanoScience*, 9. 1. (2019) 96–104. https://doi.org/10.1007/s12668-018-0569-5.

[2] An, C., Wang, S., Diameter-selected synthesis of single crystalline trigonal selenium nanowires. *Materials Chemistry and Physics*, 101. 2–3. (2007) 357–361. https://doi.org/10.1016/j.matchemphys.2006.06.011.

[3] Andreoni, V., Luischi, M. M., Cavalca, L., Erba, D., Ciappellano, S., Selenite tolerance and accumulation in the *Lactobacillus* species. *Annals of Microbiology*, 50. (2000) 77–88.

[4] Angamuthu, A., Venkidusamy, K., Muthuswami, R. R., Synthesis and characterization of nano-selenium and its antibacterial response on some important human pathogens. *Current Science*, 116. 2. (2019) 285. https://doi.org/10.18520/cs/v116/i2/285-290.

[5] Anu, K., Singaravelu, G., Murugan, K., Benelli, G., Green-synthesis of selenium nanoparticles using garlic cloves (*Allium sativum*): Biophysical characterization and cytotoxicity on vero cells. *Journal of Cluster Science*, 28. 1. (2017) 551–563. https://doi.org/10.1007/s10876-016-1123-7.

[6] Bai, K., Hong, B., He, J., Hong, Z., Tan, R., Preparation and antioxidant properties of selenium nanoparticles-loaded chitosan microspheres. *International Journal of Nanomedicine*, 12. (2017) 4527–4539. https://doi.org/10.2147/IJN.S129958.

[7] Barnaby, S., Sarker, N., Dowdell, A., Bannerjee, I., The spontaneous formation of selenium nanoparticles on gallic acid assemblies and their antioxidant properties. *The Fordham Undergraduate Research Journal*, 1. 1. (2013) 3.

[8] Boroumand, S., Safari, M., Shaabani, E., Shirzad, M., Faridi-Majidi, R., Selenium nanoparticles: Synthesis, characterization and study of their cytotoxicity, antioxidant and antibacterial activity. *Materials Research Express*, 6. 8. (2019) 0850d8. https://doi.org/10.1088/2053-1591/ab2558.

[9] Cavalu, S., Kamel, E., Laslo, V., Fritea, L., Costea, T., Antoniac, I. V., Vasile, E., Antoniac, A., Semenescu, A., Mohan, A., Saceleanu, V., Vicas, S., Eco-friendly, facile and rapid way for synthesis of selenium nanoparticles production, structural and morphological characterization. *Revista de Chimie*, 68. 12. (2018) 2963–2966. https://doi.org/10.37358/RC.17.12.6017.

[10] Chapman, J., Sullivan, T., Regan, F., *Nanoparticles in anti-microbial materials: Use and characterisation*. RSC Pub. (2012).

[11] Chen, H., Yoo, J.-B., Liu, Y., Zhao, G., Green synthesis and characterization of Se nanoparticles and nanorods. *Electronic Materials Letters*, 7. 4. (2011) 333–336. https://doi.org/10.1007/s13391-011-0420-4.

[12] Chen, T., Wong, Y.-S., Zheng, W., Bai, Y., Huang, L., Selenium nanoparticles fabricated in *Undaria pinnatifida* polysaccharide solutions induce mitochondria-mediated apoptosis in A375 human melanoma cells. *Colloids and Surfaces B: Biointerfaces*, 67. 1. (2008) 26–31. https://doi.org/10.1016/j.colsurfb.-2008.07.010.

[13] Cogun, H. Y., Fırat, Ö., Fırat, Ö., Yüzereroğlu, T. A., Gök, G., Kargin, F., Kötemen, Y., Protective effect of selenium against mercury-induced toxicity on hematological and biochemical parameters of *Oreochromis niloticus*. *Journal of Biochemical and Molecular Toxicology*, 26. 3. (2012) 117–122. https://doi.org/10.1002/jbt.20417.

[14] Cremonini, E., Zonaro, E., Donini, M., Lampis, S., Boaretti, M., Dusi, S., Melotti, P., Lleo, M. M., Vallini, G., Biogenic selenium nanoparticles: Characterization, antimicrobial activity and effects on human dendritic cells and fibroblasts. *Microbial Biotechnology*, 9. 6. (2016) 758–771. https://doi.org/10.1111/1751-7915.12374.

[15] Cui, D., Liang, T., Sun, L., Meng, L., Yang, C., Wang, L., Liang, T., Li, Q., Green synthesis of selenium nanoparticles with extract of hawthorn fruit induced HepG2 cells apoptosis. *Pharmaceutical Biology*, 56. 1. (2018) 528–534. https://doi.org/10.1080/13880209.2018.1510974.

[16] Dhanjal, S., Cameotra, S. S., Aerobic biogenesis of selenium nanospheres by *Bacillus cereus* isolated from coalmine soil. *Microbial Cell Factories*, 9. 1. (2010) 52. https://doi.org/10.1186/1475-2859-9-52.

[17] Dodane, V., Vilivalam, V. D., Pharmaceutical applications of chitosan. *Pharmaceutical Science & Technology Today*, 1. 6. (1998) 246–253. https://doi.org/10.1016/S1461-5347(98)00059-5.

[18] Estevam, E. C., Griffin, S., Nasim, M. J., Denezhkin, P., Schneider, R., Lilischkis, R., Dominguez-Alvarez, E., Witek, K., Latacz, G., Keck, C., Schäfer, K.-H., Kieć-Kononowicz, K., Handzlik, J., Jacob, C., Natural selenium particles from *Staphylococcus carnosus*: Hazards or particles with particular promise? *Journal of Hazardous Materials*, 324. (2017) 22–30. https://doi.org/10.1016/j.jhazmat.2016.02.001.

[19] Eszenyi, P., Sztrik, A., Babka, B., Prokisch, J., Elemental, nano-sized (100–500 nm) selenium production by probiotic Lactic acid bacteria. *International Journal of Bioscience, Biochemistry and Bioinformatics*, 1. 2. (2011) 148–152. https://doi.org/10.7763/IJBBB.2011.V1.27.

[20] Fardsadegh, B., Jafarizadeh-Malmiri, H., *Aloe vera* leaf extract mediated green synthesis of selenium nanoparticles and assessment of their in vitro antimicrobial activity against spoilage fungi and pathogenic bacteria strains. *Green Processing and Synthesis*, 8. 1. (2019) 399–407. https://doi.org/10.1515/gps-2019-0007.

[21] Fardsadegh, B., Vaghari, H., Mohammad-Jafari, R., Najian, Y., Jafarizadeh-Malmiri, H., Biosynthesis, characterization and antimicrobial activities assessment of fabricated selenium nanoparticles using *Pelargonium zonale* leaf extract. *Green Processing and Synthesis*, 8. 1. (2019) 191–198. https://doi.org/10.1515/gps-2018-0060.

[22] Fernandes, A. P., Wallenberg, M., Gandin, V., Misra, S., Tisato, F., Marzano, C., Rigobello, M. P., Kumar, S., Björnstedt, M., Methylselenol formed by spontaneous methylation of selenide is a superior selenium substrate to the thioredoxin and glutaredoxin systems. *PloS One*, 7. 11. (2012) e50727. https://doi.org/10.1371/journal.pone.0050727.

[23] Fernández-Llamosas, H., Castro, L., Blázquez, M. L., Díaz, E., Carmona, M., Biosynthesis of selenium nanoparticles by *Azoarcus* sp. CIB. *Microbial Cell Factories*, 15. 1. (2016) 109. https://doi.org/10.1186/s12934-016-0510-y.

[24] Fritea, L., Laslo, V., Cavalu, S., Costea, T., Vicaş, I. S., Green biosynthesis of selenium nanoparticles using parsley (*Petroselinum crispum*) leaves extract. *Studia Universitatis Vasile Goldis Arad, Seria Stiintele Vietii*, 27. (2017) 203–208.

[25] Galbraith, M. L., Vorachek, W. R., Estill, C. T., Whanger, P. D., Bobe, G., Davis, T. Z., Hall, J. A., Rumen microorganisms decrease bioavailability of inorganic selenium supplements. *Biological Trace Element Research*, 171. 2. (2016) 338–343. https://doi.org/10.1007/s12011-015-0560-8.

[26] Garousi, F., The essentiality of selenium for humans, animals, and plants, and the role of selenium in plant metabolism and physiology. *Acta Universitatis Sapientiae, Alimentaria*, 10. 1. (2017) 75–90. https://doi.org/10.1515/ausal-2017-0005.

[27] Giadinis, N. D., Loukopoulos, P., Petridou, E. J., Panousis, N., Konstantoudaki, K., Filioussis, G., Tsousis, G., Brozos, C., Koutsoumpas, A. T., Chaintoutis, S. C., Karatzias, H., Abortions in three beef cattle herds attributed to selenium deficiency. *Pakistan Veterinary Journal*, 36. 2. (2016) 145–148.

[28] Gunti, L., Dass, R. S., Kalagatur, N. K., Phytofabrication of selenium nanoparticles from *Emblica officinalis* fruit extract and exploring its biopotential applications: Antioxidant, antimicrobial, and biocompatibility. *Frontiers in Microbiology*, 10. (2019). https://doi.org/10.3389/fmicb.2019.00931.

[29] Hao, P., Zhu, Y., Wang, S., Wan, H., Chen, P., Wang, Y., Cheng, Z., Liu, Y., Liu, J., Selenium administration alleviates toxicity of chromium(VI) in the chicken brain. *Biological Trace Element Research*, 178. 1. (2017) 127–135. https://doi.org/10.1007/s12011-016-0915-9.

[30] Kessi, J., Hanselmann, K. W., Similarities between the abiotic reduction of selenite with glutathione and the dissimilatory reaction mediated by *Rhodospirillum rubrum* and *Escherichia coli*. *Journal of Biological Chemistry*, 279. 49. (2004) 50662–50669. https://doi.org/10.1074/jbc.M405887200.

[31] Kora, A. J., *Bacillus cereus*, selenite-reducing bacterium from contaminated lake of an industrial area: A renewable nanofactory for the synthesis of selenium nanoparticles. *Bioresources and Bioprocessing*, 5. 1. (2018) 30. https://doi.org/10.1186/s40643-018-0217-5.

[32] Kora, A. J., Rastogi, L., Biomimetic synthesis of selenium nanoparticles by *Pseudomonas aeruginosa* ATCC 27853: An approach for conversion of selenite. *Journal of Environmental Management*, 181. (2016) 231–236. https://doi.org/10.1016/j.jenvman.2016.06.029.

[33] Kora, A. J., Rastogi, L., Bacteriogenic synthesis of selenium nanoparticles by *Escherichia coli* ATCC 35218 and its structural characterisation. *IET Nanobiotechnology*, 11. 2. (2017) 179–184. https://doi.org/10.1049/iet-nbt.2016.0011.

[34] Lampis, S., Zonaro, E., Bertolini, C., Bernardi, P., Butler, C. S., Vallini, G., Delayed formation of zero-valent selenium nanoparticles by *Bacillus mycoides* SeITE01 as a consequence of selenite reduction under aerobic conditions. *Microbial Cell Factories*, 13. 1. (2014) 35. https://doi.org/10.1186/1475-2859-13-35.

[35] Li, Q., Chen, T., Yang, F., Liu, J., Zheng, W., Facile and controllable one-step fabrication of selenium nanoparticles assisted by L-cysteine. *Materials Letters*, 64. 5. (2010) 614–617. https://doi.org/10.1016/j.matlet.2009.12.019.

[36] Liang, T., Qiu, X., Ye, X., Liu, Y., Li, Z., Tian, B., Yan, D., Biosynthesis of selenium nanoparticles and their effect on changes in urinary nanocrystallites in calcium oxalate stone formation. *3 Biotech*, 10. 1. (2019) 23. https://doi.org/10.1007/s13205-019-1999-7.

[37] Ma, J., Liu, X., Wu, Y., Peng, P., Zheng, W., Controlled synthesis of selenium of different morphologies at room temperature. *Crystal Research and Technology*, 43. 10. (2008) 1052–1056. https://doi.org/10.1002/crat.200800058.

[38] Malhotra, S., Jha, N., Desai, K., A superficial synthesis of selenium nanospheres using wet chemical approach. *International Journal of Nanotechnology and Application (IJNA)*, 3. 4. (2014) 7–14.

[39] Medina Cruz, D., Mi, G., Webster, T. J., Synthesis and characterization of biogenic selenium nanoparticles with antimicrobial properties made by *Staphylococcus aureus*, methicillin-resistant *Staphylococcus aureus* (MRSA), *Escherichia coli*, and *Pseudomonas aeruginosa*. *Journal of Biomedical Materials Research. Part A*, 106. 5. (2018) 1400–1412. https://doi.org/10.1002/jbm.a.36347.

[40] Menon, S., Shrudhi Devi, K. S., Agarwal, H., Shanmugam, V. K., Efficacy of biogenic selenium nanoparticles from an extract of ginger towards evaluation on anti-microbial and anti-oxidant activities. *Colloid and Interface Science Communications*, 29. (2019) 1–8. https://doi.org/10.1016/j.colcom.2018.12.004.

[41] Mishra, R. R., Prajapati, S., Das, J., Dangar, T. K., Das, N., Thatoi, H., Reduction of selenite to red elemental selenium by moderately halotolerant *Bacillus megaterium* strains isolated from Bhitarkanika mangrove soil and characterization of reduced product. *Chemosphere*, 84. 9. (2011) 1231–1237. https://doi.org/10.1016/j.chemosphere.2011.05.025.

[42] Mulla, N. A., Otari, S. V., Bohara, R. A., Yadav, H. M., Pawar, S. H., Rapid and size-controlled biosynthesis of cytocompatible selenium nanoparticles by *Azadirachta indica* leaves extract for antibacterial activity. *Materials Letters*, 264. (2020) 127353. https://doi.org/10.1016/j.matlet.2020.127353.

[43] Prasad, K. S., Patel, H., Patel, T., Patel, K., Selvaraj, K., Biosynthesis of Se nanoparticles and its effect on UV-induced DNA damage. *Colloids and Surfaces B: Biointerfaces*, 103. (2013) 261–266. https://doi.org/10.1016/j.colsurfb.-2012.10.029.

[44] Prasad, K. S., Selvaraj, K., Biogenic synthesis of selenium nanoparticles and their effect on As(III)-induced toxicity on human lymphocytes. *Biological Trace Element Research*, 157. 3. (2014) 275–283. https://doi.org/10.1007/s12011-014-9891-0.

[45] Prokisch J., Zommara M., Process for producing elemental selenium nanospheres (Patent No. US 8003071 B2) (2011).

[46] Qin, Y., Ji, X., Jing, J., Liu, H., Wu, H., Yang, W., Size control over spherical silver nanoparticles by ascorbic acid reduction. *Colloids and Surfaces A: Physicochemical and Engineering Aspects*, 372. 1–3. (2010) 172–176. https://doi.org/10.1016/j.colsurfa.2010.10.013.

[47] Ramamurthy, Ch., Sampath, K. S., Arunkumar, P., Kumar, M. S., Sujatha, V., Premkumar, K., Thirunavukkarasu, C., Green synthesis and characterization of selenium nanoparticles and its augmented cytotoxicity with doxorubicin on cancer cells. *Bioprocess and Biosystems Engineering*, 36. 8. (2013) 1131–1139. https://doi.org/10.1007/s00449-012-0867-1.

[48] Ramya, S., Shanmugasundaram, T., Balagurunathan, R., Biomedical potential of actinobacterially synthesised selenium nanoparticles with special reference to anti-biofilm, anti-oxidant, wound healing, cytotoxic and anti-viral activities. *Journal of Trace Elements in Medicine and Biology: Organ of the Society for Minerals and Trace Elements (GMS)*, 32. (2015) 30–39. https://doi.org/10.1016/j.jtemb.2015.05.005.

[49] Sasidharan, S., Sowmiya, R., Balakrishnaraja, R., Biosynthesis of selenium nanoparticles using *Citrus Reticulata* peel extract. *World Journal of Pharmaceutical Research*, 4. (2015) 1322–1330.

[50] Satgurunathan, T., Bhavan, P., Komathi, S., Green synthesis of selenium nanoparticles from sodium selenite using garlic extract and its enrichment on *Artemia nauplii* to feed the freshwater prawn *Macrobrachium rosenbergii* post-larvae. *Research Journal of Chemistry and Environment*, 21. 10. (2017) 1–12.

[51] Shi, L., Xun, W., Yue, W., Zhang, C., Ren, Y., Shi, L., Wang, Q., Yang, R., Lei, F., Effect of sodium selenite, Se-yeast and nano-elemental selenium on growth performance, Se concentration and antioxidant status in growing male goats. *Small Ruminant Research*, 96. 1. (2011) 49–52. https://doi.org/10.1016/j.smallrumres.2010.11.005.

[52] Shoeibi, S., Mashreghi, M., Biosynthesis of selenium nanoparticles using *Enterococcus faecalis* and evaluation of their antibacterial activities. *Journal of Trace Elements in Medicine and Biology*, 39. (2017) 135–139. https://doi.org/10.1016/j.jtemb.2016.09.003.

[53] Sowndarya, P., Ramkumar, G., Shivakumar, M. S., Green synthesis of selenium nanoparticles conjugated *Clausena dentata* plant leaf extract and their insecticidal potential against mosquito vectors. *Artificial Cells, Nanomedicine, and Biotechnology*, 45. 8. (2017) 1490–1495. https://doi.org/10.1080/21691401.-2016.1252383.

[54] Sribenjarat, P., Jirakanjanakit, N., Jirasripongpun, K., Selenium nanoparticles biosynthesised by garlic extract as antimicrobial agent. *Science, Engineering and Health Studies.* (2020) 22–31. https://doi.org/10.14456/sehs.2020.3.

[55] Srivastava, N., Mukhopadhyay, M., Biosynthesis and structural characterization of selenium nanoparticles mediated by *Zooglea ramigera*. *Powder Technology*, 244. (2013) 26–29. https://doi.org/10.1016/j.powtec.2013.03.050.

[56] Srivastava, N., Mukhopadhyay, M., Biosynthesis and structural characterization of selenium nanoparticles using *Gliocladium roseum*. *Journal of Cluster Science*, 26. 5. (2015a) 1473–1482. https://doi.org/10.1007/s10876-014-0833-y.

[57] Srivastava, N., Mukhopadhyay, M., Green synthesis and structural characterization of selenium nanoparticles and assessment of their antimicrobial property. *Bioprocess and Biosystems Engineering*, 38. 9. (2015b) 1723–1730. https://doi.org/10.1007/s00449-015-1413-8.

[58] Sun, K., Qiu, J., Liu, J., Miao, Y., Preparation and characterization of gold nanoparticles using ascorbic acid as reducing agent in reverse micelles. *Journal of Materials Science*, 44. 3. (2009) 754–758. https://doi.org/10.1007/s10853-008-3162-4.

[59] Tejo Prakash, N., Sharma, N., Prakash, R., Raina, K. K., Fellowes, J., Pearce, C. I., Lloyd, J. R., Pattrick, R. A. D., Aerobic microbial manufacture of nanoscale selenium: Exploiting nature's bio-nanomineralization potential. *Biotechnology Letters*, 31. 12. (2009) 1857–1862. https://doi.org/10.1007/s10529-009-0096-0.

[60] Torres, S. K., Campos, V. L., León, C. G., Rodríguez-Llamazares, S. M., Rojas, S. M., González, M., Smith, C., Mondaca, M. A., Biosynthesis of selenium nanoparticles by *Pantoea agglomerans* and their antioxidant activity. *Journal of Nanoparticle Research*, 14. 11. (2012) 1236. https://doi.org/10.1007/s11051-012-1236-3.

[61] Tóth, R. J., Csapó, J., The role of selenium in nutrition – A review. *Acta Universitatis Sapientiae, Alimentaria*, 11. 1. (2018) 128–144. https://doi.org/10.2478/ausal-2018-0008.

[62] Tugarova, A. V., Kamnev, A. A., Proteins in microbial synthesis of selenium nanoparticles. *Talanta*, 174. (2017) 539–547. https://doi.org/10.1016/j.talanta.2017.06.013.

[63] Vetchinkina, E., Loshchinina, E., Kursky, V., Nikitina, V., Reduction of organic and inorganic selenium compounds by the edible medicinal basidiomycete *Lentinula edodes* and the accumulation of elemental selenium nanoparticles in its mycelium. *Journal of Microbiology (Seoul, Korea)*, 51. 6. (2013) 829–835. https://doi.org/10.1007/s12275-013-2689-5.

[64] Vieira, A., Stein, E., Andreguetti, D., Cebrián-Torrejón, G., Doménech-Carbó, A., Colepicolo, P., Ferreira, A. M., "Sweet chemistry": A green way for obtaining selenium nanoparticles active against cancer cells. *Journal of the Brazilian Chemical Society*, 28. 10. (2017) 2021–2027. https://doi.org/10.21577/0103-5053.20170025.

[65] Visha, P., Nanjappan, K., Jayachandran, S., Selvaraj, P., Elango, A., Kumaresan, G., Biosynthesis and structural characteristics of selenium nanoparticles using *Lactobacillus acidophilus* bacteria by wet sterilization process. *International Journal of Advanced Veterinary Science and Technology*, 4. 1. (2015) 178–183.

[66] Vyas, J., Rana, S., Antioxidant activity and green synthesis of selenium nanoparticles using *Allium sativum* extract. *International Journal of Phytomedicine*, 9. 4. (2017) 634–641. https://doi.org/10.5138/09750185.2185.

[67] Vyas, J., Rana, S., Biosynthesis of selenium nanoparticles using aloe vera leaf extract. *International Journal of Advanced Research*, 6. 1. (2018a) 104–110. https://doi.org/10.5281/zenodo.1173991.

[68] Vyas, J., Rana, S., Synthesis of selenium nanoparticles using *Allium sativum* extract and analysis of their antimicrobial property against gram positive bacteria. *The Pharma Innovation Journal*, 7. 9. (2018b) 262–266.

[69] Wang, H., Chen, B., He, M., Yu, X., Hu, B., Selenocystine against methyl mercury cytotoxicity in HepG2 cells. *Scientific Reports*, 7. 1. (2017) 147. https://doi.org/10.1038/s41598-017-00231-7.

[70] Wang, R. R., Pan, X. J., Peng, Z. Q., Effects of heat exposure on muscle oxidation and protein functionalities of pectoralis majors in broilers. *Poultry Science*, 88. 5. (2009) 1078–1084. https://doi.org/10.3382/ps.2008-00094.

[71] Wang, T., Yang, L., Zhang, B., Liu, J., Extracellular biosynthesis and transformation of selenium nanoparticles and application in H_2O_2 biosensor. *Colloids and Surfaces B: Biointerfaces*, 80. 1. (2010) 94–102. https://doi.org/10.1016/j.colsurfb.2010.05.041.

[72] Xiong, Y., Xia, Y., Shape-controlled synthesis of metal nanostructures: The case of palladium. *Advanced Materials*, 19. 20. (2007) 3385–3391. https://doi.org/10.1002/adma.200701301.

[73] Xu, C., Guo, Y., Qiao, L., Ma, L., Cheng, Y., Roman, A., Biogenic synthesis of novel functionalized selenium nanoparticles by *Lactobacillus casei* ATCC 393 and its protective effects on intestinal barrier dysfunction caused by enterotoxigenic *Escherichia coli* K88. *Frontiers in Microbiology*, 9. (2018) 1129. https://doi.org/10.3389/fmicb.2018.01129.

[74] Yazdi, M. H., Mahdavi, M., Varastehmoradi, B., Faramarzi, M. A., Shahverdi, A. R., The immunostimulatory effect of biogenic selenium nanoparticles on the 4T1 breast cancer model: An in vivo study. *Biological Trace Element Research*, 149. 1. (2012) 22–28. https://doi.org/10.1007/s12011-012-9402-0.

[75] Zare, B., Babaie, S., Setayesh, N., Shahverdi, A. R., Isolation and characterization of a fungus for extracellular synthesis of small selenium nanoparticles. *Nanomedicine Journal*, 1. 1. (2013) 13–19. https://doi.org/10.7508/nmj.2013.01.002.

[76] Zhang, J., Wang, X., Xu, T., Elemental selenium at nano size (nano-Se) as a potential chemopreventive agent with reduced risk of selenium toxicity: Comparison with Se-methylselenocysteine in mice. *Toxicological Sciences*, 101. 1. (2008) 22–31. https://doi.org/10.1093/toxsci/kfm221.

[77] Zhang, W., Chen, Z., Liu, H., Zhang, L., Gao, P., Li, D., Biosynthesis and structural characteristics of selenium nanoparticles by *Pseudomonas alcaliphila*. *Colloids and Surfaces B: Biointerfaces*, 88. 1. (2011) 196–201. https://doi.org/10.1016/j.colsurfb.2011.06.031.

Acta Univ. Sapientiae, Alimentaria, **14** (2021) 44–56

DOI: 10.2478/ausal-2021-0003

Physiological benefits of a honeydew-based functional food fortified with selected bioactive agents justified by trials

E. Némedi[1]
e-mail: expeditnodum@expeditnodum.com

J. Nemes[1]
e-mail: jpnemes@gmail.com

I. Mirmazloum[2]
e-mail: imanmedica@gmail.com

D. Pituk[1]
e-mail: pituk.dora@gmail.com

V. Szarka[1]
e-mail: nika.szarka@gmail.com

A. Kiss[3]
e-mail: attilakiss.eger@gmail.com

[1] Expedit Nodum Ltd. Budapest, Hungary
[2] Department of Plant Physiology and Plant Ecology, Institute of Plant Production, Hungarian University of Agriculture and Life Sciences (MATE), Budapest, Hungary
[3] Agricultural and Food Industrial Innovation and Knowledge Centre, Debrecen University (DU), Debrecen, Hungary

Abstract. Honey is a consumer-preferred, highly esteemed natural product with a broad variety of distinct bioactive components. In recent days, the consumption of high-added-value, honey-based products are increasingly coming to the forefront of interest, and thus huge efforts are being made by researchers/developers to elaborate honey variants with fortified biological value. Relevant human clinical trials have scarcely been accomplished; thus, the biological impact of honey and its derivatives has not been thoroughly revealed. In this work, we present our experiments on the development of a novel honey-based prototype and its plausible physiological impacts certified via human clinical trials. The investigated product was a newly elaborated honeydew-based prototype fortified with pumpkin, sea buckthorn, and inulin, which was subjected to a 13-week-long, double-blind, placebo-controlled human clinical trial. The prototypes were applied to 20 adult volunteers to establish the complex impact of the newly developed product. Conclusions drawn at the end of the trial were based on results of blood tests taken at diverse phases of the study. The positive physiological effects of consumption of the investigated products are underpinned by the fact that no significant elevations have been measured in terms of the blood glucose level and parameters featuring long-term blood sugar levels. Slight decrease of both LDL and HDL cholesterol levels were also experienced.

Keywords and phrases: inulin, honeydew, functional food, pumpkin, sea buckthorn

1. Introduction

In recent days, wellness trends and conscious nutrition are getting more and more into the forefront of interest. The consumption of healthy foodstuffs is not only a fashion currently, but it also turns out to be the conviction of many people as a health-conscious lifestyle. In accordance with changing consumer demands, food manufacturers elaborate complex foodstuffs (functional foods) of certified high added value and health-promoting effects (*Cencic & Chingwaru*, 2010; *Daliu et al.*, 2019; *Mračević et al.*, 2020).

The study presented in this paper aims at revealing the physiological impacts of a newly developed, honey-based functional foodstuff, which is in full compliance with this modern nutrition trend. A unique functional food prototype has been elaborated in the initial phase of the studies: a special blend of inulin-fortified honeydew and plant extracts of high added value.

The nutritional and physiological relevance of various honey types has already been thoroughly studied and characterized (*Siro et al.*, 2008; *Salonen et al.*, 2017). Acacia honey in particular is one of the most favoured honey types in many countries with a fructose:glucose ratio higher than that of other honey types, resulting in less likelihood of crystallization during storage (*Mădaş et al.*, 2019; *Kiss et al.*, 2019).

Honey might be considered as a healthy alternative of any artificial sweetener possessing various kinds of drawbacks in terms of health implications. The glycaemic index of saccharose is 68 while that of acacia honey is just around 50–55 (*Deibert et al.*, 2010; *Sadeghi et al.*, 2019).

The application of inulin in a variety of foodstuffs in order to replace fat or sugar or to modify the sensory characteristics has already been studied (*Tiwari et al.*, 2015). With one-tenth of sucrose sweetness, inulin comprises about 25–35% less energy than digestible carbohydrates and is considered a dietary fibre (*Shoaib et al.*, 2016; *Ahmed & Rashid*, 2019).

The application of inulin in functional foodstuffs is a sensible way of increasing the biological value due to its well-proven prebiotic activity (*Bouhnik et al.*, 2007; *González-Herrera et al.*, 2015). Inulin comprising honey-based products has not been introduced, but an inulin-rich syrup (EAT TROO) has already been developed, which is now commercially available.

Capilano Honey Ltd. has recently launched a new product called "Beeotic Honey", whose beneficial properties are to be justified via clinical tests. This prebiotic honey contains eight naturally occurring and formed oligosaccharides and is listed as a therapeutic good with the Therapeutic Goods Administration. A study conducted by the University of New South Wales (UNSW) revealed that it led to the increase of several of beneficial bacteria and suppressed harmful bacteria in the digestive tract (*Cokcetin*, 2015).

Relevant human clinical studies have been implemented by us in order to justify some of the beneficial features of the new product as well as to reveal its actual physiological impacts.

2. Materials and methods

The new product prototype

In our unique approach, the implication of not only honeydew as a healthy foodstuff but also of probiotic inulin and antioxidant-rich fruits is accomplished. Such a combination of the abovementioned components has not been described before.

The novel food prototype is composed of 84% honeydew, 10% pumpkin, 5% sea buckthorn, and 1% inulin. Several combinations have been tested, and the mentioned composition led to the most appropriate organoleptic traits as well as texture. Our primary intention was to apply the components of marked health-promoting impact in the highest possible concentrations, though the upper limits were determined by the revealed physical-chemical properties, with special regard to the solubility and homogeneity of the solution. It was observed that increasing water content resulted in shorter storage time; sea buckthorn was used as powder.

The elaborated, functional honeydew was subjected to regular quality analyses (water-content, HMF, antioxidant activity) in order to ensure the long-term excellent quality of the product. The developed honeydew-based prototype was not prone to sugar precipitation as opposed to several other honey types.

The daily dose of the product included in the diet of volunteers (chiefly as a breakfast supplement) was 6.6 g, which did not signify a stressful amount for them. The only disadvantage experienced was the product's cragged texture, which can be attributed to the applied sea buckthorn powder. The potential positive impact of our investigated product might derive from its unique composition and the multiple, synergistic effects of the intrinsic components.

Major constituents and their biological relevance

The honeydew

The honeydew honey (forest honey, pine honey) is a product with high sugar content, dark, opaque colour, balsamic aroma and strong taste, produced by bees from the body secretions of plant pests. Although honeydew honey is a special type of honey, it differs from nectar honeys in many nutritional and physiological aspects. It contains protein, vitamins, minerals, volatile compounds, alkaloids, and antioxidants. The slightly lower sugar content can be characterized by a 1:4

fructose/glucose ratio, so we can expect a higher amount of fructose compared to rapeseed and fruit honey. The content of oligosaccharides with potential prebiotic effect is much higher than that of nectar honeys.

Honeydew honey contains higher amounts of glutamic acid and tryptophan than nectar honey. Among the honeys, honeydew has outstanding mineral and essential microelement content (406 mg/100 g in total). The substantial potassium content (239–364 mg/100 g) makes up 74% of the total mineral content.

Honeydew honey is rich in volatile compounds, such as terpenes, which give it a scent. Literature findings revealed that terpenoids can exert antimicrobial, antifungal, antiviral, and anti-inflammatory effects.

Compared to nectar honey, one of the major benefits of honeydew is its three times higher content of polyphenols (140.6 mg/100 g GAE/100 g) and flavonoids, resulting in outstanding antioxidant capacity. As a consequence, liver-protective, antibacterial, antiviral, anti-inflammatory, anti-tumour, and cholesterol-lowering effects might be attributed to honeydew.

The pumpkin

Pumpkins are characterized by high water (91.6%) but low energy (108.8 kJ/100 g), protein (1 g/100 g), and fat content (0.1 g/100 g). Pumpkins may also be involved in the preventive effect against cardiovascular diseases. Most of the carbohydrates – 6.5 g/100 g – in pumpkin are polysaccharides, and just a small proportion is constituted by sugars (2.7 g/100 g).

Pumpkin fibres typically contain water-soluble, highly water-binding pectin. The pectin slows gastric emptying and prolongs the absorption of nutrients, thus increasing the amount of stool and maintaining health. Pectin consumption may also contribute to lowering total and LDL cholesterol levels.

Some pumpkin polysaccharides have both antioxidant and prebiotic effects, so they can have a beneficial effect on blood lipid values and protect against pathogenic bacteria. Out of the carotenoids, it contains beta- and alpha-carotene, lutein, and zeaxanthin in the largest amounts.

The sea buckthorn

Recently, several studies have addressed the medicinal use of some components of sea buckthorn (*Hippophae rhamnoides* L.). Potential utilizations have been demonstrated in the areas of cancer, cardiovascular diseases, gastric ulcer, inflammatory diseases, thrombosis, diabetes, tendon injuries, cholesterol reduction, and antibiotic, antiviral effects. Sea buckthorn fruit is one of the fruits of low sugar content (0.79–6.63 g/100 g).

In addition to fruit pulp, oil-rich (7–11%) sea buckthorn seeds are also present in the investigated product. Sea buckthorn seed oil consists of 35% linolic acid and 34% α-linolenic acid, so in seed oil the presented omega-3/omega-6 fatty acid ratio is nearly 1:1, which is favourable for maintaining health. Sea buckthorn oil is an outstanding source of phytosterols, containing 522–577 mg/100 g of beta-sitosterol.

Sea buckthorn is abundant in antioxidant vitamins such as vitamin C (600 mg/100 g), tocopherols (216–481 mg/100 g), but it also contains higher amounts of folate (80 mg/100 g), vitamins B_1, B_2, and K. The sea buckthorn pulp contains remarkable amounts of vitamin C and iron (4–15 mg/100 g), which can contribute to the reduction of fatigue as well as to the normal functioning of the immune system and the metabolic processes. Sea buckthorn comprises large amounts of phenolic compounds, accounting also for its outstanding antioxidant effect.

Inulin, a powerful prebiotic

The investigated honeydew-based functional product was enriched with pumpkin and sea buckthorn extract and contained 1% inulin. Several beneficial effects of prebiotic inulin consumption have been shown recently such as positive influence on bowel habits, gastric health, and immune system.

Inulin promotes calcium absorption very effectively and is able to modulate the immune function by increasing the SCFA content of the colon. Due to its immunomodulatory effect, inulin may help controlling irritable bowel syndrome. As a plausible component of potential synbiotics, it significantly reduces CRP and increases glutathione levels. In addition to the positive physiological impacts listed above, several more health-promoting effects have been confirmed in previous studies (*Markowiak & Slizewska*, 2017; *Plaza-Díaz et al.*, 2017; *Yu et al.*, 2017; *Huang et al.*, 2018).

Setup and implementation of the human clinical trial

The objective of the study was to gain information on the actual physiological impacts of the novel functional food product, and to find a way to incorporate its consumption into the daily diet of the volunteers as well as future consumers.

The study was accomplished in total compliance with all relevant EFSA requirements as well as with the ethical guidelines of the valid Declaration of Helsinki. Good clinical practice was applied in accordance with CPMP/International Conference on Harmonization ([ICH]/135/95).

The human clinical trial was a 13-week-long, crossover, double-blind, placebo-controlled randomized study with self-control groups. The study period was divided into four phases. The 1st phase included a screening and a baseline visit, where participants were randomly selected and informed of the use and dosing of the

investigated product. Thereafter (2nd phase, or first study period), the participants consumed daily a single dose of honeydew or the investigated product for 5 weeks: 5 ml (6.6 g) of the product once a day in the morning. The 3rd phase was a 3-week-long wash-out period, when the participants did not consume any honey products. Afterwards (4th stage, or second study period), in a 5-week-long period, the volunteers who had consumed functional product in the first study period, were supplied with the control substance, while those who were previously given the control product as a supplement to their food, this time consumed the functional product. This crossover feature of the study made it possible to survey the effects of both products in the case of the same volunteers.

At the beginning of this period, one on-site visit and later a telephone visit was performed, and the closing visit took place at the end of the final week. During the thirteen weeks, the condition of the participants was checked with the examination of general parameters, laboratory tests, and objective questionnaires. The results obtained after the statistical evaluation were analysed from a physiological, dietetical, and technological point of view alike.

Changes in some relevant parameters were monitored with blood tests taken at diverse phases of the study. The following laboratory parameters have been examined regarding the study's aim and by maintaining tolerability and safety: K, Na, Ca, P, Mg, Cl, Fe, total cholesterol, HDL, LDL, triglyceride, AST; ALT; GGT; alkaline phosphatase, bilirubin, HbA1c, CRP, BUN; creatinine; eGFR, albumin; total protein, MCH, MCV, polyphenol content, and antioxidant activity.

Statistical analysis

SPSS 26.0 for Windows (IBM SPSS Statistics, IBM Corporation, Armonk, NY) was used for the statistical analysis of the data. A descriptive analysis was performed for all variables. Normally distributed, continuous data were described as means and standard deviations. Results are provided as mean and its 95% confidence interval plots. The significance of differences among groups was evaluated with one-way analysis of variance (ANOVA) followed by Tukey's comparison test. Categorical data were described as numbers and proportions and analysed with a χ^2 test. The value was statistically significant at the level of $p < 0.05$.

3. Results and discussions

The justification of the physiologically beneficial properties of the new prototype was accomplished in our studies. The major laboratory safety parameters did not display significant alterations, and all the surveyed such parameters remained within the normal interval, indicating that the consumption of the investigated product is safe.

Neither honeydew nor its fortified, functional variant led to elevation of blood sugar level despite their high sugar content. It might be deduced that the daily consumption of 6.6 g of the investigated product might be considered a safe dosage even for people suffering from diabetes. It is also remarkable that parameter HbA1c, being associated with the blood sugar level, exhibited stagnant values. This phenomenon can be regarded as a health benefit of the investigated product despite the high overall sugar content; no blood-sugar-related elevations were observed (*Figures 1–2*).

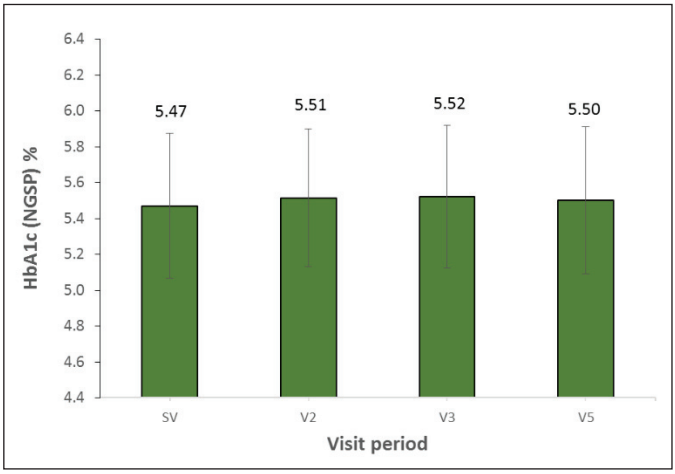

Figure 1. The impact of the consumption of the honeydew-based new prototype on HbA1c (NGSP) level (%)

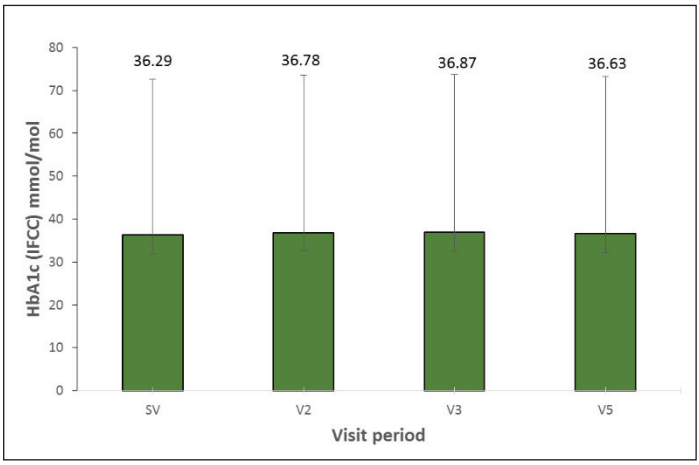

Figure 2. The effect of the honeydew-based new prototype on HbA1c (IFCC) level (mmol/mol)

Thanks to the application of pumpkin and sea buckthorn in the investigated product – being abundant in potassium and iron –, slightly improved K- and Fe-levels were observed upon completion of the study. The corresponding data for potassium are presented below, in *Figure 3*.

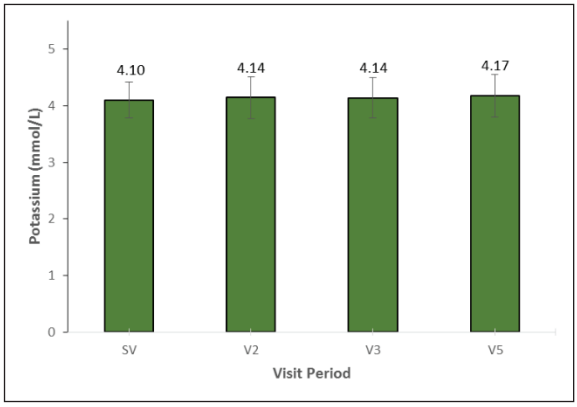

Figure 3. The impact of the consumption of the honeydew-based new prototype on potassium level

The total bilirubin level surveyed during the study exhibited an increasing tendency for the control product and a decreasing trend for the functional product (*Figure 4*). This might be considered as another beneficial consequence of consuming the investigated product, which is ascribed to the high polyphenol content of the included sea buckthorn and pumpkin.

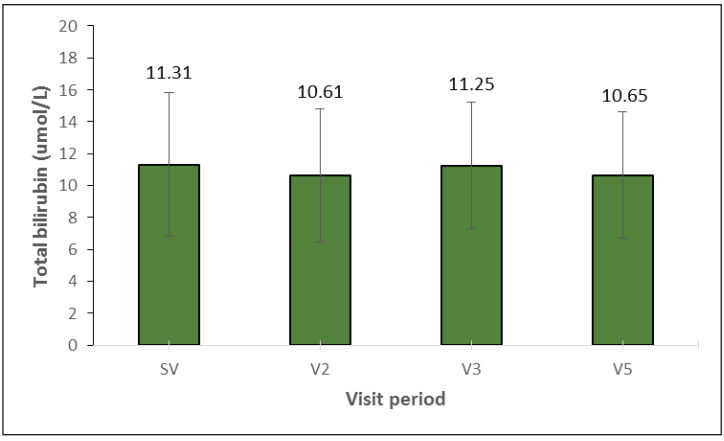

Figure 4. Changes in total bilirubin levels during the study period (13-week-long consumption of honeydew-based new prototype)

The consumption of the investigation product did not result in significant changes in any of the examined lipid parameters. The total cholesterol concentration exhibited a very slight elevation by the end of the study period, which might be accounted for by other nutrition factors apart from the used functional product (*Figure 5*). The beneficial features and high antioxidant activity of the functional product might have hindered the significant elevation of lipid parameters in spite of the fact that the increased sugar input should have triggered a marked increase in terms of these parameters.

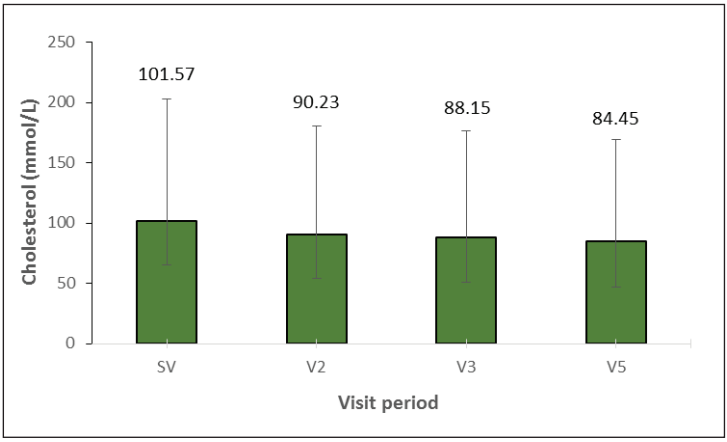

Figure 5. The impact of the consumption of the honeydew-based new prototype on cholesterol level

The consumption of the investigated product did not lead to significant alterations in the HDL cholesterol level; however, a slight decrease was observed upon completion of the study period (*Figure 6*).

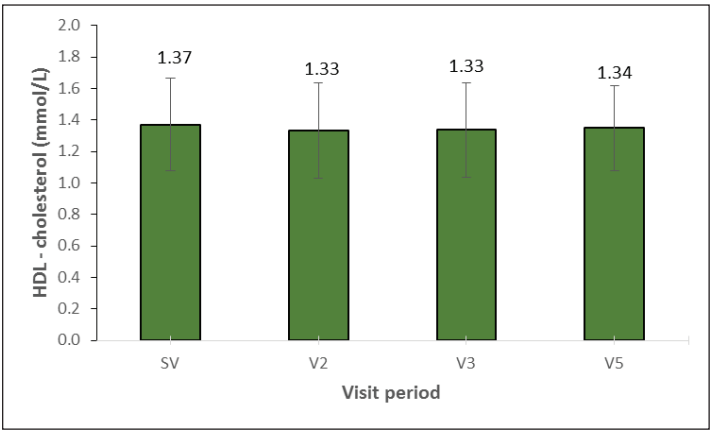

Figure 6. Changes in HDL cholesterol level during the study period

In terms of LDL cholesterol level, no significant changes were observed during the 13-week-long study period; however, a very slight increase could be observed at the last visit (*Figure 7*). This observation did not meet the expectations and might be explained by the consumption of other foodstuffs of unbeneficial impacts.

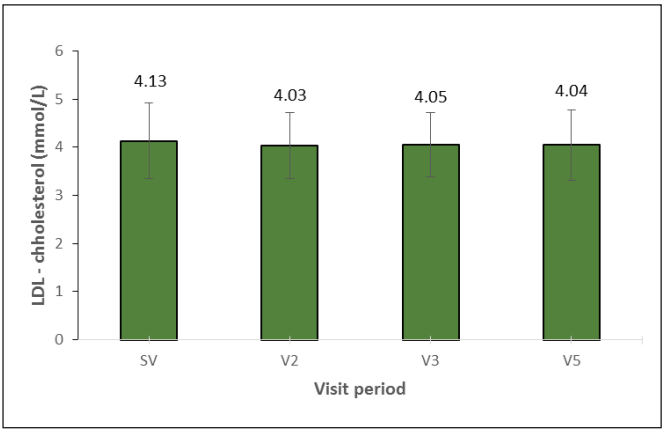

Figure 7. The impact of the consumption of the honeydew-based new prototype on LDL cholesterol level

The alkaline phosphatase activity parameter exhibited a slight decrease throughout the study period as follows: the high polyphenol content of sea buckthorn might have played a crucial role in the development of this tendency. The same parameter of the control product displayed a slight increase throughout the study period, and thus the observed trend can be regarded as a remarkable distinction (*Figure 8*).

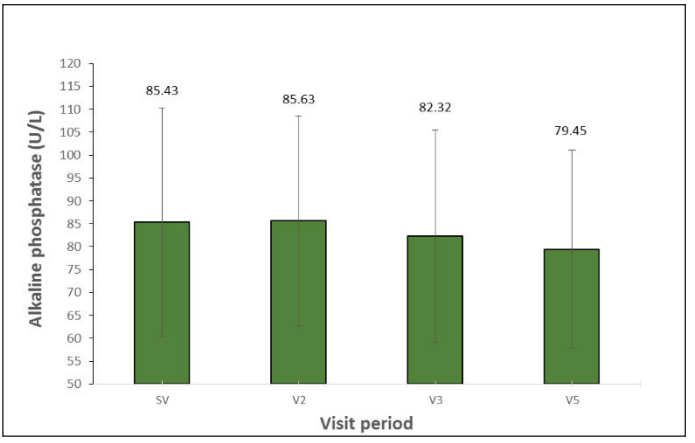

Figure 8. The effect of the honeydew-based new prototype on alkaline phosphatase level

4. Conclusions

In this study, the actual physiological effects triggered by the consumption of a special, newly developed functional foodstuff pointed out that the investigated product's high added value is reinforced.

Most significantly, it should be noted that the new product's long-term consumption is regarded as not only safe but also physiologically beneficial. Multiple synergistic effects of the investigated product's intrinsic bioactive components have been observed. Special emphasis should be laid on the fact that the consumption of the product does not lead to increase in blood sugar; hence, under controlled conditions, even clients with diabetes might be recipients of this food type. HbA1c, the most reliable blood sugar indicator parameter, displayed no increase at all.

Total cholesterol levels displayed negligible changes during the study, which is regarded as a beneficial impact of consumption of the new food prototype. The high antioxidant activity as well the abundance of other types of bioactive molecules present in the investigated product hindered the significant elevation of lipid parameters, which might be regarded as a beneficial consequence.

The new food prototype can be regarded as a healthy alternative for sweeteners due to its relatively low impact on blood sugar level and its high level of diverse, beneficial bioactive substances.

Most of the involved volunteers were impressed by the flavours of our functional product and claimed that they would purchase it in case of commercialization. In the long run, this new product might constitute an integral part of people's regular breakfast meal. The implemented human clinical study facilitated the introduction of the product as well as the elaboration of scientifically grounded marketing activities.

Acknowledgements

The publishing of this paper is supported by the *Programs for Supporting the Research, Development, and Innovation Activities of Enterprises* financed by the Hungarian National Research and Development Innovation Agency under the auspices of the GINOP-2.1.1-15-2015-00461 project.

References

[1] Ahmed, W., Rashid, S., Functional and therapeutic potential of inulin: A comprehensive review. *Critical Reviews in Food Science and Nutrition*, 59. 1. (2019) 1–13.

[2] Bouhnik, Y., Raskine, L., Champion, K., Andrieux, C., Penven, S., Jacobs, H., Simoneau, G., Prolonged administration of low-dose inulin stimulates the growth of bifidobacteria in humans. *Nutrition Research*, 27. 4. (2007) 187–193.

[3] Cencic, A., Chingwaru, W., The role of functional foods, nutraceuticals, and food supplements in intestinal health. *Nutrients*, 2. (2010) 611–625.

[4] Cokcetin, N., *An investigation of the prebiotic properties of Australian honeys*. PhD dissertation, School of Biotechnology and Biomolecular Sciences, Faculty of Science, University of New South Wales, Australia (2015).

[5] Daliu, P., Santini, A., Novellino, E., From pharmaceuticals to nutraceuticals: Bridging disease prevention and management. *Expert Review of Clinical Pharmacology*, 12. 1. (2019) 1–7.

[6] Deibert, P., König, D., Kloock, B., Groenefeld, M., Berg, A., Glycaemic and insulinaemic properties of some German honey varieties. *European Journal of Clinical Nutrition*, 64. 7. (2010) 762–764.

[7] González-Herrera, S. M., Herrera, R. R., López, M. G., Rutiaga, O. M., Aguilar, C. N., Esquivel, J. C., Martínez, L. A., Inulin in food products: Prebiotic and functional ingredient. *British Food Journal*, 9. 2. (2015) 121–127.

[8] Huang, L., Zhu, Q., Qu, X., Qin, H., Microbial treatment in chronic constipation. *Science China Life Sciences*, 61. 7. (2018) 744–752.

[9] Kiss, A., Mirmazloum, I., Naár, Z., Némedi, E., Supplementation of lingzhi or reishi medicinal mushroom, *Ganoderma lucidum* (Agaricomycetes) extract enhanced the medicinal values and prebiotic index of Hungarian acacia honey. *International Journal of Medicinal Mushrooms*, 21. 12. (2019) 1167–1179.

[10] Mădaş, N. M., Mărghitaş, L. A., Dezmirean, D. S., Bonta, V., Bobiş, O., Fauconnier, M. L., Francis, F., Haubruge, E., Nguyen, K. B., Volatile profile and physico-chemical analysis of acacia honey for geographical origin and nutritional value determination. *Foods*, 8. (2019) 445.

[11] Markowiak, P., Slizewska, K., Effects of probiotics, prebiotics, and synbiotics on human health. *Nutrients*, 9. 9. (2017) 1021.

[12] Mračević, S. Đ., Krstić, M., Lolić, A., Ražić, S., Comparative study of the chemical composition and biological potential of honey from different regions of Serbia. *Microchemical Journal*, 152. (2020) 104420.

[13] Plaza-Díaz, J., Ruiz-Ojeda, F. J., Vilchez-Padial, L. M., Gil, A., Evidence of the anti-inflammatory effects of probiotics and synbiotics in intestinal chronic diseases. *Nutrients*, 9. 6. (2017) 555.

[14] Sadeghi, F., Salehi, S., Kohanmoo, A., Akhlaghi, M., Effect of natural honey on glycemic control and anthropometric measures of patients with type 2 diabetes: A randomized controlled crossover trial. *International Journal of Preventive Medicine*, 10. (2019) 3.

[15] Salonen, A., Virjamo, V., Tammela, P., Fauch, L., Julkunen-Tiitto, R., Screening bioactivity and bioactive constituents of Nordic unifloral honeys. *Food Chemistry*, 237. (2017) 214–224.

[16] Shoaib, M., Shehzad, A., Omar, M., Rakha, A., Raza, H., Sharif, H. R., Shakeel, A., Ansari, A., Niazi, S., Inulin: Properties, health benefits and food applications. *Carbohydrate Polymers*, 147. (2016) 444–454.

[17] Siro, I., Kápolna, E., Kápolna, B., Lugasi, A., Functional food. Product development, marketing and consumer acceptance – A review. *Appetite*, 51. 3. (2008) 456–467.

[18] Tiwari, A., Sharma, H. K., Kumar, N., Kaur, M., The effect of inulin as a fat replacer on the quality of low-fat ice cream. *International Journal of Dairy Technology*, 68. 3. (2015) 374–380.

[19] Yu, T., Zheng Y. P., Tan, J. C., Xiong, W. J., Wang, Y., Lin, L., Effects of prebiotics and synbiotics on functional constipation. *The American Journal of the Medical Sciences*, 353. 3. (2017) 282–292.

Acta Univ. Sapientiae, Alimentaria, **14** (2021) 57–83

DOI: 10.2478/ausal-2021-0004

The role of resistant starch in human nutrition

Zs. Zurbó[1,2]
e-mail: zurbo.zsofia@agr.unideb.hu

J. Csapó[1,3]
e-mail: csapo.janos@gmail.hu

[1] University of Debrecen, Faculty of Agricultural and Food Sciences and Environmental Management, Institute of Food Technology
[2] University of Debrecen, Doctoral School of Nutrition and Food Sciences
4032 Debrecen, Böszörményi Street 138, Hungary
[3] Sapientia Hungarian University of Transylvania, Cluj-Napoca, Faculty of Economics, Socio-Human Sciences and Engineering, Department of Food Science
530104 Miercurea Ciuc, 1 Libertății Sq., Romania

Abstract. In this paper, we examine the role and effect of resistant starch (RS) in human nutrition; further, the structure and properties of RS, the food sources based on resistance to digestion in the colon, and the physiological effects of RS are described. The nutritional value of RS, the effect of RS on short-chain fatty acid (SCFA) production, the relationships between RS and colon function, and the relationships between food starch, dietary fibre, and RS content and colon cancer development are reviewed. It has been shown that the use of RS in foods may have some benefits. Resistant starch, digestion of resistant-starch-containing foods have a number of health benefits for colon function but appear to have less effect on lipid-glucose metabolism. It has a positive effect on colon bacterial activity, promotes the growth of beneficial microbes, and reduces the activity of enzymes that are harmful to the digestive system. Under the influence of RS, increased SCFA production lowers the pH of the colon and stimulates bile acid secretion. The decreased pH protects against colon cancer and inhibits the conversion of primary and secondary bile acids, which are cytotoxic to intestinal cells. At the end of the review article, the relationships between RS and the colon microflora, its use as a prebiotic, and the relationship between RS and glucose metabolism are analysed. It was found that the use of RS in the diet might have benefits as it shortens the time it takes food to pass through the colon and increases the amount of stool. It was also found that the physicochemical properties of foods can directly affect the amount of RS and thereby the blood glucose levels and insulin response.

Keywords and phrases: resistant starch, human nutrition, short-chain fatty acid, blood sugar level, insulin response, prebiotic, probiotic bacteria

1. Effects of resistant starch in the human body

Nutritional science has recognized from the earliest years of its appearance that the body is incapable of utilizing all the nutrients in the food it consumes. An increasing number of evidence suggests that only a portion of the total nutrients consumed is available, and the term "utilization" is used to quantify this portion (*Southgate*, 1989). Nutrients measured by chemical analysis are not fully utilized, mainly due to indigestible cell walls, bulky or denser structures, low solubility, digestive inhibitors, and specific constituents (inhibitors, dietary fibre, phytic acid, and tannic acid) of foods of plant origin that can significantly reduce the absorption and utilization of certain nutrients (*Rosado et al.*, 1987).

During food processing, the ingredients are transformed, and cross-links may be formed, making them inaccessible to degrading enzymes. These types of nutrients are also "unusable" by the human body (*Erbersdobler*, 1989).

Starch is the most common storage of polysaccharides in plants and the main source of dietary carbohydrate. It can be found in the chloroplast of green leaves and the amyloplast of seeds and tubers as granules (*Ellis et al.*, 1998). Recently, it has been found that the partial digestion and absorption of starch in the small intestine is a normal phenomenon associated with indigestible starches (*Englyst & Cummings*, 1991; *Englyst et al.*, 1992). These are called resistant starch (RS). All starches and starch breakdown products that are not absorbed in the small intestine of a healthy person are classified as RS (*Nugent*, 2005). Extensive studies have shown that their physiological functions are similar to those of dietary fibre (*Asp*, 1994; *Eerlingen & Delcour*, 1995). Resistant starch (RS) is fermented by microbes in the colon, leading to the production of short-chain fatty acids (SCFAs) (*Topping & Clifton*, 2001; *Bird et al.*, 2007).

Short-chain fatty acids lower the pH in the colon, preventing the excessive growth of pathogenic bacteria (*Roy et al.*, 2006). Acetic acid, propionic acid, and butyric acid are the main SCFAs produced in the colon, and the last of these has the most health benefits. The health-promoting effects of butyric acid are prevention and inhibition of carcinogenesis in the colon, protection of the mucosa from oxidative stress, and strengthening the barrier of the colon. Butyric acid also has anti-inflammatory properties (*Hamer et al.*, 2008). Propionic acid can lower blood cholesterol levels (*Hosseini et al.*, 2011). In addition, short-chain fatty acids are thought to play a role in the development of satiety (*Sleeth et al.*, 2010). RS contributes to health protection by promoting the formation of short-chain fatty acids (*Haenen et al.*, 2013).

2. Characterization of starch and resistant starch

Chemically, starches are polysaccharides in which the glucose molecules are linked together by α-1-4 and/or α-1-6 bonds. There are two main structural types of starch: amylose, which is a linear α-1-4 molecule and typically accounts for 15–30% of starch, and amylopectin, which is a larger branched chain – α-1-4 and α-1-6 molecules that also contain bonds – and accounts for 70–85% of starch.

In vivo studies of dietary-fibre-like non-starch polysaccharides by *Englyst et al.* (1992) revealed that certain starches remain after enzymatic hydrolysis. Follow-up studies with a healthy ileostomy (an operation in the abdominal wall through which a small section of the small intestine (ileum) is passed to the body surface) confirmed the presence of similar starches that resisted digestion in the small intestine (*Cummings et al.*, 1996).

RS is classified into five general types, numbered from RS1 to RS5 (*Englyst et al.*, 1992; *Brown et al.*, 1995; *Asp et al.*, 1996; *Nugent*, 2005; *Sajilata et al.*, 2006; *Fuentes-Zaragoza et al.,* 2011). *Table 1* gives an overview of the RS types, the different classification criteria, and the food origin.

Table 1. Types of resistant starch and their food sources

RS type	Description	Food sources
RS1	Physically protected starch	Wholly or partly ground cereals and seeds, legumes, pasta
RS2	Non-gelatinized resistant starch granules with type B crystallinity, which can be slowly hydrolysed by α-amylases	High amylose starch, some legumes, raw potatoes, and green bananas
RS3	Retrograded starch	Boiled and chilled potatoes, bread, cornflakes, long-lasting and/or repeated wet heat-treated foods
RS4	Chemically modified starches (with ether, ester groups, other chemicals)	Some fibre drinks, foods in which modified starch is used, in some breads and cakes
RS5	Amylose-lipid complexes	Stearic acid-complexed high-amylose starch

Sources: *Nugent*, 2005; *Sajilata et al.*, 2006; *Lunn & Buttriss*, 2007; *Sharma et al.*, 2008; *Birt et al.*, 2013; *Lockyer & Nugent*, 2017; *Metzler-Zebeli et al.*, 2019; *Gutiérrez & Tovar*, 2021
RS, resistant starch

In RS1, starch is physically inaccessible to digestion because the intact cell walls in grains, seeds, or tubers prevent their digestion. RS2 are native starch granules, which contain granular starch that is resistant to digestion because of the conformation or structure of the granules. RS3 represents non-particulate

starch-derived substances that are resistant to digestion. RS4 is a group of starches containing chemically modified starch that is etherified, esterified, or cross-linked with chemicals in a way that reduces the digestibility of the starch (*Brown*, 2004; *Fuentes-Zaragoza et al.*, 2011). RS5 is a group of starches that contain an amylose-lipid complex (*Birt et al.*, 2013; *Lockyer & Nugent*, 2017; *Metzler-Zebeli et al.*, 2019; *Gutiérrez & Tovar*, 2021).

Resistant starch can be found in a variety of everyday foods. However, depending on the degree of processing or cooking, as well as the length and circumstances of storage to which the starch is subjected, these levels can be variable and unexpected (*Brown*, 1996). Phosphate and other extreme additions can adhere to starch, making it more or less sensitive to breakdown (*Niba*, 2003). Physiological factors can also have an impact on the amount of RS in foods. Increased chewing reduces particle size (smaller particles are easier to digest in the gut) although individual differences in transit time and biological factors also play a role (*Nugent*, 2005). It is currently unknown how different types of RS4 affect digestion in vivo.

RS is a type of dietary fibre that has a number of nutritional benefits, including lowering blood sugar and insulin levels, reducing calorie intake, increasing faecal excretion and decreasing faecal transit time, promoting the growth of beneficial intestinal bacteria and the colonic production of short-chain fatty acids (SCFA), etc. (*Zhao et al.*, 2018).

The many definitions of dietary fibre derive from the method of its definition, i.e. dietary fibre is defined as a plant component or as a chemical (*Champ et al.*, 2003a). In 2000, the American Association of Cereal Chemists (AACC) defined dietary fibre as edible components that resist digestion and absorption in the human small intestine and are fully or partially fermented in the large intestine. Dietary fibres include oligosaccharides, polysaccharides, lignin, and other plant compounds. These dietary fibres have beneficial physiological effects such as lowering blood glucose and blood cholesterol levels, assisting bowel movements and defecation (*Jones*, 2000).

The National Academies' Institute of Medicine's Food and Nutrition Board recently issued a definition of dietary fibre that includes RS. The same definition is being worked on by the Codex Alimentarius Commission. In the UK, the definition of dietary fibre is based on the method developed by *Englyst et al.* (1992); it does not include RS (*EFSA*, 2017) and applies only to non-starch polysaccharides and lignin. Manufacturers use the method developed by the Association of Official Analytical Chemists (AOAC) to measure dietary fibre, so food tables used in practice for nutritional purposes for all foods in the UK continue to include data according to the *Englyst* principle.

When RS is found naturally in food, it is classified as dietary fibre. If it is produced artificially, such as through physical, enzymatic, or chemical means, it must give physiological benefits to be deemed dietary fibre (*Dai & Chau*, 2017).

3. Physiological effects of resistant starch

A number of physiological effects are attributed to RS and are listed in *Table 2*.

Table 2. Physiological effects of resistant starch

Possible physiological effects	Circumstances in which they are required
Improves glycaemic and insulin responses	Diabetes, decreased glucose and insulin response, metabolic syndrome
Normalization of intestinal function	Colorectal cancer, ulcerative colitis, inflammatory bowel disease, colonic abscess, constipation
Better lipid profile	Cardiovascular disease, lipid metabolism, metabolic syndrome
Prebiotics and intestinal flora protective components	Colon dysfunction
Increased feeling of satiety and decreased energy intake	Obesity
Increased micronutrient absorption	Increased mineral absorption, osteoporosis
Oral rehydration therapies	Cholera treatment, chronic diarrhoea
Synergistic interactions with other dietary components, e.g. dietary fibre, protein, lipids	Improved metabolic control and increased intestinal health
Thermogenesis (heat generation)	Obesity, diabetes

Source: *Brown*, 2004; *Champ*, 2004; *Bindels et al.,* 2017; *Snelson et al.*, 2019; *Tian & Sun*, 2020

As it passes through the small intestine, RS interacts weakly with digestive enzymes in the upper gastrointestinal tract and ferments strongly in the colon to produce fermentation products such as carbon dioxide, methane, hydrogen, and organic acids (lactic acid and SCFAs). However, it is believed that RS results in little gas production compared to other indigestible polysaccharides (fructooligosaccharides, lactulose) (*Christl et al.*, 1992). Fermentation products, such as butyric acid, acetic acid, and propionic acid, are thought to contribute to the exertion of the physiological effects of RS (*Topping et al.*, 2003).

Dietary fibre is divided into two types: insoluble and soluble. Insoluble fibre resists fermentation, but soluble fibre is easily digested by gut bacteria (*Singh et al.*, 2018). The consumption of soluble fibre may be beneficial in cardiovascular diseases as it affects both lipid and glucose metabolism. RS shares certain characteristics with soluble fibre in that it is poorly digested in the small intestine and highly digested and metabolized (fermented) in the large intestine, which releases SCFA. However, unlike soluble fibre, the RS fraction is not viscous in the

large intestine, can be easily incorporated into most starchy foods in the diet, and is considered much more palatable (*Demigne et al.*, 2001).

Other beneficial physiological effects of RS have also been demonstrated in studies on rats, showing an effect on lipid metabolism, where a large reduction of fat in the body was observed. In these studies, reductions in plasma cholesterol levels of 22–32% and plasma triglyceride levels of 29–42% were observed. According to *Younes et al.* (1995), RS has been shown to be effective in lowering plasma cholesterol and triglyceride levels with cholestyramine (a bile acid sequestering agent). In genetically obese lean (*Mathé et al.*, 1993) and diabetic rats, RS has been demonstrated to be beneficial in decreasing plasma cholesterol levels (*Kim et al.*, 2003).

4. Analytical methods for the measurement of resistant starch

The methods are based on the principle of enzymatic digestion and indicate the amount of starch resistant to enzymatic digestion at 37 °C. The first step in any method for measuring the resistant starch content of food is to remove all digestible starch from the product using thermostable α-amylases (*McCleary & Rossiter*, 2004).

In the United States, Japan, and Australia, the AOAC method 985.29 is used for the determination of Total Dietary Fibre (TDF) in food (*Prosky et al.*, 1985). After an enzymatic treatment that mimics human digestion, the amount of dietary fibre is determined gravimetrically. The method is generally used to measure total digestible dietary fibre (*Devries*, 2004). This method measures only some forms of RS (RS3, the retrograded portion, and RS2, found in high amylose corn) that appear as part of the total fibre. Therefore, additional methods are needed to quantify other forms of RS (*Champ et al.*, 2003b).

After extensive interlaboratory evaluation, AOAC methods 2009.01 and 2011.25 and AACCI methods 32-45.01 and 32-50.01 were adopted as AOAC methods 2009.01 and 2011.25 and AACCI methods 32-45.01 and 32-50.01, respectively, for measuring dietary fibre that is generally consistent with the Codex definition (*McCleary et al.*, 2010). Following that, various flaws were discovered in the procedure, the most notable of which was the use of a 16-hour incubation period, which was correctly deemed physiologically irrelevant. To preserve consistency with the Official Method for measuring resistant starch, an incubation time of 16 hours was adopted in the development of AOAC methods 2009.01 and 2011.25. (AOAC Method 2002.01; AOAC, 2012). Application of the method to different food samples and individual food ingredients revealed certain limitations. One

weakness of the method was that the incubation time with the pancreatic-α-amylase/amyloglucosidase (PAA/AMG) mixture was 16 hours, whereas the transit time to the human small intestine was probably only about 4 hours. In response to this limitation, to address it, the integrated Total Dietary Fibre (TDF) method was modified by reducing the PAA/AMG incubation time from 16 to 4 hours and increasing the enzyme concentrations accordingly, ensuring that the resistant starch values obtained for a variety of reference materials were consistent with those obtained using AOAC methods 2002.02 (*McCleary et al.*, 2002) and 2009.01 and ileostomy data (*Champ et al.*, 1999). This update (*McCleary et al.*, 2015) successfully underwent interlaboratory evaluation under the auspices of AOAC International and ICC to become AOAC Method 2017.16 and ICC Method 185 (*McCleary et al.*, 2018). The method is directly applicable to various foods and food ingredients and is significantly faster than the previously used method (*McCleary et al.*, 2015). The developed method for resistant starch is an update of current procedures and incorporates incubation conditions with pancreatic α-amylase and amyloglucosidase (AMG) equivalent to those used in AOAC Method 2017.16 for total dietary fibre (*McCleary et al.*, 2019).

5. The nutritional value of resistant starch

Under experimental conditions, the energy value of RS is about 8 kJ/g (2 kcal/g). This is significantly lower than that of fully digestible starch, which is 15 kJ/g (4.2 kcal/g) (*Liversey*, 1994). Rapidly digestible starch leads to a rapid increase in blood glucose and insulin concentrations (*Englyst et al.*, 1999), while slowly digestible starch leads to moderate glycaemic responses. The same results were observed in pigs (*Van Der Meulen et al.*, 1997a; *Noah et al.*, 2000). It was found that within 4 hrs of a meal, blood glucose and insulin levels were higher in pigs consuming a rapidly digestible starch-containing diet than in diets containing corn starch and RS (*Van Der Meulen et al.*, 1997b; *Noah et al.*, 2000).

6. Short-chain fatty acids and resistant starch

Short-chain fatty acids (SCFAs) are metabolites of anaerobic bacterial fermentation and are formed during the degradation of polysaccharides, oligosaccharides, proteins, peptides, and glycoproteins in the colon. Substrates include those derived from dietary fibre and RS (*Andoh et al.*, 2003). The major SCFAs are butyric acid, propionic acid, and acetic acid although other SCFAs are also produced in smaller amounts (*Macfarlane & Macfarlane*, 2003). SCFA is a nutrient for intestinal epithelial cells in the colon, increasing blood flow, lowering pH, and helping to

prevent the development of abnormal colon cell populations (*Topping & Clifton*, 2001). SCFAs are mainly found in the proximal colon, where fermentation intensity is the highest and their amount depends on the carbohydrate content of the diet (*Topping et al.*, 2003). The concentrations of SCFAs decrease as they pass through the colon due to absorption and utilization by colonocytes and bacteria. Any diet, any nutrient that increases the amount of SCFAs in the colon is beneficial to colon health, wherefore SCFAs are commonly used as markers of fermentation and colon health. The time spent in the colon and the composition of the diet have the greatest impact on the concentration and composition of SCFAs in the colon. Longer transit time increases the concentration of protein-derived SCFAs due to protein breakdown (*Macfarlane & Macfarlane*, 2003), while dietary fibre and the content of RS can alter the amount of SCFAs in the colon and stool (*Bird et al.*, 2000).

Butyric acid has been observed to inhibit inflammation directly by affecting the central regulation of many immune and inflammatory responses (*Segain*, 2000).

Resistant starch can increase SCFA production and thus improve intestinal function. Animal studies in pigs and rats showed that feeding RS increased total SCFAs and the concentrations of propionic acid, butyric acid, and acetic acid (*Ferguson et al.*, 2000; *Henningsson et al.*, 2003).

Following dietary supplementation with RS, most human research found increased faecal excretion and/or higher faecal concentrations (*Phillips et al.*, 1995; *Silvester et al.*, 1995; *Cummings et al.*, 1996; *Birkett et al.*, 2000; *Muir et al.*, 2004). Experiments show that RS2 (from raw potato starch) increases butyric acid concentration in humans and rats (*Cummings et al.*, 1996; *Ferguson et al.*, 2000; *Martin et al.*, 2000; *Henningsson et al.*, 2003), while the presence of RS3 (retrograded starch) increases the concentration of acetic acid in pigs (*Martin et al.*, 2000) but has no effect on the human body (*Cummings et al.*, 1996). It has also been observed that the composition of SCFAs changes only when microbes are given sufficient time to adapt during RS feeding (*Topping & Clifton*, 2001).

SCFAs stimulate the production of mucus as well as the pace of blood flow. They also provide acetyl-CoA, which is necessary for lipid biosynthesis and cell membrane formation as well as maintaining mucosal integrity. SCFAs appear to be important mediators of the positive effects of the intestinal microbiota, according to research. SCFAs also have a direct and indirect impact on risk factors for cardiovascular diseases through a range of tissue-specific pathways linked to intestinal barrier function, glucose homeostasis, immunological modulation, appetite regulation, and obesity (*Chambers et al.*, 2018).

7. Functions of resistant starch and colon

The role of starch, and colon cancer

Several studies examined the potential benefits of dietary fibre and starch in the fight against colon cancer, but there is little information on the effect of RS. Results suggest that RS enhances the beneficial effects of fibre on colorectal tumours. A large study in Europe found that in populations where fibre intake had doubled, the risk of colorectal cancer was reduced by up to 40% (*Bingham et al.*, 2003). *Cassidy et al.* (1994) found a strong negative association between starch intake and colorectal cancer in an international comparative study. Non-starch polysaccharides showed a significant positive correlation only in combination with starch. The authors hypothesized that 5% of starch is resistant and this RS contributes to its protective effect. This actually means that a significant amount of RS reaches the colon, as starch enters the digestive tract in amounts 8–10 times higher than non-starch polysaccharides (*Cassidy et al.*, 1994).

Through the creation of metabolites such as butyrate, a combination of living microbes and prebiotics has been proven to have cancer-preventive properties. Butyrate is produced when galacto-oligosaccharides are fermented (*Ambalam et al.*, 2016; *Thilakarathna et al.*, 2018), which inhibits metastasis and promotes death in colon cells. It is also known to increase the expression of enzymes involved in carcinogen inhibition (*Fernández et al.*, 2018). The clinical studies have shown the potential of synbiotics in reducing the proliferation rate, inflammatory state, and the use of antibiotics to prevent the occurrence of cancer (*Polakowski et al.*, 2019).

Resistant starch and colon functions

In animals and humans, the effect of RS on colon function has been studied. These studies focused on two main areas: the outcome of colorectal neoplasia and markers of bowel function, and colorectal cancer. Measurable features of colorectal neoplasia include tumour formation, tumour size and incidence of new diseases, cell proliferation, DNA adduct formation, presence of abnormal cryptocytes, and apoptosis. Maintenance of epithelial mass is important for the regulation of normal colon function and hyperproliferation (cellular overgrowth), which may increase the risk of developing colon cancer. Epithelial cell proliferative activity is considered an intermediate risk indicator for colorectal tumours (*Van Gorkom et al.*, 2002), but the exact utility of RS for colonic cell function is unclear, and results are often difficult to interpret. Other measurable markers of colorectal tumorigenesis and colonic function include production of SCFAs, particularly butyric acid, faecal pH, ammonia and phenol concentrations, faecal mass and

yield, secondary bile acid excretion, faecal water volume, transit time, and activity of bacterial enzymes and microbial populations.

Increased SCFA production generally improved colonic function due to decreases in pH, ammonia and phenol production and secondary bile acid excretion, decreases in faecal water volume and transit time, and changes in bacterial activity. Low pH is expected to lower primary and secondary bile acid conversion rates as well as their carcinogenic effects. Low pH paired with high SCFA concentrations is thought to inhibit pH-sensitive pathogenic bacteria from overgrowing (*Topping & Clifton*, 2001). Phenol and ammonia are products of protein fermentation, and their reduced concentrations suggest that RS reduces protein degradation in the colon and possibly shortens transit time (retention time). The inhibition of certain bacterial enzymes (e.g. β-glucuronidase) may reduce the formation of toxic and carcinogenic metabolites from food and endogenous compounds (*Young & Le Leu*, 2004; *Yang et al.*, 2017).

The effects of resistant starch on colon function in animal studies

Animal studies thus suggest that RS has a protective effect on colon function, increases SCFA concentration, and lowers pH. The results are less clear in terms of tumour formation, size, cell proliferation, and DNA damage. The different results may be partly due to the animal models and the carcinogens used, but the results may also have been influenced by different types of RS (mainly RS2 or RS3) or even different diets. The effect of RS on colon function and colon cancer development in animals has been studied in pigs, mice, and rats, using previously experimentally induced colon cancer (mostly using dimethylhydrazine, azoxymethane) or colitis (dextran sodium sulphate) and genetic models of colon cancer. Rats and mice are more commonly used than pigs to study gut function, but it should be kept in mind that in mice genetically susceptible to colorectal cancer, the cancerous areas are predominantly in the small intestine rather than the large intestine, but the maximal benefits of RS fermentation are in the large intestine (*Young & Le Leu*, 2004; *Shen et al.*, 2017).

Dietary RS2 effectively lowers digesta pH throughout the colon and increases lactic-acid-producing bacteria in swine faeces, which may limit the growth of opportunistic pathogens in the hindgut (*Metzler-Zebeli et al.*, 2019).

The ability of resistant starch type 2 (RS2) – a dietary fibre made entirely of glucose – to promote metabolic and systemic health has been widely explored in human trials and animal models. These studies frequently incorporate assessments of RS2-mediated changes in gut microbiome composition and function since the health-modulatory effects of RS2 and other dietary fibres are assumed to be caused by changes in the gut microbiota (*Bendiks et al.*, 2020).

Table 3 shows the effects of resistant starch on colon function in animal studies. The protective effect of RS aberrant crypt foci (ACF) was observed in two animal studies (*Thorup et al.*, 1995; *Cassand et al.*, 1997). However, according to *Young et al.* (1996), raw potato starch (RS2) containing 20% carbohydrate (14.4 g/100 g diet) increased ACF density. This effect disappeared when RS was mixed with wheat bran (*Young et al.*, 1996).

Table 3. Animal intervention studies examining the effects of resistant starch on colonic function

Animal model studied	Intervention	Measured parameter	Result
Wistar rats (azoxymethane) (*Thorup et al.*, 1995)	The carbohydrate content of the meal can be replaced by: sucrose, corn starch, or RPS (RS2, 67g/100 g)	ACF	All RPS decreases and ACF increases
Sprague-Dawley rats (*Caderni et al.*, 1996)	Sucrose, glucose, fructose, corn starch, or HYLON VII (RS2)	Cell proliferation Bladder pH SCFA concentration in the caecum	NSD Decrease Decrease
Sprague-Dawley rats (*Sakamoto et al.*, 1996)	3 or 10 g/100 g of cellulose or 3 or 10 g/100 g of RS3 (high amylose-containing, hydrolysed corn starch pancreatin)	Occurrence of the tumour SCFA and butyric acid production Stool excretion	NSD Increased Increased
Sprague-Dawley rats (*Young et al.,* 1996)	Low RS, lower diet or 14.4 g/100 g dietary RPS (RS2) or 14.4 g/100 g RPS and 14.4 g/100 g wheat bran	Occurrence of the tumour Tumour size and variety ACF Cell proliferation Stool excretion	NSD It is growing Density increase It is growing
In mini-mice (*Pierre et al.*, 1997)	RS-free diet (2% cellulose without RS) or wheat bran (18.8 g/100 g) or RS3 (high amylose containing corn starch, 18.8 g/100 g)	Occurrence of the tumour	NSD

Animal model studied	Intervention	Measured parameter	Result
Sprague-Dawley rats (*Mazière et al.*, 1998)	RS-free and trend (2% cellulose) or 15 g/100 g RS3 (high amylose corn starch)	ACF Bladder pH Stool volume and efficiency Bacterial enzyme activation	Decrease Decrease growing β-glucuronidase activity is growing
Sprague-Dawley rats (*Cassand et al.*, 1997)	Retrograded high amylose-containing corn starch (RS3)	ACF Stool excretion Stool pH SCFA	Decrease It is growing Decrease Increased total and butyric acid content
Wistar rats (*Kleessen et al.*, 1997)	RPS or retrograded potato starch (RS2) 10 g/100 g	SCFA	SCFA is growing Butyric acid is growing
Wistar rats (*Ebihara et al.*, 1998)	Potato starch or CMS	Stool excretion Appendix SCFA Appendix bile acids	It is growing Decreases the butyric CMS and increases the CMS
Fisher rats (*Silvi et al.*, 1999)	RS- and cellulose-free food (2.1%) or retrograde amylose starch (15 g/100 g)	Appendix SCFA Bacterial enzyme activation Ammonia production Cell proliferation	Butyric acid is growing Decreased β-glucuronidase activity Decrease NSD
Mini-mouse (*Williamson et al.*, 1999)	RS- and NSP-free diet or 1:1 RPS (RS2) and high amylose corn diet (RS3)	Tumour presence	It is growing
Pigs (*Bird et al.*, 2000)	Brown rice or white rice and bran	SCFA selection Mass digested in the colon	It is growing It is growing
Wistar rats (*Ferguson et al.*, 2000)	RS- and NSP-free diet, or potato starch, or high amylose corn starch, or α-amylase-treated Hi-corn (35 g/100 g)	Stool excretion SCFA Transit time	It is growing It grows, including butyric acid It is growing treated with potato starch and α-amylase Hi-maize dosing
Sprague-Dawley rats (*Le Leu et al.*, 2003)	High amylose content of corn starch	pH	Decrease

Animal model studied	Intervention	Measured parameter	Result
Sprague-Dawley rats (*Conlon & Bird,* 2003)	10 g/100 g of fish oil or sunflower oil and 10 g/100 g of dietary fibre (wheat bran or cellulose) or 10 g/100 g of RS (hybrid or NOVELOSE)	Colon DNA damage	There is less DNA damage with RS / sunflower oil than with RS / fish oil combinations
Sprague-Dawley rats (*Toden et al.*, 2005)	15 or 25 g/100 g of casein 48% Hi-maize or without	DNA damage Thinning of the mucosal layer	Decrease Decrease

Source: *Young & Le Leu* (2004) and *Nugent* (2005)

Notes: ACF, aberrant crypt foci; CMS, chemically modified starch; RS, resistant starch; RPS, raw potato starch; SCFA, short-chain fatty acid; NSD, no significant difference.

Various forms of RS (especially RS2 and RS3) continuously increase the number of defaecations and stool weight (*Cassand et al.*, 1997; *Ebihara et al.*, 1998; *Mazière et al.*, 1998; *Ferguson et al.*, 2000; *Bird et al.*, 2000), decrease faecal pH and/or appendix pH (*Caderni et al.*, 1996; *Cassand et al.*, 1997; *Mazière et al.*, 1998; *Le Leu et al.*, 2003), reduce ammonia levels (*Silvi et al.*, 1999), and have a positive effect on bacterial enzyme activity (*Mazière et al.*, 1998; *Silvi et al.*, 1999). Feeding RS had no effect on tumour incidence in four animal experiments (*Young et al.*, 1996; *Sakamoto et al.*, 1996; *Pierre et al.*, 1997; *Mazière et al.*, 1998), decreased tumour incidence in other experiments, and resulted in an increase in tumour size, with increased cell proliferation also observed (*Young et al.*, 1996; *Williamson et al.*, 1999), while *Silvi et al.* (1999) reported no such effects.

It appears that feeding RS in combination with macronutrients can directly influence outcomes. According to *Conlon & Bird* (2003), it provided protection against DNA damage in male Sprague-Dawley rats fed RS (Hi-maize or Novelose) supplemented with 10% sunflower oil and 10% fish oil. Toden et al. (2003) showed that when male Sprague-Dawley rats were fed a high protein (15 or 25% casein) and RS (48% Hi-corn) diet, the diet containing RS alleviated colonic damage and thinning of the colonic mucosa in a high-protein diet.

8. Resistant starch and the colonic microflora; prebiotics and probiotics

Prebiotics were defined by *Gibson & Roberfroid* (1995) as "growth substrates" for potentially beneficial bacteria in the colon. Prebiotics are non-digestible food components that promote the growth and/or activity of bacteria in the colon, enhancing the health of the host (*Topping et al.*, 2003). By this definition, a resistant starch is a prebiotic that promotes the growth of probiotic bacteria when co-administered with synbiotics (*Brown et al.*, 1997; *Wang et al.*, 1999). Studies in humans and pigs showed that high RS food intake causes a time-dependent shift in the SCFA profile of faecal and colonic content, suggesting a change in the original (autochthonous) microbial population, and that RS can interact with gut bacteria (*Topping et al.*, 2003). RS probably functions differently from known prebiotics (e.g. fructooligosaccharides). When co-administered with fructooligosaccharides, faecal bacteria growth was higher than when administered alone (*Brown et al.*, 1997).

RS may act as a nutrient for *Bifidobacteria* in vitro (*Wang et al.*, 1999) and may also provide protection for these bacteria in vivo as they pass through the upper gastrointestinal tract (*Wang et al.*, 1999). In vitro studies have also demonstrated that different types of RS (RS2 and RS4) can nourish the *Bifidobacterium* strain (*Brown et al.*, 1997), which protects them from the physical effects of food preparation and storage (*Brown et al.*, 1997) and as they pass through the gastrointestinal tract (*Wang et al.*, 1999). Because of these protective effects, RS can be considered an adjuvant of intestinal flora (*Conway*, 2001). To exploit this effect, RS was combined with *Bifidobacteria* in yogurt (*Crittenden et al.*, 2001). RS may provide physical protection and slow down the rate of bacterial excretion as long as they are consumed. RS in combination with fructooligosaccharides was not observed to reduce the local number of bacteria (*Brown et al.*, 1997). Therefore, *Topping et al.* (2003) concluded that probiotics should not be consumed as frequently in combination with foods rich in RS or fructooligosaccharides.

Because of these prebiotic effects, RS also appears to exert other health-promoting effects in the intestinal tract. In the context of hydration therapy with RS, it has been observed to reduce fluid loss and halve recovery time when fed to people with cholera-induced diarrhoea, for example (*Ramakrishna et al.*, 2000). Similar effects were observed after feeding green bananas following diarrhoeal illness in children (*Rabbani et al.*, 2001).

It is believed that the use of RS has a greater benefit by improving fluid absorption due to higher SCFA production (*Topping et al.*, 2003). SCFA stimulates the absorption of water and cations (sodium, potassium, and calcium) in the proximal colon and may directly reduce the severity of diarrhoea by increasing muscle activity and stimulating blood flow in the colon. The beneficial effect may

be triggered by the fact that RS impairs the viability of cholera bacteria in the intestine as these microbes, such as *Bifidobacteria*, can adhere to RS and thus be excreted in the faeces (*Topping et al.*, 2003).

9. Resistant starch and glucose metabolism

The hormone insulin regulates the uptake of glucose into muscle and fat cells, thereby lowering blood glucose levels. It inhibits the breakdown of body fat and can affect appetite and satiety. Glucose is released slowly from foods rich in RS, reducing the insulin response, aiding the breakdown of fat deposits, and satisfying hunger. These effects may help with metabolic diseases such as treating diabetes and decreased glucose tolerance, but probably also obesity. Several studies have been conducted on the effects of various forms and doses of RS on glucose concentration and insulin response, but a consensus on the exact effects of RS is still pending. In diabetic patients, improvement after consumption of a diet rich in RS was reported in 15 cases, while in 10 cases there was no effect, or the effect was physiologically irrelevant. On a positive note, however, no RS-induced adverse insulinaemia and glycaemic response has been reported to date. In general, beneficial effects occurred within a short period of time, after the first 2–8 hrs of ingestion, following consumption of foods high in RS (*Higgins et al.*, 1996).

Consumption of RS appears to reduce postprandial glycaemia only slightly, but is associated with a significant reduction in postprandial insulinaemia. It has been concluded that the proportion of RS should be at least 14% to show a beneficial effect on glycaemic or insulin response (*Higgins et al.*, 1996; *Behall & Hallfrish*, 2002; *Brown et al.*, 2003).

Intravenous glucose tolerance studies on rats have shown that digestible starch causes insulin resistance during 16 weeks of feeding, whereas feeding RS caused no such problems (*Higgins et al.*, 1996; *Byrnes et al.*, 1995; *Wiseman et al.*, 1996; *Snelson et al.*, 2019).

10. Conclusions

RS-related studies have been conducted on healthy animals (mainly on animal models such as pigs). The use of RS as a dietary ingredient may have beneficial effects on digestive system function by shortening the transit time of food in the colon and increasing the volume of stool. It has a positive effect on the bacterial activity of the colon by promoting the proliferation of beneficial microbes and reducing the activity of certain enzymes (β-glucuronidase).

RS has an indirect effect through SCFAs, which are important in maintaining colon function by regulating colonocyte gene expression, cell cycle, and apoptosis. Increased SCFA production lowers colon pH and stimulates bile acid secretion. Because secondary bile acids are cytotoxic to colon cells, the lower pH protects against colon cancer and slows the conversion of primary and secondary bile acids. SCFA acetates inhibit the breakdown of cholesterol and may reduce the bioavailability of free fatty acids because high concentrations of free fatty acids are harmful to the body since they reduce insulin activity.

Starchy foods significantly affect metabolism, blood glucose levels, and insulin response. Resistant starch, digestion-resistant starch, and starchy foods have several health benefits for gut function but appear to have less effect on lipid-glucose metabolism. Further studies are needed to understand the responses of RS to insulin and glucose in pigs. Most of the effects of RS are mediated by SCFAs, but the use of RS as a prebiotic has also become a focus of interest.

References

[1] Ambalam, P., Raman, M., Purama, R. K., Doble, M., Probiotics, prebiotics and colorectal cancer prevention. *Best Practice & Research: Clinical Gastroenterology*, 30. 1. (2016) 119–131.

[2] Andoh, A., Tsujikawa, T., Fujiyama, Y., Role of dietary fiber and short-chain fatty acids in the colon. *Current Pharmaceutical Design*, 9. 4. (2003) 347–358.

[3] Asp, N. G., Nutritional classification and analysis of food carbohydrates. *The American Journal of Clinical Nutrition*, 59. 3. (1994) 679–681.

[4 Asp, N. G., Van Amelsvoort, J. M. M., Hautvast, J. G. A. J., Nutritional implications of resistant starch. *Nutrition Research Reviews*, 9. (1996) 1–31.

[5] Behall, K. M., Hallfrisch, J., Plasma glucose and insulin reduction after consumption of breads varying in amylose content. *European Journal of Clinical Nutrition*, 56. (2002) 913–920.

[6] Bendiks, Z. A., Knudsen, K. E. B., Keenan, M. J., Marco, M. L., Conserved and variable responses of the gut microbiome to resistant starch type 2. *Nutrition Research (New York, N.Y.)*, 77. (2020) 12–28.

[7] Bindels, L. B. et al., Resistant starch can improve insulin sensitivity independently of the gut microbiota. *Microbiome*, 5. 12. (2017).

[8] Bingham, S. A., Day, N. E., Luben, R., Ferrari, P., Slimani, N., Norat, T., Riboli, E., Dietary fibre in food and protection against colorectal cancer in the European prospective investigation into cancer and nutrition (EPIC): An observational study. *The Lancet (British Edition)*, 361. (2003) 1496–1501.

[9] Bird, A. R., Brown, I. L., Topping, D. L., Starches, resistant starches, the gut microflora and human health. *Current Issues in Intestinal Microbiology*, 1. (2000) 25–37.

[10] Bird, A. R., Vuaran, M., Brown, I., Topping, D. L., Two high-amylose maize starches with different amounts of resistant starch vary in their effects on fermentation, tissue and digesta mass accretion, and bacterial populations in the large bowel of pigs. *British Journal of Nutrition*, 97. (2007) 134–144.

[11] Birkett, A. M., Mathers, J. C., Jones, G. P., Walker, K. Z., Roth, M. J., Muir, J. G., Changes to the quantity and processing of starchy foods in a Western diet can increase polysaccharides escaping digestion and improve in vitro fermentation variables. *British Journal of Nutrition*, 84. (2000) 63–72.

[12] Birt, D. F., Boylston, T., Hendrich, S., Jane, J., Hollis, J., Li, L., Whitley, E. M., Resistant starch: Promise for improving human health. *Advances in Nutrition (Bethesda, Md.)*, 4. (2013) 587–601.

[13] Brown, I., Complex carbohydrates and resistant starch. *Nutrition Reviews*, 54. 11. (1996) 115–119.

[14] Brown, I., Applications and uses of resistant starch. *Journal of AOAC International*, 87. (2004) 727–732.

[15] Brown, I., McNaught, K. J., Moloney, E., Hi-maize™: New directions in starch technology and nutrition. *Food Australia*, 47. (1995) 272–275.

[16] Brown, I., Warhurst, M., Arcot, J., Playne, M., Illman, R. J., Topping, D. L., Fecal numbers of *Bifidobacteria* are higher in pigs fed *Bifidobacterium longum* with a high amylose cornstarch than with a low amylose cornstarch. *The Journal of Nutrition*, 127. (1997) 1822–1827.

[17] Brown, M. A., Storlien, L. H., Brown, I. L., Higgins, J. A., Cooking attenuates the ability of high-amylose meals to reduce plasma insulin concentrations in rats. *British Journal of Nutrition*, 90. (2003) 823–827.

[18] Byrnes, S. E., Miller, J. C., Denyer, G. S., Amylopectin starch promotes the development of insulin resistance in rats. *The Journal of Nutrition*, 125. (1995) 1430–1437.

[19] Caderni, G., Luceri, C., Lancioni, L., Dolara, P., Dietary sucrose, glucose, fructose, and starches affect colonic functions in rats. *Nutrition and Cancer*, 25. (1996) 179–186.

[20] Cassand, P., Maziere, S., Champ, M., Meflah, K., Bornet, F., Narbonne, J., Effects of resistant starch- and vitamin A-supplemented diets on the promotion of precursor lesions of colon cancer in rats. *Nutrition and Cancer*, 27. (1997) 53–59.

[21] Cassidy, A., Bingham, S. A., Cummings, J. H., Starch intake and colorectal cancer risk: An international comparison. *British Journal of Cancer*, 69. (1994) 937–942.

[22] Chambers, E. S., Preston, T., Frost, G., Morrison, D. J., Role of gut microbiota-generated short-chain fatty acids in metabolic and cardiovascular health. *Current Nutrition Reports*, 7. 4. (2018) 198–206.

[23] Champ, M. M., Physiological aspects of resistant starch and in vivo measurements. *Journal of AOAC International*, 87. (2004) 749–755.

[24] Champ, M., Langkilde, A., Brouns, F., Kettlitz, B., Le Bail Collet, Y., Advances in dietary fibre characterisation. 1. Definition of dietary fibre, physiological relevance, health benefits and analytical aspects. *Nutrition Research Reviews*, 16. (2003a) 71–82.

[25] Champ, M., Langkilde, A., Brouns, F., Kettlitz, B., Le Bail Collet, Y., Advances in dietary fibre characterisation. 2. Consumption, chemistry, physiology and measurement of resistant starch; implications for health and food labelling. *Nutrition Research Reviews*, 16. (2003b) 143–161.

[26] Champ, M., Martin, L., Noah, L., Gratas, M., Analytical methods for resistant starch. In: *Complex Carbohydrates in Foods*, (1999) 169–187.

[27] Christl, S., Murgatroyd, P., Gibson, G., Cummings, J., Production, metabolism, and excretion of hydrogen in the large intestine. *Gastroenterology (New York, N.Y. 1943)*, 102. (1992) 1269–1277.

[28] Conlon, M. A., Bird, A. R., Interactions of dietary fibre and resistant starch with oil on genetic damage in the rat colon. *Asia Pacific Journal of Clinical Nutrition*, 12. (2003) S54.

[29] Conway, P. L., Prebiotics and human health: The state-of-the-art and future perspectives. *Naringsforskning*, 45. (2001) 13–21.

[30] Crittenden, R. G., Morris, L. F., Harvey, M. L., Tran, L. T., Mitchell, H. L., Playne, M. J., Selection of a *Bifidobacterium* strain to complement resistant starch in a synbiotic yoghurt. *Journal of Applied Microbiology*, 90. (2001) 268–278.

[31] Cummings, J. H., Beatty, E. R., Kingman, S. M., Bingham, S. A., Englyst, H. N., Digestion and physiological properties of resistant starch in the human large bowel. *British Journal of Nutrition*, 75. (1996) 733–747.

[32] Dai, F., Chau, C., Classification and regulatory perspectives of dietary fiber. *Journal of Food and Drog Analysis*, 25. 1. (2017) 37–42.

[33] Demigne, C., Remesy, C., Morand, C., Resistant starches and lipid metabolism. *Journal of Food Science and Technology*, 17. (2001) 159–168.

[34] Devries, J. W., Dietary fiber: The influence of definition on analysis and regulation. *Journal of AOAC International*, 87. (2004) 682–706.

[35] Ebihara, K., Shiraishi, R., Okuma, K., Hydroxypropyl-modified potato starch increases fecal bile acid excretion in rats. *The Journal of Nutrition*, 128. (1998) 848–854.

[36] Eerlingen, R. C., Delcour, J. A., Formation, analysis, structure and properties of type III enzyme resistant starch. *Journal of Cereal Science*, 22. (1995) 129–138.

[37] EFSA. *Overview of nutritional benchmarks. The values of the EU population, as described in the European Food Safety Authority (EFSA) on dietary products, nutrition and allergies (NDA).* (2017).

[38] Ellis, R. P., Cochrane, M. P., Dale, M. F. B., Duffus, C. M., Lynn, A., Morrison, I. M., Tiller, S. A., Starch production and industrial use. *Journal of the Science of Food and Agriculture,* 77. (1998) 289–311.

[40] Englyst, H. N., Cummings, J. H., Measurement of starch fermentation in the human large intestine. *Canadian Journal of Physiology and Pharmacology*, 69. (1991) 121–129.

[39] Englyst, K. N., Englyst, H. N., Hudson, G. J., Cole, T. J., Cummings, J. H., Rapidly available glucose in foods: An in vitro measurement that reflects the glycemic response. *The American Journal of Clinical Nutrition*, 69. (1999) 448–454.

[41] Englyst, H. N., Kingman, S. M., Cummings, J. H., Classification and measurement of nutritionally important starch fractions. *European Journal of Clinical Nutrition*, 46. (1992) 533–550.

[42] Erbersdobler, F. H., Factors affecting uptake and utilization of macro nutrients. In: Southgate, D., Johnson, I. T., Fenwick, G. R. (eds.), *Nutrient availability: Chemical and biological aspects.* Cambridge: Royal Society of Chemistry. (1989) 330–339.

[43] Ferguson, L. R., Tasman-Jones, C., Englyst, H., Harris, P. J., Comparative effects of three resistant starch preparations on transit time and short-chain fatty acid production in rats. *Nutrition and Cancer*, 36. (2000) 230–237.

[44] Fernández, J., Moreno, F. J., Olano, A., Clemente, A., Villar, C. J., Lombó, F., Galactooligosaccharides derived from lactulose protects against colorectal cancer development in an animal model. *Frontiers in Microbiology*, 9. 2004. (2018) 1–14.

[45] Fuentes-Zaragoza, E., Sánchez-Zapata, E., Sendra, E., Sayas, E., Navarro, C., Fernández-López, J., Pérez-Alvarez, J. A., Resistant starch as prebiotic: A review. *Starch – Stärke*, 63. (2011) 406–415.

[46] Gibson, G. R., Roberfroid, M. B., Dietary modulation of the human colonic microbiota: Introducing the concept of prebiotics. *Journal of Nutrition, 125*, (1995) 1401–1412.

[47] Gutiérrez, T. J., Tovar, J., Update of the concept of type 5 resistant starch (RS5): Self-assembled starch V-type complexes. *Trends in Food Science & Technology*, 109. (2021) 711–724.

[48] Haenen, D., Zhang, J., Souza Da Silva, C., Bosch, G., Meer, V. D., Arkel, V. J., Hooiveld, G. J., A diet high in resistant starch modulates microbiota composition, SCFA concentrations, and gene expression in pig intestine. *The Journal of Nutrition*, 143. (2013) 274–283.

[49] Hamer, H. M. H., Jonkers, D., Venema, K., Vanhoutvin, S., Troost, F. J., Brummer, R. J. M., Review article: The role of butyrate on colonic function. *Alimentary Pharmacology & Therapeutics*, 27. (2008) 104–119.

[50] Henningsson, Å. M., Margareta, E., Nyman, G. L., Björck, I. M. E., Influences of dietary adaptation and source of resistant starch on short-chain fatty acids in the hindgut of rats. *British Journal of Nutrition*, 89. (2003) 319–327.

[51] Higgins, J. A., Brand Miller, J. C., Gareth, A., Denver, S., Biochemical and molecular roles of nutrients. Development of insulin resistance in the rat is dependent on the rate of glucose absorption from the diet. *The Journal of Nutrition*, 126. 3. (1996) 596–602.

[52] Hosseini, E., Grootaert, C., Verstraete, W., Van de Wiele, T., Propionate as a health promoting microbial metabolite in the human gut. *Nutrition Reviews*, 69. (2011) 245–258.

[53] Jones, J., Update on defining dietary fiber. *Cereal Foods World*, 45. (2000) 219–220.

[54] Kim, W. K., Chung, M. I. K., Kang, N. E., Kim, M. H., Park, O. J., Effect of resistant starch from corn or rice on glucose control, colonic events, and blood lipid concentrations in streptozotocin-induced diabetic rats. *The Journal of Nutritional Biochemistry*, 14. (2003) 166–172.

[55] Kleessen, B., Stoof, G., Rgen Proll, J., Schmiedl, D., Noack, J., Blaut, M., Feeding resistant starch affects fecal and cecal microflora and short-chain fatty acids in rats. *Journal of Animal Science*, 75. (1997) 2453–2462.

[56] Le Leu, R. K., Brown, I. L., Hu, Y., Young, G. P., Effect of resistant starch on genotoxin-induced apoptosis, colonic epithelium, and lumenal contents in rats. *Carcinogenesis*, 24. (2003) 1347–1352.

[57] Liversey, G., Energy value of resistant starch. In: *Proceedings of the Concluding Plenary Meeting of EURESTA: Wageningen, Netherlands*. (1994) 56–62.

[58] Lockyer, S., Nugent, A. P., Health effects of resistant starch. *Nutrition Bulletin*, 42. 1. (2017) 10–41.

[59] Lunn, J., Buttriss, J. L., Carbohydrates and dietary fibre. *Nutrition Bulletin*, 32. (2007) 21–64.

[60] Macfarlane, S., Macfarlane, G. T., Regulation of short-chain fatty acid production. *Proceedings of the Nutrition Society*, 62. (2003) 67–72.

[61] Martin, L. J. M., Dumon, H. J. W., Lecannu, G., Champ, M. M. J., Potato and high-amylose maize starches are not equivalent producers of butyrate for the colonic mucosa. *British Journal of Nutrition*, 84. (2000) 689–696.

[62] Mathé, D., Riottot, M., Rostaqui, N., Sacquet, E., Navarro, N., Lécuyer, B., Lutton, C., Effect of amylomaize starch on plasma lipoproteins of lean and obese zucker rats. *Journal of Clinical Biochemistry and Nutrition*, 14. (1993) 17–24.

[63] Mazière, S., Meflah, K., Tavan, E., Champ, M., Narbonne, J., Cassand, P., Effect of resistant starch and/or fat-soluble vitamins A and E on the initiation stage of aberrant crypts in rat colon. *Nutrition and Cancer*, 31. (1998) 168–177.

[64] McCleary, B. V., An integrated procedure for the measurement of total dietary fiber (including resistant starch), non-digestible oligosaccharides and available carbohydrates. *Analytical and Bioanalytical Chemistry*, 389. (2007) 291.

[65] McCleary, B. V., Cox, J., Ivory, R., Delaney, E., Definition and analysis of dietary fiber in grain products. In: Beta, T., Camire, M. E. (eds.), *Grain-based functional foods: Carbohydrate and phytochemical components (food chemistry, function and analysis). Chapter 6. Royal Society of Chemistry*. (2018) 103–126.

[66] McCleary, B. V., DeVries, J. W., Rader, J. I., Cohen, G., Prosky, L., Mugford, D. C., Okuma, K., Determination of total dietary fiber (CODEX definition) by enzymatic-gravimetric method and liquid chromatography: Collaborative study. *Journal of AOAC International*, 93. (2010) 221–233.

[67] McCleary, B. V., McLoughlin, C., Charmier, L., McGeough, P., Measurement of available carbohydrates, digestible and resistant starch in food ingredients and products. *Cereal Chemistry*, 97. (2019) 114–137.

[68] McCleary, B. V., McNally, M., Rossiter, P., Measurement of resistant starch by enzymic digestion in starch samples and selected plant materials: Collaborative study. *Journal of AOAC International*, 2002. 85. (2002) 1103–1111.

[69] McCleary, B. V., Rossiter, P., Measurement of novel dietary fibers. *Journal of AOAC International*, 87. (2004) 707–717.

[70] McCleary, B. V., Sloane, N., Draga, A., Determination of total dietary fibre and available carbohydrates: A rapid integrated procedure that simulates in vivo digestion. *Starch – Stärke*, 67. (2015) 860–883.

[71] Metzler-Zebeli, B. U. et al., Resistant starch reduces large intestinal pH and promotes fecal lactobacilli and bifidobacteria in pigs. *Animal*, 13. 1. (2019) 64–73.

[72] Muir, J. G., Yeow, E. G. W., Keogh, J., Pizzey, C., Bird, A. R., Sharpe, K., Macrae, F. A., Combining wheat bran with resistant starch has more beneficial effects on fecal indexes than does wheat bran alone. *The American Journal of Clinical Nutrition*, 79. (2004) 1020–1028.

[73] Niba, L. L., Processing effects on susceptibility of starch to digestion in some dietary starch sources. *International Journal of Food Sciences and Nutrition*, 54. (2003) 97–109.

[74] Noah, L., Krempf, M., Lecannu, G., Maugère, P., Champ, M., Bioavailability of starch and postprandial changes in splanchnic glucose metabolism in pigs. *American Journal of Physiology – Endocrinology and Metabolism*, 278. (2000) 181–188.

[75] Nugent, A. P., Health properties of resistant starch. *Nutrition Bulletin*, 30. (2005) 27–54.

[76] Phillips, J., Muir, J. G., Birkett, A., Lu, Z. X., Jones, G. P., O'Dea, K., Young, G. P., Effect of resistant starch on fecal bulk and fermentation-dependent events in humans. *The American Journal of Clinical Nutrition*, 62. (1995) 121–130.

[77] Pierre, F., Perrin, P., Champ, M., Bornet, F., Meflah, K., Menanteau, J., Short-chain fructo-oligosaccharides reduce the occurrence of colon tumors and develop gut-associated lymphoid tissue in min mice. *Cancer Research*, 57. (1997) 225–228.

[78] Polakowski, C. B., Kato, M., Preti, V. B., Schieferdecker, M. E. M., Campos, A. C. L., Impact of the preoperative use of synbiotics in colorectal cancer patients: A prospective, randomized, doubleblind, placebo-controlled study. *Nutrition*, 58. (2019) 40–46.

[79] Prosky, L., Asp, N. G., Furda, I., DeVries, J. W., Schweizer, T. F., Harland, B. F., Determination of total dietary fiber in foods and food products: Collaborative study. *Journal – Association of AOAC International*, 68. (1985) 677–679.

[80] Rabbani, G. H., Teka, T., Zaman, B., Majid, N., Khatun, M., Fuchs, G. J., Clinical studies in persistent diarrhea: Dietary management with green banana or pectin in Bangladeshi children. *Gastroenterology (New York, N.Y. 1943)*, 121. (2001) 554–560.

[81] Ramakrishna, B. S., Venkataraman, S., Srinivasan, P., Dash, P., Young, G. P., Binder, H. J., Amylase-resistant starch plus oral rehydration solution for cholera. *New England Journal of Medicine*, 342. 5. (2000) 308–313.

[82] Rosado, J. L., Morales, M., Allen, L. H., Energy and macronutrient bioavailability from rural and urban Mexican diets. In: Southgate, D., Johnson, I., Fenwick, G. R., (eds.), *Nutrient availability: Chemical and biological aspects.* Cambridge: Royal Society of Chemistry. (1987) 327–329.

[83] Roy, C. C., Kien, C. L., Bouthillier, L., Levy, E., Short-chain fatty acids: Ready for prime time? *Nutrition in Clinical Practice*, 21. (2006) 351–366.

[84] Sajilata, M. G., Singhal, R. S., Kulkarni, P. R., Resistant starch – A review. *Comprehensive Reviews in Food Science and Food Safety*, 5. (2006) 1–17.

[85] Sakamoto, J., Nakaji, S., Sugawara, K., Iwane, S., Munakata, A., Comparison of resistant starch with cellulose diet on 1,2-dimethylhydrazine-induced colonic carcinogenesis in rats. *Gastroenterology*, 110. (1996) 116–120.

[86] Segain, J., Butyrate inhibits inflammatory responses through NF kappa B inhibition: Implications for Crohn's disease. *Gut*, 47. (2000) 397–403.

[87] Sharma, A., Yadav, B. S., Ritika, Resistant starch: Physiological roles and food applications. *Food Reviews International*, 24. (2008) 193–234.

[88] Shen, D., Bai, H., Li, Z., Yu, Y., Zhang, H., Chen, L., Positive effects of resistant starch supplementation on bowel function in healthy adults: A systematic review and meta-analysis of randomized controlled trials. *International Journal of Food Sciences and Nutrition*, 68. 2. (2017) 149–157.

[89] Silvester, K. R., Englyst, H. N., Cummings, J. H., Ileal recovery of starch from whole diets containing resistant starch measured in vitro and fermentation of ileal effluent. *American Journal of Nutrition*, 62. (1995) 403–411.

[90] Silvi, S., Rumney, C. J., Cresci, A., Rowland, I. R., Resistant starch modifies gut microflora and microbial metabolism in human flora associated rats inoculated with faeces from Italian and UK donors. *Journal of Applied Microbiology*, 86. (1999) 521–530.

[91] Singh, V. et al., Dysregulated microbial fermentation of soluble fiber induces cholestatic liver cancer. *Cell*, 175. 3. (2018) 679–694.

[92] Sleeth, M. L., Thompson, E. L., Ford, H. E., Zac-Varghese, S. E. K., Frost, G., Free fatty acid receptor 2 and nutrient sensing: A proposed role for fibre, fermentable carbohydrates and short-chain fatty acids in appetite regulation. *Nutrition Research Reviews*, 23. (2010) 135–145.

[93] Snelson, M., Jong, J., Manolas, D., Kok, S., Louise, A., Stern, R., Kellow, N. J., Metabolic effects of resistant starch type 2: A systematic literature review and meta-analysis of randomized controlled trials. *Nutrients*, 11. 8. (2019) 1833.

[94] Southgate, D. A. T., Conceptual issues concerning the assessment of nutrient bioavailability. In: Southgate, D. A. T. (ed.), *Nutrient availability: Chemical and biological aspect*. Cambridge: Royal Society of Chemistry. (1989) 10–12.

[95] Thilakarathna, W. W., Langille, M. G., Rupasinghe, H. V., Polyphenol-based prebiotics and synbiotics: Potential for cancer chemoprevention. *Current Opinion in Food Science*, 20. (2018) 51–57.

[96] Thorup, I., Meyer, O., Kristiansen, E., Effect of potato starch, corn starch and sucrose on aberrant crypt foci in rats exposed to azoxymethane. *Anticancer Research*, 15. (1995) 2101–2105.

[97] Tian, S., Sun, Y., Influencing factor of resistant starch formation and application in cereal products: A review. *International Journal of Biological Macromolecules*, 149. (2020) 424–431.

[98] Toden, S., Bird, A. R., Topping, D. L., Conlon, M. A., Resistant starch attenuates colonic DNA damage induced by higher dietary protein in rats. *Nutrition and Cancer*, 51. (2005) 45–51.

[99] Topping, D. L., Clifton, P. M., Short-chain fatty acids and human colonic function: Roles of resistant starch and nonstarch polysaccharides. *Physiological Reviews*, 81. (2001) 1031–1064.

[100] Topping, D. L., Fukushima, M., Bird, A. R., Resistant starch as a prebiotic and synbiotic: State of the art. *Proceedings of the Nutrition Society*, 62. 1. (2003) 171–176.

[101] Van Der Meulen, J., Bakker, J. G. M., Smits, B., De Visser, H., Effect of source of starch on net portal flux of glucose, lactate, volatile fatty acids and amino acids in the pig. *British Journal of Nutrition*, 78. (1997a) 533–544.

[102] Van Der Meulen, J., Bakker, J. G. M., Smits, B., De Visser, H., Effect of resistant starch on net portal-drained viscera flux of glucose, volatile fatty acids, urea, and ammonia in growing pigs. *Journal of Animal Science*, 75. (1997b) 2697–2704.

[103] Van Gorkom, B. A. P, Karrenbeld, A., Van der Sluis, T., Zwart, N., Van der Meer, R., De Vries, E. G. E, Kleibeuker, J. H., Calcium or resistant starch does not affect colonic epithelial cell proliferation throughout the colon in adenoma patients: A randomized controlled trial. *Nutrition and Cancer*, 43. (2002) 31–38.

[104] Wang, X., Conway, P. L., Brown, I. L., Evans, A. J., In vitro utilization of amylopectin and high-amylose maize (amylomaize) starch granules by human colonic bacteria. *Applied and Environmental Microbiology*, 65. (1999) 4848–4854.

[105] Williamson, S. L. H., Kartheuser, A., Coaker, J., Kooshkghazi, M. D., Fodde, R., Burn, J., Mathers, J. C., Intestinal tumorigenesis in the Apc1638N mouse treated with aspirin and resistant starch for up to 5 months. *Carcinogenesis (New York)*, 20. (1999) 805–810.

[106] Wiseman, C. E., Higgins, J. A., Denyer, G. S., Brand, J. C., Biochemical and molecular roles of nutrients: Amylopectin starch induces nonreversible insulin resistance in Rats. *Journal of Nutrition*, 126. 2. (1996) 410–415.

[107] Yang, X., Darko, K. O., Huang, Y., He, C., Yang, H., He, S., Li, J., Hocher, B., Yin, Y., Resistant starch regulates gut microbiota: Structure, biochemistry and cell signalling. *Cellular Physiology and Biochemistry*, 42. (2017) 306–312.

[108] Younes, H., Levrat, M. A., Demigné, C., Rémésy, C., Resistant starch is more effective than cholestyramine as a lipid-lowering agent in the rat. *Lipids*, 30. 9. (1995) 847–853.

[109] Young, G., McIntyre, A., Albert, V., Folino, M., Muir, J., Gibson, P., Wheat bran suppresses potato starch-potentiated colorectal tumorigenesis at the aberrant crypt stage in a rat model. *Gastroenterology*, 110. (1996) 508–514.

[110] Young, G. P., Le Leu, R. K., Resistant starch and colorectal neoplasia. *Journal of AOAC International*, 87. (2004) 775–786.

[111] Zhao, X., Andersson, M., Andersson, R., Resistant starch and other dietary fiber components in tubers from a high-amylose potato. *Food Chemistry*, 251. (2018) 58–63.

Acta Univ. Sapientiae, Alimentaria, **14** (2021) 84–94

DOI: 10.2478/ausal-2021-0005

Influence of milk used for cheese making on microbiological aspects of Camembert-type cheese

É. György
e-mail: gyorgyeva@uni.sapientia.ro

É. Laslo
e-mail: lasloeva@uni.sapientia.ro

I. Onodi
e-mail: onodiizabella@uni.sapientia.ro

Sapientia Hungarian University of Transylvania, Cluj-Napoca,
Faculty of Economics, Socio-Human Sciences and Engineering,
Department of Food Science, RO-530104 Miercurea Ciuc, 1 Libertății Sq.

Abstract. Camembert-type cheeses are surface mould-ripened soft cheeses obtained with *Penicillium camemberti*. Soft cheeses are more frequently associated with foodborne disease outbreaks than hard and semi-hard cheeses. During our work, three Camembert-type cheeses were prepared on a pilot/small industrial scale. The first cheese was made from bulk milk and pasteurized at 74 °C for 15 seconds. The second and third cheese were prepared from one type of milk and were heat-treated at 72 °C for 60 seconds. The microbial contamination with *Salmonella* spp. and *Staphylococcus aureus* of the three Camembert-type cheeses was evaluated. The food-related stress survival of *Salmonella* spp. and *S. aureus* isolates originated from the cheese samples was assayed. The antibiotic susceptibility of the bacterial isolates was determined by the disk diffusion method, using 12 and 16 different antibiotics respectively. Based on the results, the first cheese sample contained the highest number of *Salmonella* bacteria; *S. aureus* was detected only in the first sample. According to the results of antibiotic susceptibility of the *Salmonella*, isolates showed susceptibility to the majority of assayed antibiotics and resistance to trimethoprim, chloramphenicol, amikacin, and cefotaxime. The *S. aureus* isolates showed resistance to trimethoprim and displayed intermediate resistance to levofloxacin and ciprofloxacin.

Keywords and phrases: Camembert-type cheese, *Salmonella* spp., *Staphylococcus aureus*, food-related stress, antibiotic resistance

1. Introduction

Cheese, being a dairy product, is an integral part of human diet with its high micro- and macronutrient content and is a good source of proteins, vitamins, fat, fatty acids, and lactose. Due to the rich calcium content, it contributes to skeleton and teeth integrity (*Hamdaoui et al.*, 2021). Globally, 35% of produced raw milk

is transformed into cheese, which is equal approx. to 19×10^6 tons per year, representing a large part of the food industry (*Fox et al.*, 2017).

The Camembert-type cheese belongs to the soft surface-ripened group of cheeses, originated from the Normandy region of France from the 18th century. This speciality of cheese is manufactured all over the world. Traditionally, this type of cheese is made using raw cows' milk, obtaining a product of approximately 10 cm in diameter, having 200–250 g weight. The industrial process uses pasteurized milk (*Fox et al.*, 2017).

Soft ripened cheeses are produced by the fermentation of milk inoculated with mesophilic starter culture to lower the pH. The technology does not include the cooking and pressing steps. These specialities have two types: one with washed rind and the other one with bloomy rind. The *Penicillium camemberti* mould is responsible for the formation of the specific, roughly 3 mm thick white/grey rind. Other microorganisms as *Geotrichum candidum*, *Debaryomyces hansenii*, *Kluyveromyces* spp., and some bacterial species grow on the surface of the cheese contributing to the development of very dark orange or brown layer with a thickness of about 0.5 mm. During the ripening period (3–5 weeks), the cheese undergoes different physicochemical and biochemical changes, becoming soft, fluid, and viscous. As the result of the enzymatic activity of the surface moulds, the pH increases during ripening, which finally leads to mineral migration from the centre to the surface of the cheese. This phenomenon contributes to the swelling and hydration of the proteins (*Leclercq-Perlat*, 2011; *Spinnler*, 2017; *Batty et al.*, 2019).

The mould *P. camemberti* has a key role in the production of different aroma and flavour compounds (*Hong et al.*, 2018). Besides them, other microbes are also involved in the ripening, such as *Lactococcus lactis*, *Leuconostoc mesenteroides*, and surface bacteria *Brevibacterium linens* (*Leclercq-Perlat*, 2011).

The sensory properties of the industrial Camembert-type cheese were improved with the addition of *Lactobacillus rhamnosus* in the case of pasteurized milk (*Galli et al.*, 2019). Some of the predominant characteristics of Camembert-type cheeses include ethyl esters and the ethanol formed by fermentation, while the adjunct cultures with ester-synthesising ability contribute to the formation of the fruity flavour of cheese *(Hong et al.*, 2018).

Cheese quality is determined by multiple parameters, including the raw material, curd formation, and ripening process. Ripening is also influenced by different microbiological, physicochemical, and biochemical factors. The stabilized composition and quality of Camembert-type cheese are achieved by: the use of proper starter species; suitable fermentation conditions, including time/temperature, adequate rate of acidification; curd handling practices; cut size (*Batty et al.*, 2019).

Despite being a popular dairy product, cheese has been frequently associated with foodborne disease outbreaks. The source of pathogens could be direct contamination or cross-contamination during the manufacturing steps. Cheeses

were implicated in severe cases of salmonellosis (*Robinson et al.*, 2020). According to European Regulation No. 2073/2005, 25 g of product should not contain *Salmonella* spp.

Another foodborne pathogen with high prevalence rate in raw milk cheeses is *Staphylococcus aureus*. Their primary source is bovine mastitis, while secondarily they appear as a result of human contamination. These enterotoxin-producing bacteria favour cheese environment due to their high osmotolerance and can survive in low water activity ($a_w = 0.86$) conditions. The heat tolerant enterotoxin in milk can cause food poisoning (*Possas et al.*, 2021).

The aim of the present study was to manufacture Camembert-type cheese from pasteurized milk on a pilot/small industrial scale. To determine the effect of single source and bulk milk on cheese quality, we evaluated the presence of *Salmonella* spp. and *Staphylococcus aureus* as markers in the obtained products. Also, we determined the food-related stress tolerance and antibiotic resistance of the isolated bacteria.

2. Materials and methods

During our work, three Camembert-type cheeses were prepared on a pilot/small industrial scale. The first cheese was made using bulk milk, obtained by mixing milk from several vendors. The raw milk supposed heat treatment at 74 °C for 15 seconds. The second and third cheeses were prepared from one type of milk and were heat treated at 72 °C for 60 seconds. After one week of maturation, the third cheese was placed in a vacuum bag for further maturation.

The manufacturing procedure involved the main technological steps as follows: the refrigerated (4 °C) milk was pasteurized, the calcium chloride (200 g/1,000 L) was added to cooled milk, was inoculated with starter culture (100 DCU/1000 L), renneted (33 ml/1,000 L) and mould-inoculated. After inoculation, coagulation time was 60 minutes, whereafter the curd was cut with harps into cubes with edge lengths of 5 cm. Following the whey separation, the clot was placed into forms and rotated at regular intervals (in every 6 hours) for a day. Finally, the formed wheels were immersed in 22% brine at 14-15 °C for 45 minutes. After the drainage of the solution had taken place, the cheeses were dried on surface at 14-15 °C, relative humidity being 75-80%, and afterwards it was matured (at 16 °C, relative humidity of 80-85%) for a period of three weeks (*Molnár & Molnár*, 1999).

The microbial contamination of three Camembert-type cheeses was carried out in three steps, as follows: firstly, the stock suspension (10 g sample and 90 ml physiological solution) was obtained; secondly, the preparation of dilution series (10^{-1}–10^{-2}) was performed; thirdly, the spreading of a volume of 0.1 ml of the solutions on the used selective agar mediums was made. For detecting the presence

of *Staphylococcus aureus* and *Salmonella* spp., the following mediums were used: Mannitol Salt Agar and ChromoBio® Salmonella Base.

Bacterial isolates with characteristic colony morphology were isolated, and pure cultures were made. The isolated bacterial strains were subjected to confirmation and biochemical tests, which included: Gram-type determination with 3% KOH test, catalase test, indole test, methyl red test, lactose fermentation, gelatine hydrolysis test, and inoculation in medium with 16% NaCl content (*Dunca et al.*, 2004).

The food-related stress survival of five bacterial isolates originated from the Camembert-type cheese was assayed. Osmotic stress was determined in nutrient broth with different NaCl content as: 4%, 6%, 10%, 15%, and 20%. Each of the above mentioned broths were inoculated with 1 ml suspension of bacterial isolates (10^8 CFU/ml) taken in study and incubated at 37 °C for 24 hours. After incubation, the bacterial isolates growth was marked by + or ++ where the survival was positive (*György*, 2020).

With a view to exposing the bacterial isolates to the most selective acid stress possible, they were (10^8 CFU/ml) inoculated in nutrient broth with pH of 3 and 5.5, were adjusted with 1 M HCl with pH 3.5 and 5.5 respectively, and adjusted with lactic acid. The inoculated nutrient broth with different pH was incubated at 37 °C for 1 hour (*Horlbog et al.*, 2018). After this, an amount of 1 ml from each broth was transferred in 9 ml sterile nutrient broth and incubated at 37 °C for 24 hours. Following the incubation, the positive bacterial isolates' survival was marked by + or ++. Bacterial growth at different temperatures (8 °C, 20 °C, and 37 °C) was assayed. The bacterial isolates were inoculated on nutrient agar medium and incubated at the above-mentioned temperatures, and the growth after incubation was evaluated.

The antibiotic susceptibility of the bacterial isolates was determined by the disk diffusion method. A volume of 0.1 ml suspension of bacterial isolates (10^8 CFU/ml) was spread on Mueller–Hinton agar medium plates (Himedia), and the antibiotic disks were placed. A total of 12 different antibiotic discs containing the antibiotics imipenem 10 µg (IPM), meropenem 10 µg (MRP), tigecycline 15 µg (TGC), levofloxacin 5 µg (LE), amikacin 30 µg (AK), cefotaxime 30 µg (CTX), ofloxacin 5 µg (OF), tobramycin 10 µg (TOB), amoxyclav (amoxicillin/clavulonic acid) 30 µg (AMC), trimethoprim 5 µg (TR), gentamicin 10 µg (GEN), and chloramphenicol 30 µg (C) were used for *Salmonella* spp. isolates. For the *Staphylococcus aureus* isolates' antibiotic susceptibility study, 16 antibiotics were used: nalidixic acid 30 µg (NA), rifampicin 5 µg (RIF), tigecycline 15 µg (TGC), erythromycin 15 µg (E), levofloxacin 5 µg (LE), amikacin 30 µg (AK), linezolid 30 µg (LZ), kanamycin 30 µg (K), cefotaxime 30 µg (CTX), clindamycin 2 µg (CD), tobramycin 10 µg (TOB), ciprofloxacin 5 µg (CIP), trimethoprim 5 µg (TR), tetracycline 30 µg (TE), gentamicin 10 µg (GEN), and chloramphenicol 30 µg (C). It was incubated for 24

hrs at 37 °C. The diameter of the inhibition zone was measured, and the results of antimicrobial resistance were interpreted according to the European Committee on Antimicrobial Susceptibility Testing (EUCAST) guidelines as susceptible (S), intermediate (I), and resistant (R) (*EUCAST*, 2016; *György et al.*, 2021).

3. Results and discussions

On the surface of the manufactured cheeses, the characteristic rind was properly formed by the mould, and the inside of the cheese was creamy and soft, with mushroom taste.

The pathogens and spoilage microorganisms from raw milk can survive the processing technology. In cheese, different factors contribute to the survival of pathogens, such as temperature, acidification, or the salt and moisture content (*Bachmann et al.*, 2011; *Martin et. al.*, 2021).

S*almonella* is most frequently associated with foodborne infections. Outbreaks caused by *Salmonella* represent a worldwide problem. The infectious dose depends on serotype, host defence, immune status, and, of course, the mode of transmission. The symptoms of salmonellosis include from mild to severe diarrhoeal disease (*Gharpure et al.*, 2021). All over the world, many salmonellosis outbreaks are associated with the consumption of raw milk cheese (*Lobacz & Zulewska*, 2021). The infective dose for gastroenteritis is usually > 10,000 cells, but in high-fat foods, such as cheese, it may be < 100 cells. The infective dose for enteric fever is < 1,000 cells (*Fox et al.*, 2017).

Evaluation of the microbiological quality of the three cheeses resulted that the first sample contained the highest number of *Salmonella* bacteria $3.1 \cdot 10^4$ CFU/g, while the second and third samples contained $9 \cdot 10^2$ CFU/g and $2.7 \cdot 10^2$ CFU/g. *Salmonella* species are Gram-negative, catalase-positive, non-lactose-fermenting, and not indole-producing bacteria. Gram staining and biochemical tests resulted that *Salmonella* isolates originated from cheese samples belong to the *Salmonella* group (*Table 1*).

The nutritional content of cheese favours the growth of *S. aureus.* This ubiquitous bacterium can cause food poisoning with symptoms such as abdominal cramps, vomiting, nausea, and diarrhoea. Coagulase-positive staphylococci can appear in raw milk due to cross-contamination (*Baran et al.*, 2017). Udder infections may be derived from *S. aureus.* Second transmission routes of *S. aureus* are the environment, milking equipment, human handling, and water (*Rosengren et al.*, 2010; *Bachmann et al.*, 2011). Rosengren et al. (2010) determined different types of *S. aureus* strains in cheeses. This suggests the different contamination sources such as human, animal, or environment. *S. aureus* could not be detected from the assayed Camembert-type cheese prepared from pasteurized milk. Only 33% of raw milk cheese contained it.

Table 1. Biochemical characteristics of *Salmonella spp.* isolates originated from Camembert samples

Sample	Gram staining	Catalase test	Lactose fermentation	Indole probe
Sal. 10^{-1} (1)	Gram-negative	Catalase-positive	negative	negative
Sal. 10^{-2} (1)	Gram-negative	Catalase-positive	negative	negative
Sal. A (Vák.)	Gram-negative	Catalase-positive	negative	negative

Notes: Sal. 10^{-1} (1): *Salmonella*, 10-fold dilution, first sample; Sal. 10^{-2} (1): *Salmonella*, 100-fold dilution, first sample; Sal. A (Vák.): *Salmonella*, stock solution, vacuum-packed sample; Sal. A: *Salmonella*, stock solution, second sample.

The high content (100000 CFU g^{-1}) of *S. aureus* is associated with high enterotoxin content, which remains in curd for a long time, whereas the number of *S. aureus* is decreasing during cheese ripening. Based on European Regulation (EC) No. 2073/2005, determination of coagulase-positive staphylococci is required during the manufacturing (*Bachmann et al.*, 2011).

Staphylococcus aureus was detected from the first sample – $3.1 \cdot 10^3$ CFU/g.

Characteristics of *Staphylococcus aureus* are: Gram-positive, catalase-positive, indole-negative, gelatinase-positive, and methyl red positive. Based on the results of biochemical tests, two isolates (S.a. A, S.a. 10^{-2}) were identified as *S. aureus* (notes for isolates: S.a. A: *Staphylococcus aureus*, stock, first sample; S.a. 10^{-2}: *Staphylococcus aureus*, 100-fold dilution, first sample).

The survival rate of the five bacterial isolates in different environmental stress conditions, including osmotic stress, acidic stress, and temperature, was almost the same (*Table 2*).

Table 2. Food-related stress survival of *Salmonella* spp. and *S. aureus* isolates

Bacterial isolates	NaCl					pH				Temperature		
	4%	6%	10%	15%	20%	3.5 (L.a.)	5.5 (L.a.)	3	5.5	8 °C	20 °C	37 °C
Sal. 10^{-1} (1)	++	++	-	-	-	++	++	+	++	+	++	++
Sal. 10^{-2} (1)	++	++	++	+	+	++	++	+	++	+	++	++
Sal. A (Vák.)	++	++	++	+	+	++	++	+	++	+	++	++
S.a. A	++	++	++	+	+	++	++	++	++	+	++	++
S.a. 10^{-2}	++	++	++	+	+	++	++	+	++	+	++	++

L.a.: pH adjusted with lactic acid

No remarkable differences between the isolates were observed. The tested bacteria were more tolerant to 4%, 6%, and 10% NaCl. Slower growth could be detected in the presence of 15% and 20% NaCl.

Bacteria with salt can be eliminated or its growth mitigated. The osmotic pressure effect is the disruption of the osmotic balance between the cytoplasmic and the intracellular membrane. The activation of osmoregulatory systems protects the bacteria from osmotic pressure. For example, in *S. aureus*, osmoprotective compounds are produced. Also, it has been shown that osmotic stress can contribute to the increase of antibiotic resistance (*Horn & Bhunia*, 2018). The growth and development of microorganisms in cheese are determined by different factors (*Picón*, 2018; *György & Laslo*, 2021).

None of the *Salmonella* spp. and *Staphyloccocus* isolates were inactivated by the acidic treatment. With the exception of 3 pH adjusted with 1 M HCl, the isolates grow well, whereas a slight growth was observed in the case of the three *Salmonella* isolates at the mentioned pHs. Isolates were considered as acid tolerant.

In the food matrices, microbial inactivation could be reached through acid stress. This could be achieved through fermentation, addition of organic acids as preservatives, or by acid washes. This stress may lead to cell injury, cell death, or inactivation of enzymes or may affect the transmembrane proton motive force (*Horn & Bhunia*, 2018; *Horlbog et al.*, 2018). It has been shown that *Salmonella* is an acid-adapted bacterium that can survive the acidic condition due to expression of acid shock proteins (*Horn & Bhunia*, 2018).

The bacterial isolates grow well at 20 °C and 37 °C. Also, the low temperature of 8 °C did not affect the growth. It has been shown that cold temperatures (4 °C) did not affect cell number reduction in *S. aureus*. Further, it was demonstrated that the alteration of cytoplasmic metabolites contributes to the survival of *S. aureus* in and its adaptability to different stress conditions (*Alreshidi*, 2020).

According to the results of antibiotic susceptibility, the three *Salmonella* isolates showed susceptibility to the majority of antibiotics. The isolates showed resistance to trimethoprim, chloramphenicol, amikacin, and cefotaxime. These three *Salmonella* isolates can be defined as multi-drug-resistant strains. They exhibit resistance to four classes of antibiotics, which makes them multi-drug-resistant (*Magiorakos et al.*, 2012).

The two *S. aureus* isolates showed resistance to trimethoprim and displayed intermediate resistance to levofloxacin and ciprofloxacin.

Salmonella serotypes with multiple antibiotic resistance has been detected increasingly in the food chain. It has been demonstrated that the spreading of antibiotic resistance in *Salmonella* species, the horizontal transmission of resistance genes plays a crucial role (*Nair et al.*, 2018; *Xu et al.*, 2020).

4. Conclusions

During the production of Camembert-type cheese, it is essential to follow exactly the technological process steps and to assure the proper hygienic conditions. Microbiologically, the raw material quality, the adequate heat treatment, the temperature profile during processing, and the hygienic conditions are of paramount importance.

The microbiological contamination of the cheese sample made from bulk milk was significantly higher in comparison with cheese samples made from milk from a single source. Based on the results of biochemical confirmation tests, *Salmonella* spp. was detected in all of the three cheese samples, whereas the highest cell number was detected in the first sample, in sufficient amount to infect a host. *S. aureus* was present in the first sample as well, but the infestation did not reach the threshold limit to produce enterotoxin.

The presence of *Salmonella* isolates with multiple antibiotic resistance in the cheese sample should be considered a risk indicator.

From the results of the study, it can be concluded that improper food-processing practices could contribute to the survival of foodborne pathogens. To ensure the safety of cheese, raw milk microbiological analysis and adequate pasteurization is needed.

References

[1] Alreshidi, M. M., Selected metabolites profiling of *Staphylococcus aureus* following exposure to low temperature and elevated sodium chloride. *Frontiers in Microbiology*, 11. (2020) 834.

[2] Bachmann, H. P., Fröhlich-Wyder, Jacob, E., Roth, E., Wechsler, D., Raw milk cheeses. In: Fuquay, J. W., Fox, P. F., McSweeney, P. L. H. (eds.), *Encyclopedia of Dairy Science*, 2nd ed. Elsevier Academic Press. (2011).

[3] Baran, A., Erdoğan, A., Turgut, T., Adigüzel, M. C., A review on the presence of *Staphylococcus aureus* in cheese. *Turkish Journal of Nature and Science*, 6. 2. (2017) 100–105.

[4] Batty, D., Waite-Cusic, J. G., Meunier-Goddik, L., Influence of cheese-making recipes on the composition and characteristics of Camembert-type cheese. *Journal of Dairy Sci*ence, 102. (2019) 164–176.

[5] Dunca, S., Ailiesei, O., Nimițan, E., Ştefan, M., *Microbiologie aplicată*. Tehnopress, Iaşi. (2004).

[6] Fox, P. F., Guinee, T. P., Cogan, T. M., McSweeney, P. L. H., *Fundamentals of Cheese Science*, 2nd ed. Springer, New York. (2017).

[7] Galli, B. D., Baptista, D. P., Cavalheiro, G., Gigante, M. L., *Lactobacillus rhamnosus* GG improves the sensorial profile of Camembert-type cheese: An approach through flash-profile and CATA. *LWT – Food Science and Technology*, 107. (2019) 72–78.

[8] Gharpure, R., Healy, J. M., Lauer, A. C., Tauxe, R. V., *Salmonella* infections. In: Morris, J. G., Vugia, D. J. (eds.), *Foodborne Infections and Intoxications*. Elsevier Academic Press. (2021).

[9] György, É., Élelmiszer-mikrobiológia laboratóriumi gyakorlatok. Scientia Publishing House, Cluj-Napoca. (2020).

[10] György, É., Laslo, É., Microbial diversity of traditionally processed cheese from Northeastern Region of Transylvania (Romania). In: Laranjo M. (ed.), *Fermentation – Processes, benefits and risks*. Intechopen. DOI: 10.5772/intechopen. 97591 (2021).

[11] György, É., Laslo, É., Antal, M., András, C. D., Antibiotic resistance pattern of the allochthonous bacteria isolated from commercially available spices. *Food Science & Nutrition*, 9. (2021) 4550–4560.

[12] Hamdaoui, N., Mouncif, M., Mennane, Z., Omari, A., Meziane, M., Development of the technology of soft Camembert-type cheese with flowery rind in Morocco. *Research Square* [preprint]. (2021).

[13] Hong, Q., Liu, X. M., Hang, F., Zhao, J. X., Zhang, H., Chen, W., Screening of adjunct cultures and their application in ester formation in Camembert-type cheese. *Food Microbiology*, 70. (2018) 33–41.

[14] Horlbog, J. A., Kent, D., Stephan, R., Guldimann, C., Surviving host- and food-relevant stresses: Phenotype of *L. monocytogenes* strains isolated from food and clinical sources. *Scientific Reports*, 8. (2018) 12931.

[15] Horn, N., Bhunia, A. K., Food-associated stress primes foodborne pathogens for the gastrointestinal phase of infection. *Frontiers in Microbiology*, 9. (2018) 1962.

[16] Leclercq-Perlat, M. N., Camembert, Brie, and related varieties. In: Fuquay, J. W., Fox, P. F., McSweeney, P. L. H. (eds.), *Encyclopedia of Dairy Sciences*, 2nd ed. Elsevier Academic Press. (2011).

[17] Lobacz, A., Zulewska, J., Fate of *Salmonella* spp. in the fresh soft raw milk cheese during storage at different temperatures. *Microorganisms*, 9. (2021) 938.

[18] Magiorakos, A. P. et al., Multidrug-resistant, extensively drug-resistant and pandrug-resistant bacteria: An international expert proposal for interim standard definitions for acquired resistance. *Clinical Microbiology and Infection*, 18. 3. (2012) 268–281.

[19] Martin, N. H., Torres-Frenzel, P., Wiedmann, M., Invited review: Controlling dairy product spoilage to reduce food loss and waste. *Journal of Dairy Science*, 104. 2. (2021) 1251–1261.

[20] Molnár, A., Molnár, J., *A sajtkészítés ABC-je*. GAIA Alapítvány Kiadó, Galgahévíz. (1999).

[21] Nair, D. V. T., Venkitanarayanan K., Johny, A. K., Antibiotic-resistant *Salmonella* in the food supply and the potential role of antibiotic alternatives for control. *Foods*, 7. 10. (2018) 167.

[22] Picón, A., Cheese microbial ecology and safety. In: Papademas P., Bintsis T. (eds.), *Global cheesemaking technology*. John Wiley & Sons, Ltd. (2017).

[23] Possas, A., Bonilla-Luque, O. M., Valero, A., From cheese-making to consumption: Exploring the microbial safety of cheeses through predictive microbiology models. *Foods*, 10. (2021) 355.

[24] Robinson, E. et al., Outbreak of *Salmonella* Newport associated with internationally distributed raw goats' milk cheese, France, 2018. *Epidemiology & Infection*, 148. (2020).

[25] Rosengren, Å., Fabricius, A., Guss, B., Sylvén, S., Lindqvist, R., Occurrence of foodborne pathogens and characterization of *Staphylococcus aureus* in cheese produced on farm dairies. *International Journal of Food Microbiology*, 144. (2010) 263–269.

[26] Spinnler, H.-E., Surface mold-ripened cheeses. In: McSweeney P. L. H., Fox P. F., Cotter P. D., Everett D. W. (eds.), *Cheese. Chemistry, physics & microbiology*, vol. 1., *General aspects*, 4th ed. Elsevier Academic Press, London. (2017).

[27] The European Committee on Antimicrobial Susceptibility Testing (2016). Breakpoint tables for interpretation of MICs and zone diameters (EUCAST). Retrieved from: http://www.eucast.org.

[28] Xu, X., Biswas, S., Gu, G., Elbediwi, M., Li, Y., Yue, M., Characterization of multidrug resistance patterns of emerging *Salmonella enterica* serovar Rissen along the food chain in China. *Antibiotics*, 9. 10. (2020) 660.

Acta Univ. Sapientiae, Alimentaria, **14** (2021) 95–116

DOI: 10.2478/ausal-2021-0006

The comparative analysis of some Hungarian and Moldovan wines: The promise of protected geographical indication

E. Savchina[1]
e-mail: ec.savchina@gmail.com

A.-M. Borta[1]
e-mail: anna.maria.borta@gmail.com

L. Csige[2]
e-mail: csigelaszlo@unideb.hu

Z. Győri[1]
e-mail: gyori.zoltan@unideb.hu

J. Szepesi[1]
e-mail: szepesi@agr.unideb.hu

E. Máthé[1]
e-mail: endre.mathe@agr.unideb.hu

[1] University of Debrecen, Faculty of Agricultural, Food Sciences and Environmental Management, Institute of Nutrition, HU-4032 Debrecen, 138 Böszörményi St, Hungary
[2] University of Debrecen, Wine Academy of Mád, HU-3909, 37–39 Mád St, Hungary

Abstract. Hungary and Moldova are excelling in unique wines and alcoholic beverages that could qualify for the protected geographical indication (PGI) by emphasizing parameters attributable to the geographical area, production or processing methods. In this study, we have assessed some parameters of wine and brandy samples looking for specificities. The studied samples were of Moldovan and Hungarian Cabernet Sauvignon red wines, Hungarian Furmint white wines, and Moldovan wine distillate/brandy called Divin. The assessed samples were evaluated for: total polyphenol and flavonoid, ethanol, malic, citric, lactic, tartaric acids, reducing sugar, glycerol, carbon dioxide, total and free SO_2 content as well as for total acidity, volatile acidity, pH, and wine density.

Our results indicate that despite the relatively close geographical vicinity of Hungary and Moldova, the wines produced in the two countries have specific composition, antioxidant activity, and sensorial properties. Thus, the registration of such wines as PGI is clearly justified, and such a label itself does represent a competitive advantage worth promoting.

Keywords and phrases: wine quality, geographical indications, FTIR spectroscopy, Protected Designations of Origin (PDO)

1. Introduction

Historical features of Moldovan winemaking

Winemaking in the historical Moldavia has a rich past. In ancient times, the Dacians and the Getae, the two Scythian tribes, were engaged in agriculture, livestock husbandry, and winemaking. Around 50 BC, King Burebista issued a decree compelling the Dacians and the Getae to destroy vineyards, give up wine making and consumption. Until the Roman invasion of Dacia (106 AD), the order was in force for nearly 150 years. By introducing new grape types and farming practices and sharing their winemaking technology with the locals, the Romans in this area supported the growth of wine-grapes and wine production.

In the Middle Ages, when Moldavia comprised the entire territory from the Dniester to the Carpathians, the Moldavian princes – Matei Basarab, Negru Vodă, Ştefan cel Mare, and Mihai Viteazul – planted new vineyards, brought new varieties of wine-grapes and experienced workers from the Hungarian Kingdom. After the death of Ştefan cel Mare (1504), Moldavia was partly conquered by the Ottoman Empire, and table varieties of grapes were cultivated in the colonized areas. During the Russo–Turkish war of 1806–1812, the southern wine-producing region of Moldavia was destroyed (*Taran*, 2010).

After the annexation of the eastern side of Moldavia (also called Bessarabia) by the Russian Empire, the viticulture and wine production started to develop intensively in this part of Moldavia. In 1832, the first special school for viticulture and winemaking was established. During the period of 1880–1915, winemaking in Bessarabia entered a period of crisis caused by wine adulteration practices at large scale, which was aggravated by the appearance of phylloxerae in the vineyards (*Taran*, 2010). Following World War I, the eastern part of Moldavia, called Moldavian Democratic Republic, became part of the Soviet Union, while the western part of Moldavia remained an integrated part of Romania.

In the following, we will refer only to the grapes and wines of the eastern part of Moldavia (today called Republic of Moldova), where approx. 54 wineries were built and rebuilt by the 1960s. Due to the technological modernization of the wine enterprises in 1970–1985, new types of high-quality wines were obtained, which made the Soviet Moldova known in the USSR and abroad as an important wine-producing country. The decline of the Soviet Moldovan wine industry began in 1985 with the issuance of Gorbachev's decree on combating alcoholism in the USSR, which led to the destruction of 50% of the wine-grape plantations (*Taran*, 2010).

Nowadays, the wine sector in the Republic of Moldova is of a strategic importance for the entire economy (*Taran*, 2010). Moldova was the first post-Soviet republic to join the International Organization of Vine and Wine as a member state (OIV). The *Law on Vine and Wine* was enacted by the Parliament of the Republic of Moldova

in 1994, and it was the first law on this issue in the CIS countries (no such law had existed before either in the USSR or in European winegrowing countries). This law pays particular attention to the process of wine production as well as other wine products with a designation of origin. In 2005, the Republic of Moldova was one of the top-ten wine exporters of the world. In March 2006, the Russian Federation issued a nearly two-year embargo on Moldovan wines, denying Moldovan winemakers from access to the Russian wine market. In September 2013, the same scenario occurred, but this time the consequences were less harmful as the Moldovan companies diversified their export routes to Belarus, Kazakhstan, Ukraine, the EU, and Asia. Due to the severe crises of 2006 and 2011, the Moldovan wine industry focused on the development of high-quality wines, market diversification, and industrial modernization (*Wine of Moldova*, 2021). The establishment of the National Office of Wine (2013) was a significant step forward for the public and private sectors in implementing changes to the wine legislation and the regulatory framework. Driven mostly by marketing considerations, serious efforts were made to generate a country-specific wine brand called *Wine of Moldova. A Legend Alive*, which was further substantiated by applying a strict quality control (*Wine of Moldova*, 2021).

Besides wines, Divin is a Moldovan brandy made of wines. It is produced in accordance with its own specifications and under the supervision of the Association of Authorities and Producers. Divin is obtained by the double distillation of grapes such as Aligote, Chardonnay, Fetească Albă, Rhein Riesling, and Rkatsiteli, while the obtained wine spirit is aged for at least 3 years in oak barrels. The name Divin literally comes from the Romanian phrase "din vin", which means "from wine", and it also has the meaning of divine. Divin stands out by its hue with brownish to amber shades, balanced and soft taste with floral notes, which later develop into fine aromas of chocolate (*ADBPM*, 2012).

Regarding Moldovan grape production, there are four Moldovan grape-growing areas as follows: Valul lui Traian, Ştefan Vodă, Codru, and Divin, all having Moldovan-protected geographical indications (PGI) similar to the European Union type of regulations. The wine areas are defined by the *Law on Wine and Vineyards* of the Republic of Moldova and the Order of *Delimitation of Wine-Growing Geographical Areas for the Production of Wines with a Protected Geographical Indication* issued by the Ministry of Agriculture and Food Industry.

Red grape varieties largely cultivated in the Republic of Moldova are Cabernet Sauvignon, Cabernet Franc, Gammay Freaux, Malbec, Merlot, Pinot Gris, Pinot Noir, Saperavi, and Syrah, while the most relevant white grape varieties are Aligote, Bianca, Chardonnay, Hibernal, Muscat Frontignan, Muscat Ottonel, Müller Turgau, Pinot Blanc, Rhein Riesling, Riton, Rkatsiteli, Sauvignon, Traminer roze, and Ugni Blanc. The locally cultivated red grape varieties such as Pervomaiski, Codrinski, Fetească Neagră, and Rară Neagră and the white grape varieties such as Fetească Albă, Fetească Regală, Perveneț Magaracea, Suholimanski Belîi, Alb de Onițcani,

Floricica, Legenda, Luminița, Muscat de Ialoveni, and Viorica (*Wine of Moldova*, 2021) are also relevant for winemaking.

Besides the large number of cultivated grape varieties, it can be expected that the uniqueness of the geographical conditions would further strengthen the character of Moldovan wines. Some of the most relevant features of the Moldovan wines and regions related to the current study are shown in *tables 1* and *2*. The climate of the Codru wine-growing area is influenced by the Western European oceanic climate (Marine West Coast) and the East European Continental climate (Humid Continental) (*WADGR „Codru"*, 2017). The climate of the Ştefan Vodă region is determined mainly by the Black Sea (*AWPPGI "Ştefan Vodă"*, 2017), while the climate of the Valul lui Traian zone is affected by both the Black Sea and the Mediterranean climate (*WUDGR "Valul lui Traian"*, 2019). The delimited Divin area is again influenced by two geographical factors, namely the Carpathian Mountains and the Black Sea (*ADBPM*, 2012).

Taken together, it is impressive to notice the improvements of the Republic of Moldova regarding the quality of its own wines that have been recognized by numerous awards at major international wine competitions such as the Decanter World Wine Awards, Mundus Vini, Concours Mondial du Bruxelles, International Wine Challenge, and others (*Wine of Moldova*, 2021).

Historical features of Hungarian wine making

In historical terms, wine production and consumption was present on the territory of Hungary throughout the centuries, and the specific connotations of the different wine types are still present in the Hungarian cuisine and eating habits. Winemaking in Hungary dates back to Roman times, and by the 5th century AD, extensive vineyards are reported in Pannonia (*Bede*, 2016). The ancient Hungarians settling down in the Carpathian Basin introduced Inner Asian and Caucasian traditions into winemaking, while during the Middle Ages, abbeys of the Catholic Church continued the diversification of cultivated grapes and wine varieties. During the Austro-Hungarian period, winemaking was intensified, and several wine varieties emerged mainly related to local grape varieties. However, during the 1870s, grape phylloxerae spread following the Danube river route, first to Upper and Lower Austria and Burgenland and then to Czech, Slovakian, and Hungarian regions, affecting dramatically the grape and wine production (*Tello et al.*, 2019). After the "Great phylloxera attack", more emphasis was put on creating new resistant grape varieties by using own-rooted local *V. vinifera* varieties grafted onto partially resistant American *non-vinifera Vitis* spp. or hybrids used as rootstocks (*This et al.*, 2006).

The cultivated red grape varieties in Hungary are the Kékfrankos, Cabernet Franc, Cabernet Sauvignon, Merlot, Nero, Pinot Noir, and Syrah. The most popular

white grape varieties cultivated in Hungary are Chardonnay, Italian Riesling, Sauvignon, Muscat Blanc, Pinot Blanc, Pinot Gris, and Bianca. Local red grape varieties are Kadarka, Kékfrankos, Kékoportó, and Zweigelt, while the locally cultivated white grape varieties are Ottonel muskotály and Tramini. Indigenous Hungarian red wine-grapes are, e.g. Bíborkadarka, Csókaszőlő, Rubintos, and Turán, while Cserszegi fűszeres, Furmint, Hárslevelű, Irsai Olivér, Kövérszőlő, Zengő, and Zenit are based on local white grape-wine varieties (*TWRAC*, 2014; *ABUWR*, 2016; *EBWRAC*, 2017; *BWRAC*, 2018).

Currently in Hungary, there are several grape varieties and cultivars, largely grouped into six wine regions as follows: (1) Észak-Dunántúl (North Transdanubia or Upper Pannonia) with subregions as Ászár-Neszmély, Etyek-Buda, Mór, Pannonhalma, and Sopron; (2) Lake Balaton, divided into subregions as Badacsony, Balatonfelvidék, Balatonfüred-Csopak, Dél-Balaton, Somló, and Zala; (3) Dél-Dunántúl (South Transdanubia or Pannonia) consisting of subregions as Pécs, Villány, Szekszárd, and Tolna; (4) Duna or Alföld with subregions as Csongrád, Hajós-Baja, and Kunság; (5) Észak-Magyarország (Northern Hungary or Upper Hungary) including sub-regions as Eger, Mátra, and Bükkalja; and (6): Tokaj (*Smyth*, 2016). Some of the most relevant features of the Hungarian wines and the corresponding regions related to the current study are shown in *tables 1* and *2*, and further details about the Hungarian wine regions can be found on the following webpage: https://winesofhungary.hu/wine-regions.

The aforementioned six Hungarian wine regions are associated with specific soil and climatic conditions, and together with local grape and wine varieties are attributable features that suggest the inclusion of such wines into the EU Protected Food Name (PFN) quality scheme. Four types of protected names were established under the EU PFN general rules, and they are the following: (1) Protected Designations of Origin (PDO); (2) Protected Geographical Indications (PGI); (3) Traditional Specialties Guaranteed (TSG), and (4) the so-called optional quality terms. By definition, the PDO and PGI foodstuffs look similar in terms of identity, as the product originates from a particular geographical area, which, associated with natural and human factors, conveys particular qualities to that product. The differences between the two above-mentioned PFN quality categories are related to the foodstuff manufacturing, so that in case of PDO the entire production should take place in the defined geographical area, while in the case of PGI only one of the production steps must take place in the defined area. It is worth mentioning that geographically defined manufacturing areas could be as large as a whole country in exceptional cases. The TSG quality category is attributed to foods obtained through traditional practices, including the ingredients, technology, and the food name. The PFN optional quality terms are intended to describe some specific features of a locally obtained foodstuff, with additional meaning in a European dimension.

Comparing wines to transform their specific features into competitive advantages

It has become a common fact that the wine offer is increasingly overwhelming across the markets of highly developed countries, yet wine producing still continues to grow. Therefore, new strategies and practices are needed to introduce and position wine brands on markets, while the health-conscious consumer category is looking for novel keynotes related to the beneficial effects of wine. Moreover, to promote the circular bioeconomy and sustainability, there is a stringent need for the promotion of local knowledge even in the case of foodstuffs like wine and nutrition. In the light of the above-mentioned considerations, efforts should be made to promote local wines made of locally grown grapes. Identifying the specific features of such wines made from local resources can bring about new knowledge that might confer competitive advantage on both local and global levels. The chemical analysis of Hungarian and Moldovan wines suggests the use of PDO, PGI, and TSG categories under the auspices of the EU Protected Food Name (PFN) quality scheme.

2. Materials and methods

Several wines from Hungary and Moldova together with two Divin brandies were included into the present study as they are considered top alcoholic beverages. The dry white wines were made from Furmint, while the dry red wines were obtained from Cabernet Sauvignon wine-grapes. Some features of the selected wine regions and study objects are shown in *tables 1* and *2*.

Table 1. Wine/wine brandy samples selected for the study

Product type	Code	Vintage year	Ethanol content	Origin (Wine region)
White dry Furmint wine	WW1	2017	14.5%	Tokaj
	WW2	2017	14.0%	Tokaj
	WW3	2017	13.5%	Tokaj
	WW4	2017	14.5%	Tokaj
	WW5	2017	13.5%	Tokaj

Product type	Code	Vintage year	Ethanol content	Origin (Wine region)
Red dry Cabernet Sauvignon wine	WR1	2018	15.0%	Lake Balaton
	WR2	2017	14.0%	Lake Balaton
	WR3	2018	12.0%	Upper Hungary
	WR4	2018	14.0%	South Transdanubia
	WR5	2017	13.5%	Ştefan Vodă
	WR6	2018	14.5%	Codru
	WR7	2017	14.5%	Valul lui Traian
Divin Brandy VSOP	D1		40.0%	Divin
	D2		40.0%	

Note: VSOP – Divin brandy aged for 5 years.

Table 2. Some characteristics of the selected wine regions from Hungary and Moldova

Characteristics	Wine regions							
	Divin	**Codru**	**Valul lui Traian**	**Ştefan Vodă**	**Lake Balaton**	**Upper Hungary**	**South T. danubia**	**Tokaj**
Vineyards' area (ha)		61,200	43,203	10,000	10,718	78,092	6,700	88,124
Elevation (m)	150–250	150–400	5–311	120–190	120–350	160–500	120–450	100–300
Annual precipitation (mm)	400–700	450–550	450–550	450–550	650	592.6	600–800	525
Yearly clear days	300–320	310–320	310–320	310–320	nd	nd	nd	nd
Yearly insolation hours	2,100–2,200	2,100–2,200	nd.	nd.	1,900	1,964	1,900	2,009
Sum of active temperatures (°C)	2,900–3,100	3,000–3,450	3,000–3,450	3,000–3,450	nd.	nd.	nd.	1,600–1,800
Average annual temperature (°C)	10–12	9.0–9.5	9.5–10.0	9.0–10.0	9.0–11.0	10.65	9.0–11.0	10.8
Soil types	Alfisol, brown earth soil, common Chernozems (typical, cambic), mostly well-aerated and light		Chernozems (typical, cambic), mostly well-aerated and light	Chernozems (typical, cambic), mostly heavy and rich	Clay washed brown earth soil, volcanic rhyolite tuff	Volcanic rhyolite tuff, dacite tuff and andesite brown earth soil and loess	Brown earth soil (luvisols)	Brown earth soil (luvisols) volcanic rhyolite tuff

Note: nd – non-determined.

The **FOSS WineScan SO_2** analyser was used to determine the wine- and brandy-specific chemical parameters. The system uses an FTIR interferometer to scan the entire infrared spectrum of the sample. Phosphoric acid is employed as a hydrolysing agent to liberate SO_2 gas from the wine sample, which is then scanned using an FTIR analyser (*FOSS*, 2019).

The **Folin–Ciocâlteu method** was applied to determine the total polyphenol content in wines and cognacs, as described by Pisoschi et al. (2016).

3. Results and discussion

Evaluation of the quality parameters of the studied wines' and brandies' distillate was conducted in order to identify specific traits that might lead to the definition of wine/wine distillate profiles with respect to the geographical location of vineyards, the used wine-grape varieties, and the manufacturing technologies.

The **phenolic compounds** are known to influence the wine's organoleptic properties such as colour, astringency, bitterness, flavour as well as antimicrobial properties (*Jackson*, 2020). It has been suggested that higher total phenolic content (TPC) is correlated with higher antioxidant activity (*Burns et al.*, 2000). Apart from caffeic, ferulic, and p-coumaric acids, the concentration of the rest of the phenolic compounds found in the wines declines over time (*Kallithraka et al.*, 2009), leading to TPC diminution. The relationship between the TPC and the vintage of wines is still an open question. All the analysed red wine samples (WR1-7) featured significantly higher TCP values as compared to the white wine samples (WW1-WW5) (for details, see *Table 3*). The brandy samples showed equally low levels of TCP as compared to the red wines, but the TPC values were almost similar to the white wine values.

Relying on reference literature, the TPC of young red wines is about 1,300 mg GAE/l on average, while for white wines is about 190–290 mg GAE/l (Jackson, 2020). Apart from WR1 and WR2 featuring relatively higher TPC values, the rest of the red wines showed TPC values specific for young wines. The WR1-2 was from the Lake Balaton region, having the same vintage year like all the other analysed red wine samples, which suggests the relevance of soil and climatic conditions with respect to TPC.

Jackson reported that increased pH and ethanol concentration positively affect the extraction of phenolic compounds (*Jackson*, 2020). This is confirmed only in red samples in this study. The pH decrease is known to affect wine colour, paling its blueness and shifting it to red. Thus, as white wines mostly contain colourless (leucoform) phenolics, the pH does not influence their extraction yield.

The increased amounts of TPC in Balaton wine samples are due to their geographical provenance, characterized by volcanic soils and intense solar UV

radiation. It was demonstrated that such environmental factors create stressful growth conditions, forcing the plant to activate its natural defence (*Heras-Roger et al.*, 2017). In order to increase the TPC values of wines, producers are recommended to prolong the maturation stage, stick to traditional winemaking technology, which implies longer contact between skins and must and implicitly with the formed ethanol (*Fuhrman et al.*, 2001). At the same time, carbonic maceration, thermo-vinification procedures, or commercial pectolytic enzymes should be avoided (*Generalić-Mekinić et al.*, 2019; *Jackson*, 2020).

Speaking of Divin type of wine distillates, sample D1 showed an amount of TPC comparable to white wines, while sample D2 contained 2.2 times less polyphenols. As the main source of phenolic compounds in distilled spirits are wooden barrels, the observed relevant difference can be justified by the use of older barrels made of Hungarian oak on a par with French limousine oak that was used for sample D1. The seasoning and maturation of the wood, the heat treatment and size of the barrel, the cellar microclimate, and the technological operations used could also be among the influencing factors (*Canas*, 2017).

In order to continue the characterization of the studied wines/brandies, we decided to assess several parameters that are considered conventional markers used to describe wine products. Based on oenological considerations, great wines are described as fully balanced when their four fundamental traits, i.e. acidity, tannin content, alcohol strength, and sweetness, reach a sensation harmony that could be preserved by acidity, as the wines are aged. The importance of acidity cannot be underestimated from the consumers' point of view, so that many of them would prefer more sourness than sweetness. Interestingly, sweetness decreases the sensation of acidity, and consumers preferring sweet wines would be more appreciative of the sweetness sensation. Reaching the right combination of sourness and sweetness together with the proper alcohol content remains a permanent open question for wine manufacturers that they must face on yearly basis, and the challenges are enormous as several variables should be considered, while the cause-effect type of correlations remain largely elusive.

In the following, we will present the data of the current study referring to the analysed red and white wines' specific parameters affecting acidity.

Looking at the **citric acid** concentration, all the assessed white wines, with the exception of WW3, were showing higher values than the reference of 270 mg/l (*IARC*, 1988), which could be explained most likely by the grape varieties involved. In the case of red wines, citric acid values were reduced all the way from the WR1 to WR6. It is known that the addition of citric acid to wine as a stabilizer could prevent ferric haze and enhances acidity. It is possible that applying such a consideration could explain the higher concentration of citric acid in sample WR7.

L-malic and **L-lactic acid** content is an important quality parameter of wines and is related to malolactic fermentation, decreasing the fixed acidity in wine

together with the formation of volatile acids and esters that greatly influence the wine "bouquet". The L-malic acid is essential for determining grape ripeness, and it gives sourness and stability to the finished wine (*Volschenk et al.*, 2006). L-lactic acid is a by-product of malolactic fermentation, rather than an indigenous acid found in grapes, and it is considered ideal for controlling secondary fermentation (*Virdis et al.*, 2021; *Volschenk et al.*, 2006).

Regarding the assessed red wines, samples WR2, WR4, WR5, and WR6 had the highest lactic acid values, all associated with non-detectable malic acid levels. Higher levels of malic acid in association with lower levels of lactic acid were detected in WR1, WR3, and WR7, probably indicating that the malolactic fermentation was not fully completed. As expected in the case of white wines, high levels of malic acid with reduced levels of lactic acid were observed, indicating that the malolactic fermentation does not play an important role in "bouquet" formation. However, WW3 represents an exception among the analysed white wines, so that it shows reduced malic acid and greatly increased lactic acid levels, indicating that malic and lactic acid content could be used for "bouquet" profiling even in the case of Tokaj white wines.

Tartaric acid has a great impact on the pH, general stability, and sensory qualities of wines (*Volschenk et al.*, 2006). With the exception of WR3, the other Hungarian red wines had lower tartaric acid content as compared to the Moldovan samples, which could be due to the differences in soil type, as tartaric acid concentration is highly dependent on the potassium content of soil (Robinson, 2006). The tartaric acid content of the assessed Tokaj white wines is not surprising since the Tokaj region, with its volcanic origin soil, is rich in potassium (*O'Geen et al.*, 2008). However, tartaric acid is also a grape-specific acid, and its concentration could also be highly influenced by the grape variety, so the relevance of cultivated grapes remains to be clarified with respect to the observed tartaric acid values exceeding the internationally accepted average level of ~2,120 mg/l (*IARC*, 1988).

Volatile acidity is another important quality parameter indicating microbial activity during fermentation (*Nyknen* & *Suomalainen*, 1983), and its normal range falls between 0.3 and 0.7 g/L (*Tsakiris et al.*, 2014), though the EU legal limit is about 1.2 g/L of acetic acid. It has been observed that volatile acidity exceeding 0.8 g/L acetic acid could confer unpleasant acidic taste and vinegar aroma to wine. With the exception of WR1 (0.8 g/L acetic acid), all the other wines included in the present study have normal volatile acidity.

Wine-specific **total acidity** (TA) indicates the concentration of acids present in wine, and its normal values range between 3.6 and 5.5 g/L, expressed as sulphuric acid (*Jackson*, 2020). With the exception of WR7, the red wines' specific values indicate normal TA, while the white wines' TA values exceed the upper limit of the normal range.

Usually, all wines have an acidic **pH** ranging between 2.5 and 4.5. Wine-specific pH level indicates the intensity of acidic taste. As expected, all the analysed white wines fall into the pH range of 3.1–3.3, which is a characteristic of sweet and light-bodied white wines. The studied red wines showed a wider pH spectrum (3.4 – 3.8), suggesting that the red wines situated closer to pH = 3.5 could be regarded as of normal category, while those that reach pH = 3.8 would fall into the low-acid red wine type. The assessed brandies had a higher pH than all analysed wines, but this does not pose any problem for the stability because their high ethanol content will prevent microbial deterioration.

In order to explain the acidity-specific parameters of wines, numerous factors could come into play, but in the present situation we can also think of the influence of climate. All the assessed white wines were from the Tokaj region and were based on the Furmint grapevine, while the studied red wines were obtained using Cabernet Sauvignon grapevine produced in different Hungarian and Moldovan wine regions. The relatively low values and narrower pH spectrum of Tokaj wines could be associated with either cooler night-time temperatures or a shorter wine-grape growing season (see *Table 2*). It is believed that cool nights and cold weather stop the grapes from losing their acidity, but the scientific confirmation of such a presumption is still awaiting further proof. Some genomic studies indicate that temperature might desynchronize the sugar and organic acid metabolism in ripening wine-grape fruits, as shown by transcriptome analysis (*Rienth et al.*, 2016), but such studies should comprise more wines and regions.

Talking about wine-grapes, they contain fermentable sugars such as glucose, fructose, and sucrose and pentose as a non-fermentable sugar. Based on their reducing ability, the above-mentioned sugars can be included into (i) the reducing (glucose, fructose, pentose) and (ii) the non-reducing (sucrose) sugar categories.

In wines, some **reducing sugars** remain after fermentation, and their quantity may rise during oak barrel aging. If the reducing sugar content is higher than 1.5 g/L, the wine's ability to resist spoiling could be affected, and wine stewards can perceive sweetness at a value of 2 g/L (*Jackson*, 2020). All studied red wines had the reducing sugar concentration exceeding 2 g/L. Interestingly, WR1 and WR7 scored higher values than 4 g/L reducing sugar concentration, which is most probably due to some technological reasons. The reducing sugar content of the analysed white wine samples falls between 1 and 1.7 g/L, with the exception of WW2, were a value of 3.7 g/L was detected. Our data cannot be considered of absolute relevance since the applied FTIR assay does not detect pentose and other non-sugar reducing compounds (*Wilkes et al.*, 2019). No reducing sugars were found in the analysed Divin brandies, though sucrose-derived caramel colorant (E150) is used to set the colour of the product.

The **ethanol** content of the analysed wines and distillates was also determined (see *Table 3*), and for wines it ranged between 12.12 and 14.62%, while for

distillates it was at about 42%. When compared, no obvious differences were observed between red and white wines. The ethanol content of wines contributes to their stability, but through its antimicrobial property – further strengthened with some polyphenols and proper pH – it could have bacteriocidal and/or bacteriostatic effects on human pathogens such as *Helicobacter pylori, Salmonella enterica* serovar *Enteritidis*, and *Escherichia coli* (*Jackson*, 2020; *Boban et al.*, 2010; *Ruggiero et al.,* 2007). However, it remains an open question whether the ethanol content of wines might have harmful effects on the microbiota of human gut. Nevertheless, some experimental data indicate that polyphenols and ethanol can influence gut microbiota and some inflammatory markers (*Queipo-Ortuño et al.*, 2012). When several alcoholic beverages were investigated in three independent cohort studies, it turned out that moderate red wine consumption was associated with an increased gut microbiota α-diversity (*Le Roy et al.*, 2020). White wines showed a lesser but relevant positive association with α-diversity, while no associations were observed with other alcohol categories. Interestingly, these gut-microbiota-related effects were attributed to the wine polyphenols (*Nash et al.*, 2018).

Another alcohol found in wine is the **glycerol**, which in normal condition is produced by *Saccharomyces cerevisiae*, *Candida pulcherrima* during fermentation, and it is produced in concentrations ranging between 2 and 36 g/L *(Nykänen* & *Suomalainen*, 1983). Higher glycerol concentrations (26 g/L and above) increase wine viscosity (*Jackson*, 2020) and are rot indicators (*Restani et al.*, 2007). Clearly, there is no indication of putrefaction since all the analysed red wines showed values ranging between 7.2 and 10 g/L, the white wines were between 7 and 9 g/L, and the wine distillates had a glycerol content of 3.4–4 g/L. When the glycerol concentration exceeds 13 g/L, the sweeter taste sensation increases (*Jackson*, 2020), but this was certainly not the case of any of the analysed wines (see *Table 3*). Our data is in good agreement with the known facts that usually red wines have a greater glycerol content in comparison to white wines. The studied brandy samples contained traces of glycerol, most probably due to the distillation process (*Sarvarova et al.*, 2011).

The **sulphur dioxide** (E220) content evaluation was also included into the present study to provide further conclusions regarding wine quality. SO_2 is added to the wine to prevent undesired residual fermentation activities, for the inhibition of the oxidative processes, and to avoid spoilage (*Jackson*, 2020). Usually, three chemical forms of SO_2 are distinguished in wines: the total (TSD), the free (FSD), and the bound forms. FSD accounts for the preservative effects of SO_2, and the bound SO_2 arises from the reaction of bisulphite and other wine components. Both bound SO_2 and FSD count towards TSD, which is regulated in most wine-producing countries.

In our experiments, samples WR5 and WR7 indicate low FSD, which may jeopardize safety during storage (see *Table 3*).

Table 3. The analysed wine/Divin brandy parameters

Parameter	Wine/Distillate Sample ID													
	WR1	**WR2**	**WR3**	**WR4**	**WR5**	**WR6**	**WR7**	**WW1**	**WW2**	**WW3**	**WW4**	**WW5**	**D1**	**D2**
TPC, mg GAE/L	1892.24 ±6.52	1743.58 ±11.75	1158.38 ±8.62	1515.90 ±11.29	1203.54 ±3.26	1434.99 ±3.26	1295.75 ±5.65	194.26 ±1.63	179.24 ±1.84	167.89 ±5.40	187.48 ±1.63	194.82 ±4.39	180.51 ±5.08	82.02 ±1.00
Ethanol, % vol.	14.62 ±0.01	13.95 ±0.00	12.12 ±0.01	13.95 ±0.00	13.59 ±0.00	14.37 ±0.01	14.53 ±0.02	14.39 ±0.01	13.79 ±0.01	13.32 ±0.01	14.38 ±0.02	13.24 ±0.02	42.12 ±0.04	42.05 ±0.04
pH	3.86 ±0.00	3.79 ±0.00	3.43 ±0.00	3.69 ±0.00	3.60 ±0.00	3.75 ±0.00	3.56 ±0.00	3.13 ±0.00	3.16 ±0.00	3.35 ±0.01	3.25 ±0.00	3.13 ±0.00	3.59 ±0.00	3.49 ±0.00
Total acidity, g/L	5.30 ±0.01	4.80 ±0.01	5.20 ±0.01	5.00 ±0.02	5.20 ±0.01	5.10 ±0.00	6.50 ±0.02	6.50 ±0.01	6.50 ±0.00	5.80 ±0.00	6.50 ±0.01	6.70 ±0.02	0.50 ±0.00	0.60 ±0.00
Volatile acidity, g/L	0.80 ±0.00	0.70 ±0.01	0.50 ±0.00	0.70 ±0.01	0.70 ±0.00	0.70 ±0.00	0.70 ±0.01	0.50 ±0.00	0.30 ±0.00	0.70 ±0.00	0.40 ±0.00	0.50 ±0.00		
Malic acid, g/L	0.50 ±0.01	0.00 ±0.02	0.30 ±0.00	0.00 ±0.01	0.00 ±0.02	0.00 ±0.01	1.30 ±0.03	1.00 ±0.00	1.50 ±0.00	0.10 ±0.00	1.70 ±0.00	1.50 ±0.00		
Citric acid, g/L	0.180 ±0.009	0.080 ±0.002	0.160 ±0.006	0.130 ±0.002	0.110 ±0.004	0.100 ±0.002	0.240 ±0.000	0.280 ±0.000	0.340 ±0.004	0.220 ±0.002	0.340 ±0.006	0.310 ±0.001		
Lactic acid, g/L	1.00 ±0.01	1.80 ±0.01	1.20 ±0.02	1.50 ±0.05	1.40 ±0.00	1.50 ±0.01	0.50 ±0.01	0.80 ±0.01	0.70 ±0.02	1.80 ±0.04	0.60 ±0.02	0.60 ±0.01		
Tartaric acid, g/L	1.70 ±0.02	1.50 ±0.02	2.00 ±0.01	1.50 ±0.03	2.20 ±0.04	1.80 ±0.00	2.10 ±0.01	2.80 ±0.00	2.60 ±0.03	2.30 ±0.01	2.40 ±0.03	2.60 ±0.02	0.50 ±0.04	0.80 ±0.09
Reducing sugar, g/L	4.20 ±0.22	2.00 ±0.03	2.30 ±0.04	3.60 ±0.17	3.50 ±0.02	3.00 ±0.10	4.90 ±0.07	1.20 ±0.04	3.70 ±0.02	1.70 ±0.02	1.70 ±0.11	1.00 ±0.01		
Glycerol, g/L	10.00 ±0.01	8.20 ±0.09	7.20 ±0.01	8.70 ±0.05	8.30 ±0.07	8.90 ±0.02	10.0 ±0.00	7.50 ±0.03	7.30 ±0.01	9.00 ±0.00	7.60 ±0.02	7.00 ±0.01	3.40 ±0.04	4.00 ±0.02
Density, g/cm^3	0.9960 ±0.0001	0.9935 ±0.0000	0.9935 ±0.0000	0.9936 ±0.0000	0.9933 ±0.0000	0.9934 ±0.0000	0.9947 ±0.0000	0.9886 ±0.0000	0.9903 ±0.0000	0.9906 ±0.0000	0.9893 ±0.0000	0.9899 ±0.0000	0.9709 ±0.0000	0.9702 ±0.0000
CO_2, mg/L	199.37 ±0.11	735.62 ±3.35	466.36 ±3.07	453.7 ±3.09	478.8 ±2.48	384.03 ±2.12	259.26 ±0.69	430.90 ±9.32	1004.04 ±6.91	246.37 ±0.43	704.31 ±4.46	550.40 ±1.00	230.05 ±0.99	226.91 ±0.27
Total SO_2, mg/L	92.0 ±1.0	48.0 ±0.0	81.0 ±2.0	65.0 ±1.0	34.0 ±1.0	73.0 ±0.0	59.0 ±0.0	347.5 ±17.4	80.0 ±4.0	89.0 ±4.5	44.0 ±2.2	65.0 ±3.3		
Free SO_2, mg/L	7.6 ±0.07	5.9 ±0.08	8.3 ±0.15	10.4 ±0.06	0.7 ±0.39	6.2 ±0.10	1.6 ±0.33	212.3 ±10.62	24.0 ±1.20	11.0 ±0.55	7.0 ±0.35	15.0 ±0.75		

In sample WR2, with the lowest level of reducing sugars among the tested red wines, it seems likely that the production of a substantial amount of bound SO_2 was prevented, minimizing the requirement for additional SO_2 during processing. Samples WR1 and WR4 had the highest FSD values, while the white wines, with the exception of WW1, had FSD values between 7 and 24 mg/L. The assessed brandies did not reveal the presence of any SO_2, which complies with the international trends and food safety regulations.

Carbon dioxide (E290) is a by-product of fermentation that exerts a stabilizing-preservative effect, antioxidant activity, and brings a fizzy taste to wines (*Easton*, 2009). Winemaking technologies deal with CO_2 in multiple ways, so that it can be intentionally kept in the wine, gradually removed while the wine is getting processed, or removed intentionally by sparging, while during force carbonation the CO_2 can be intentionally introduced into wine. It is also important to notice the sensory impact of dissolved CO_2 in wine, so it can boost the perception of freshness and acidity together with bitterness and astringency, decreasing sweetness. It should be pinpointed that wines usually contain between 0.4 and 1.0 g/L of CO_2, and, regularly, white wines show higher CO_2 levels than red ones to accentuate their acidity. The assessed red wines had their CO_2 content varying between 0.19 and 0.73 g/L, while in the case of the white wines, the CO_2 concentration seemed to vary at a much larger range: 0.24–1 g/L (see *Table 3*). Samples WR2, WW2, and WW4 contain considerably greater levels of CO_2, allowing winemakers to lower the total sulphur dioxide addition. These samples are likely to have a more acidic taste. On the other hand, WR1 featured the lowest CO_2 level, and it will be regarded as "flat" by wine stewards. As expected, the analysed brandies exhibited the lowest CO_2 levels due to the distillation process.

Finally, it should be mentioned that the assessment of water content, or more specifically the **density** of wines and wine distillates, offers general but important data on the quality of alcoholic beverages. In normal conditions, wine densities above the water-specific value (~1 g/cm^3 depending on the ambient temperature) indicate an increased sugar and/or acid content, while lower wine density values suggest increased ethanol content. Statistically, consumers would rate wines with a lower density (elevated ethanol level) as being of higher quality (*Miadad*, 2015). All the assessed red and white wines had their density values integrated into the 0.98–0.99 g/cm^3 interval, while the Divin brandy densities were about 0.97 g/cm^3 (see *Table 3*).

4. Conclusions

The characterization of alcoholic beverages and in particular of wines and wine distillates is of particular interest for both those involved in such businesses and the gourmet consumers. The competition on the wine market is fierce, and we are often facing adulteration and misguidance. The effort to make wine business

safe and trustworthy is becoming an imperative, and defining validated methods to describe the specific features of wine/wine distillates are increasingly needed (*Palade & Popa*, 2014). Analytical chemistry has been called into action, and the methodology is steadily improving, while a great deal of data continues to emerge (*González-Centeno et al.*, 2015). Despite all the accomplishments, the relevant conclusions regarding wine/brandy authenticity are still missing, though some promising results, by combining advanced analytical chemistry and statistics, look rather promising (*Hu et al.*, 2019). On the other hand, sommeliers have come to the fore, and they are considered knowledgeable wine professionals having a formal training regarding all aspects of wine service, wine and food matching, and wine ageing. It is interesting that at the crossroads of food chemistry coupled with microbiology and wine manufacturing together with marketing, the concept of oenology has emerged as the science of wine and winemaking, with a lot of subjectivism. However, oenology is not completely separable from viticulture, which is the science addressing the cultivation and harvesting of grapes.

By now, wine specialists and enthusiasts all have agreed that in order to define the profile of a certain wine, all relevant measurable parameters of the assessed wine should be included into the evaluation. The history of wine should indicate the geographical conditions specific to a particular wine region, the wine-grape variety, the annual specificity of the chemical composition of the wine-grape(s), the applied wine manufacturing technology, the obtained wine parameters that will be monitored throughout the ageing process, together with the appreciations of sommeliers and consumers.

Taken all together, the presented data on the chemical parameters of several Hungarian and Moldovan red and white wines, including some Moldovan wine distillates too, clearly demonstrate the efficiency of the applied FTIR methodology. According to the current national and international standards, the assessed wines/wine distillates can be considered of high quality. It was our aim to perform a comparative chemical assessment, hoping that some specific features of the analysed wines might be revealed (see *Table 4*). It seems obvious that the total polyphenol content (TPC) of red wines is significantly higher as compared to white wines or wine distillates. It is our opinion that the polyphenols and other phytonutrients of the wines should be more carefully assessed both qualitatively and quantitatively as they might hold relevant information for the wine-specific features, including both traceability and authenticity. In a recent study by Kalló and collaborators (2021), several compounds with antiviral, anti-inflammatory, and anticancer activity were identified in wines from the Tokaj region, using high-resolution mass spectrometry, statistics, and bioinformatics. It is noteworthy that the qualitative and quantitative chemical analysis of the phytonutrient profile including TPC could be an influential tool for the definition of wine specificity.

Table 4. The relative comparison of some representative wine parameters

Product type	Code	TPC	Total acidity (g/L)	Malic acid (g/L)	Lactic acid (g/L)	Tartaric acid (g/L)	Reducing sugar (g/L)	Glycerol (g/L)	CO_2 (g/L)	Origin (Wine region)
White dry Furmint wine	WW1		6.5–6.7	0.5–1.7	0.6–1.8	2.3–2.8	1–3.7	7–9	0.2 –1	Tokaj
	WW2									
	WW3	↓↓↓								
	WW4									
	WW5									
Red dry Cabernet Sauvignon wine	WR1	↑↑↑	5–6.5	0.0–1.3	0.5–1.8	1.5–2.2	2–4.9	7.2 –10	0.2–0.7	Lake Balaton
	WR2	↑↑↑								Lake Balaton
	WR3	↑								Upper Hungary
	WR4	↑↑								South Transdanubia
	WR5	↑								Ștefan Vodă
	WR6	↑↑								Codru
	WR7	↑								Valul lui Traian
Divin VSOP	D1	↓↓↓	0.5–0.6	0	0	0.5–0.8	0	3.4–4	0.2	Divin
	D2	↓↓↓								

Note: The arrows refer to relative values. The upward arrows show increased while the downward decreased values. VSOP – aged for 5 years.

Our results indicate that Tokaj white wines have relatively higher total acidity levels as compared to all the red wines, which could be due to the wine-grape variety and the geographical conditions together with the applied grape cultivation and wine manufacturing technologies. Looking at malic acid content, again, Tokaj white wines surpass Cabernet Sauvignon red wines, and the observed variation range could indicate grapevine, geographical, and/or technological specificities. No malic acid was found in the Moldovan Divin brandy type of wine distillates. The lactic acid content does seem to vary in the same value interval for all analysed wines, while it is not detectable in Divin. Tartaric acid reaches higher values in the case of Tokaj wines, while Cabernet Sauvignon red wines showed lower values and wider variation intervals. Divin distillates did contain some reduced levels of tartaric acid. The reducing sugar content of Tokaj wines seems to be lower than in the case of the assessed red wines. The glycerol content of all studied wines looks similar, though the values for the Tokaj wines fall into a narrower interval as compared to the red wines. A lower amount of glycerol was detected in the Divin wine distillates. In the case of Tokaj wines, the level of CO_2 varied across a larger interval as compared to the red wines, and almost identical levels were visible in the case of the Moldovan wine distillates.

The present study offers clues about the relevance of wine chemistry with respect to the definition of wine specificity. Our data also suggest that after conceiving a general study plan, statistically significant amount of data should be collected on each wine parameter. The fact that the Tokaj wines are showing distinguishable features from the analysed red wines, together with the narrower variation ranges of red wine variables, plead for considering other factors than just the wine-grape variety in the context of plausible explanations. Again, we can conclude that the local climatic, soil, and anthropogenic factors all influence the characteristics of wines, even if they are made of the same grape variety. Therefore, the concept of protected geographical indication should be promoted and further substantiated through scientific proofs for specificity.

Acknowledgements

The authors are thankful to Zsófia Réka Bacsó for her technical assistance throughout the assessment of the wine-specific chemical parameters.

References

[1] Asociația Producătorilor de Divin şi Brandy de Moldova [Association of Divin and Brandy Producers of Moldova (ADBPM)], *Caiet de sarcini la fabricarea băuturii cu indicație geografică protejată „Divin”* [Specifications for the manufacturing of the beverage with the protected geographical indication “Divin”]. Chişinău, Republic of Moldova (2012).

[2] Asociația Producătorilor de Vinuri cu Indicația Geografică Protejată „Ştefan Vodă ” [Association of Wine Producers with Protected Geographical Indication (AWPPGI) “Ştefan Vodă”], *Caiet de sarcini privind fabricarea vinurilor cu indicație geografică protejată „Ştefan Vodă”* [Specifications for the manufacturing of wines with a protected geographical indication “Ş. [Sp Vodă”]. Chişinău, Republic of Moldova (2017).

[3] Asociația Vitivinicolă a Regiunii Geografice Delimitate „Codru” [Wine Association of the Delimited Geographical Region (WADGR) “Codru”], *Caiet de sarcini privind fabricarea vinurilor cu indicație geografică protejată „Codru”*. [Specifications for the production of wines with a protected geographical indication “Codru”] Chişinău, Republic of Moldova (2017).

[4] Balaton-felvidéki Borvidék Hegyközsége [Association of the Balaton Uplands Wine Region (ABUWR)], *A Balaton oltalom alatt álló földrajzi jelzés termékleírása* [Product description of the protected geographical indication Lake Balaton] (2016).

[5] Bede, B., *Wine regions of Hungary. 145 highlights* (2nd ed.) Corvina, Budapest. (2016).

[6] Boban, N., Tonkic, M., Budimir, D., Modun, D., Sutlovic, D., Punda-Polic, V., Boban, M., Antimicrobial effects of wine: Separating the role of polyphenols, pH, ethanol, and other wine components. *Journal of Food Science*, 75. 5. (2010) M322–M326.

[8] Burns, J. et al., Relationship among antioxidant activity, vasodilation capacity, and phenolic content of red wines. *Journal of Agricultural and Food Chemistry*, 48. 2. (2000) 220–230.

[7] Bükki Borvidék Hegyközségi Tanácsa [Bükk Wine Region Association Council (BWRAC)], *A Felső-Magyarország oltalom alatt álló földrajzi jelzés termékleírása* [Product description of the Upper Hungary Protected Geographical Indication] (2018).

[9] Canas, S., Phenolic composition and related properties of aged wine spirits: Influence of barrel characteristics. A review. *Beverages*, 3. 55. (2017).

[10] Etyek-Budai Borvidék Hegyközségi Tanácsa [Etyek-Buda Wine Region Association Council (EBWRAC)], *A Dunántúl oltalom alatt álló földrajzi jelzés termékleírása* [Product description of the protected geographical indication Transdanubia] (2017).

[11] FOSS (2019). *FOSS WineScan™ SO_2* (www.fossanalytics.com.). Denmark.

[12] Fuhrman, B., Volkova, N., Suraski, A., Aviram, M., White wine with red wine-like properties: Increased extraction of grape skin polyphenols improves the antioxidant capacity of the derived white wine. *Journal of Agricultural and Food Chemistry*, 49. 7. (2001).

[13] Generalić Mekinić I., Skračić, Ž., Kokeza, A., Soldo, B., Ljubenkov, I., Banović, M., Skroza, D., Effect of winemaking on phenolic profile, colour components and antioxidants in Crljenak kaštelanski (sin. Zinfandel, Primitivo, Tribidrag) wine. *Journal of Food Science and Technology*, 56. 4. (2019) 1841–1853.

[14] González-Centeno, M. R., Adrover-Obrador, S., Simal, S., Frau, M. A., Femenia, A., Rossellé, C., A multivariate methodology to distinguish among wine. Appellations of Origin. *Agron. Sustain. Dev.*, 35. (2015) 295–304.

[15] Heras-Roger, J., Díaz-Romero, C., Darias-Martín, J., Rios-Mesa, D., Characterization of red wines from Macaronesia. In: Jordão, A. (ed.), *Grapes and wines: Advances in production, processing, analysis, and valorization*. IntechOpen. DOI: 10.5772/intechopen.71795. (2017).

[16] Hu, X. Z. et al., Geographical origin traceability of Cabernet Sauvignon wines based on infrared fingerprint technology combined with chemometrics. *Scientific reports*, 9. 1. (2019) 8256.

[17] IARC. (1988). *Monographs on the evaluation of carcinogenic risks to humans no. 44. Chemical composition of alcoholic beverages, additives and contaminants.* Retrieved on: 17 April 2021, from: https://www.ncbi.nlm.nih.gov/books/NBK531662/.

[18] Jackson, R., *Wine Science* (5th ed.). Elsevier Academic Press Amsterdam. (2020).

[19] Kallithraka, S., Salacha, M., Tzourou, I., Changes in phenolic composition and antioxidant activity of white wine during bottle storage: Accelerated browning test versus bottle storage. *Food Chemistry*, 113. 2. (2009) 500–505.

[20] Kalló, G., Kunkli, B., Győri, Z., Szilvássy, Z., Csősz, É., Tőzsér, J., Compounds with antiviral, anti-inflammatory and anticancer activity identified in wine from Hungary's Tokaj region via high-resolution mass spectrometry and bioinformatics analyses. *International Journal of Molecular Sciences*, 21. 24. (2020).

[21] Le Roy, C. I., Wells, P. M., Si, J., Raes, J., Bell, J. T., Spector, T. D., Red wine consumption associated with increased gut microbiota α-diversity in 3 independent cohorts. *Gastroenterology*, 158. 1. (2020) 270–272.

[22] Miadad, R. (2015). *Wine Quality Exploration.* Retrieved from: http://rstudio-pubs-static.s3.amazonaws.com/80458_5000e31f84df449099a872ccf40747b7.html.

[23] Miller, M., *Wine from inside out. Monitoring acids and pH in winemaking.* (ebook 1). Retrieved on: 10 June 2021, from: https://www.accuvin.com/wp-content/uploads/2015/04/Monitoring-Acids-and-pH-in-Winemaking.pdf.

[24] Nash, V. et al., The effects of grape and red wine polyphenols on gut microbiota – A systematic review. *Food Research International*, 113. (2018) 277–287.

[25] Nykänen, L., Suomalainen, H., *Aroma of beer, wine and distilled alcoholic beverages*. Akademie-Verlag, Berlin. (1983).

[26] O'Geen, A., Pettygrove, S., Southard, R., Minoshima, H., Verdegaal, P., Soil-landscape model helps predict potassium supply in vineyards. *California Agriculture*, 62. 4. (2008) 195–201.

[27] Palade, M., Popa, M.-E., Wine traceability and authenticity – A literature review. *Scientific Bulletin. Series F. Biotechnologies,* 18. (2014) 226–233.

[28] Pisoschi, A. M., Pop, A., Cimpeanu, C., Predoi, G., Antioxidant capacity determination in plants and plant-derived products: A review. *Oxidative Medicine and Cellular Longevity*. (2016).

[29] Queipo-Ortuño, M. I., Boto-Ordóñez, M., Murri, M., Gomez-Zumaquero, J. M., Clemente-Postigo, M., Estruch, R., Cardona Diaz, F., Andrés-Lacueva, C., Tinahones, F. J., Influence of red wine polyphenols and ethanol on the gut microbiota ecology and biochemical biomarkers. *The American Journal of Clinical Nutrition*, 95. 6. (2012) 1323–1334.

[30] Regulation (EC) no 110/2008 of the European Parliament and of the Council of 15 January 2008 on the definition, description, presentation, labelling and the protection of geographical indications of spirit drinks and repealing Council Regulation (EEC) No 1576/89.

[31] Restani, P., Persico, A., Ballabio, C., Fuggetta, D., Moro, E., Simultaneous determination of glycerol, fructose and glucose for quality control of wines. In: *Proceedings of the XXX OIV World Congress*. Milano, Italy. (2007).

[32] Rienth, M., Torregrosa, L., Sarah, G., Ardisson, M., Brillouet, J. M. Romieu, C., Temperature desynchronizes sugar and organic acid metabolism in ripening grapevine fruits and remodels their transcriptome. *BMC Plant Biology*, 16. 1. (2016) 164.

[33] Robinson, J., *The Oxford companion to wine* (3rd ed.). Oxford University Press, Oxford. (2006).

[34] Ruggiero, P., Rossi, G., Tombola, F., Pancotto, L., Lauretti, L., Del Giudice, G., Zoratti M., Red wine and green tea reduce H pylori- or VacA-induced gastritis in a mouse model. *World Journal of Gastroenterology*, 13. 3. (2007) 349–354.

[35] Sarvarova, N., Cherkashina, Y., Evgenev, M., Application of chromatographic methods to the determination of cognac quality indicators. *Journal of Analytical Chemistry*, 66. (2011) 1190–1195.

[36] Smyth, R., *Hungarian wine: A tasting trip to the new old world* (1st ed.) Blue Guides Limited of London. (2016).

[37] Taran, N., Istoria, situația actuală şi perspectivele ramurii viti–vinicole în Republica Moldova [History, current situation, and perspectives of the wine branch in the Republic of Moldova]. *Buletinul Ştiințific al Universității de Stat „Bogdan Petriceicu Haşdeu”*, 2. 4. (2010) 16–36.

[38] Tello, J., Mammerler, R., Čajić, M., Forneck, A., Major outbreaks in the nineteenth century shaped grape phylloxera contemporary genetic structure in Europe. *Scientific Reports*, 9. 1. (2019) 17540.

[39] This, P., Lacombe, T., Thomas, M. R., Historical origins and genetic diversity of wine grapes. *Trends in Genetics*, 22. 9. (2006) 511–519.

[40] Tokaji Borvidék Hegyközségi Tanácsa [Tokaj Wine Region Association Council (TWRAC)], *A Zemplén oltalom alatt álló földrajzi jelzés termékleírása* [Product description of the Zemplén-protected geographical indication]. (2014).

[41] Tsakiris, A., Kallithraka, S., Kourkoutas, Y., Grape brandy production, composition and sensory evaluation. *Journal of the Science Food Agriculture*, 94. (2014) 404–414.

[42] Uniunea Vitivinicola a Regiunii Geografice Delimitate „Valul lui Traian” [The Wine Union of the Delimited Geographical Region (WUDGR) “Valul lui Traian”], *Caiet de sarcini privind fabricarea vinurilor cu indicație geografică protejată „Valul lui Traian”* [Specifications for the manufacturing of wines with a protected geographical indication “Valul lui Traian”]. Chişinău. (2019).

[43] Virdis, C., Sumby, K., Bartowsky, E., Jiranek, V., Lactic acid bacteria in wine: Technological advances and evaluation of their functional role. *Frontiers in Microbiology*. (2021).

[44] Volschenk, H., Vuuren, H., Viljoen-Bloom, M., Malic acid in wine: Origin, function and metabolism during vinification. *South African Journal for Enology and Viticulture*, 27. (2006) 123–136.

[45] Wilkes, E., Huckaba, P., Hodson, G., Harmonizing expression of measurement results in wine analysis: Best practices when testing and reporting sugar in wine. *BIO Web of Conferences*, 12. (2019).

[46] Wine of Moldova, *Istoria Vinului Moldovei* [History of Moldavian wine]. (2021). Retrieved on: 15 June 2021, from: *http://www.wineofmoldova.com/istoria-vinului-moldovei/*.

Acta Univ. Sapientiae, Alimentaria, **14** (2021) 117–129

DOI: 10.2478/ausal-2021-0007

Antioxidant capacity of blackcurrant (*Ribes nigrum* L.) leaves and buds

Cs. Orbán[1]
e-mail: orbancsongor@uni.sapientia.ro

É. Kis[2]
e-mail: kiseva@uni.sapientia.ro

Cs. Albert[2]
e-mail: albertcsilla@uni.sapientia.ro

É. Molnos[2]
e-mail: molnoseva@uni.sapientia.ro

[1] Sapientia Hungarian University of Transylvania,
Faculty of Economics, Socio-Human Sciences and Engineering,
Department of Bioengineering, RO-530104 Miercurea Ciuc, 1 Libertății Sq.
[2] Sapientia Hungarian University of Transylvania,
Faculty of Economics, Socio-Human Sciences and Engineering,
Department of Food Science, RO-530104 Miercurea Ciuc, 1 Libertății Sq.

Abstract. The antioxidant capacity is the combined free radical scavenging effect of all antioxidant compounds found in the studied system. There is a growing need for accurate, numerical determination of this capacity (for easier comparison), so there are many analytical procedures, methods, and measurement systems available to researchers. Neither one is able to model the totality of real, naturally occurring reactions; therefore, conclusions about the antioxidant power of the studied sample can be drawn only after using several methods. In this work, the total phenolic content (TPC) of blackcurrant leaves and buds was determined, and the antioxidant capacity was tested using the DPPH and FRAP assays. 80% methanol was the most effective in the extraction of phenolics followed by 80% ethanol, while for the antioxidant capacity the acetone (50%)/water/acetic acid (2%) mixture proved to be the best. Significant differences were observed between cultivars and sampling dates, but the pattern of variation during the harvest period was similar for all cultivars.

Keywords and phrases: polyphenols, extraction solvent, Ruben, Fertődi and Tisel cultivars

1. Introduction

Blackcurrant (*Ribes nigrum* L.) is a 1–2 m tall shrub, preferring the temperate climate. The crop is widely cultivated both for commercial and domestic use in the major part of Europe and Northern Asia as well as in Romania. The main goal

of blackcurrant growers is harvesting the berries rich in polyphenols and vitamin C, which are used in food and beverage manufacturing. The leaves and buds are also important raw materials for the food industry and cosmetics (*Ziemlewska et al.*, 2021). The leaves of the blackcurrant are simple, lobed, with 3–5 lobes; the 5–10 cm leaves are almost rounded and the leaf edge is irregularly double serrated. Blackcurrant was already popular in mediaeval German folk medicine for rheumatic complaints and as a diuretic. In modern medical terms, the leaves and fruit of the blackcurrant were used to treat patients with anuria. By the 18th century, it had become a popular herb in France, used to treat a wide range of ailments, including gout, joint pain, diarrhoea, and coughs. The health benefits of blackcurrant anthocyanins (BCA) suggested the potential for BCA use as a key ingredient of functional food or therapeutic product to treat or prevent various chronic diseases. Its antioxidant and anti-inflammatory activities have been widely studied and summarized by *Cao et al.* (2021). They protect against oxidative stress, neuron toxicity, and carcinogens. The phytoestrogenic activity also explains certain anti-aging effects of BCA. In their studies, *Nowak et al.* (2016) investigated the effects of blackcurrant leaf extract as an antioxidant and antimicrobial agent in vacuum-packed meat products.

The essential oil of blackcurrant leaves has been studied previously, and differences in the monoterpene hydrocarbon profile between different cultivars were reported (*Stevic et al.*, 2010). *Orav et al.* (2002) analysed the composition of blackcurrant aroma extracts from berries, leaves, and buds and reported that in the oils of the different blackcurrant materials the same substances, though with quantitative differences, were present.

Blackcurrant buds serve as a raw material for the preparation of essential oils and absolutes, which are used for flavouring in cosmetics and food products (*Orav et al.*, 2002). Buds of *R. nigrum* are pedicellate, ovoid, brown, towards the tip with glands, which are very well highlighted in the longitudinal section through them. They contain proanthocyanidines, flavonoids, phenolic acids, amino acids, catechin, enzymes, and vitamin C as well (*Chişe*, 2018).

Nowadays, great emphasis is placed on the study of plants with antioxidant properties. Many have studied the fruit of the blackcurrant and its berries (*Orav et al.*, 2002; *Tabart et al.*, 2006; *Teleszko & Wojdylo*, 2015), but the leaves and buds have received less attention from this point of view.

The antioxidant capacity of *R. nigrum* leaves and buds growing in the Harghita County region (Romania) has not been studied before, and no literature data is available on its antioxidant properties. Therefore, the aim of this study was to determine the total phenolic content and the antioxidant capacity of these two parts of the plants of different cultivars.

2. Materials and methods

2.1. Reagents and chemicals

Methanol (HPLC grade) and Folin–Ciocâlteu reagent (2 N) were purchased from Merck (Germany). Gallic acid (99% purity), L-ascorbic acid (reagent grade), anhydrous sodium carbonate (99% purity), iron (III)-chloride (sublimed grade, ≥ 99.9% trace metals basis), 2,4,6-Tris(2-pyridyl)-s-triazine (TPTZ, for the spectrophotometric determination of Fe, ≥ 99.0%), and 2,2-diphenyl-1-picrylhydrazyl (DPPH, 90% purity) were purchased from Sigma-Aldrich (Germany).

2.2. Plant material

Three varieties of blackcurrant (*R. nigrum* L. Ruben, *R. nigrum L.* Fertődi, and *R. nigrum L.* Tisel) leaves and buds were harvested in the village of Sânmartin, Harghita County, in the spring and summer of 2021. Bud samples were collected on 6 February and 12 April, while the leaf samples were collected on 28 June from each cultivar. The leaves and buds were air dried in shade at 22 ˚C for ten days and then ground in electric grinder.

2.3. Sample preparation

Half gram of dried samples was extracted with 10 mL of the following extraction solvents:

– 80% (v/v) methanol,
– 80% (v/v) ethanol,
– 50% (v/v) acetone with 2% (v/v) acetic acid, and
– 70% (v/v) acetone with 2% (v/v) acetic acid (*Tabart et al.*, 2007).

The mixtures were shaken for 4 hours, centrifuged at 3,461 RCF for 10 minutes, and the supernatant was removed and used for further determinations. Each sample was independently extracted in triplicate, and analyses were performed the same day.

2.4. Total phenolics content (TPC)

Total phenolics were determined according to the Folin–Ciocâlteu method (*Singleton & Rossi*, 1965). This protocol is not very accurate for phenols, but it gives a good picture of the total phenol content. 50 µL of sample diluted with 200 µL of methanol: water (4:1) solution was mixed with 0.25 mL of Folin–Ciocâlteu reagent, and, 1 minute later, 1 mL of sodium carbonate (0.7 M) was added. The mixture

was heated to 50 °C and kept at this temperature for 5 minutes. After cooling, the absorbance was measured at 760 nm on a Varian Cary 50 UV spectrophotometer (Varian Co., USA). Gallic acid (Sigma) was used as standard, and the results were expressed as milligrams of gallic acid equivalents (GAE) per gram of dry weight (DW) of plant material. Measurements were performed in triplicate on each sample.

2.5. DPPH assay

The antioxidant capacity was measured in the methanolic extracts using the DPPH (2,2-diphenyl-1-picrylhydrazyl) assay as described by *Nour et al.* (2014). Briefly, each methanol-diluted extract (50 µL) was mixed with 3 mL of DPPH methanolic solution with a concentration of 0.004% (v/v). The mixture was incubated for 30 minutes at room temperature in the dark, and the absorbance was measured at 517 nm on Varian Cary 50 UV–VIS spectrophotometer (Varian Co., USA).

The percentage of the DPPH consumed was calculated with the following equation:

$$E\% = 100 \cdot \frac{A_o - A_1}{A_o}, \quad (1)$$

where: A_o – the initial absorbance, and A_1 – the absorbance in the presence of the extract.

Measurements were performed in triplicate from all samples.

2.6. Ferric ion reducing/antioxidant power (FRAP) assay

The antioxidant potential of blackcurrant bud and leaf extracts was also determined using a FRAP assay measuring the change in absorbance at 593 nm due to the formation of a blue-coloured Fe^{2+}-tripyridyl-triazine compound from colourless oxidized Fe^{3+}-form by the action of electron-donating antioxidants (*Benzie & Strain*, 1996).

The stock solutions required for the FRAP solution were prepared as follows:

Acetate buffer: 3.1 g Na-acetate + 16 mL acetic acid + 1 L distilled water;

TPTZ solution: 0.312 g TPTZ + 100 mL distilled water + 336 µL HCl;

Ferric chloride solution: 0.54 g $FeCl_3$ + 100 mL distilled water.

The FRAP solution was prepared as follows:

25 mL acetate buffer + 2.5 mL; TPTZ solution + 2.5 mL ferric chloride solution.

The absorbance was measured spectrophotometrically at 593 nm with Varian Cary 50 UV–VIS spectrophotometer (Varian Co., USA). Calibration was performed with ascorbic acid, and results were expressed as milligrams of ascorbic acid equivalents (AsA) per gram of dry weight of plant material. Triplicate measurements were performed from all samples.

2.7. Statistical analysis

Data are expressed as the means ± standard deviation for at least three independent measurements. Statistical analysis was made using Microsoft Excel 2016. Significant differences ($p \leq 0.05$) between means were evaluated by ANOVA and *t*-test.

3. Results and discussions

Buds collected in early February were still dormant, smaller, and more closed than those collected in April. The buds collected in April were slightly swollen and had a strong scent. Leaves were between 5 and 7 cm long and varied in width from 3.5 to 4.5 cm.

In order to determine the antioxidant capacity and the total phenolic content of the samples, the responsible components must be first extracted from the plant material to exclude the possible interfering effects of other constituents during the analyses. Using the four different solvents, which were reported by *Tabart et al.* (2007), *Kowalski & de Mejia* (2021), and *Piotrowski et al.* (2016) to be the best ones to perform the extraction, the goal was to find the one that proves to be the most efficient in the analysis of the collected blackcurrant samples.

3.1. DPPH radical scavenging activity

The results obtained with this method showed that the antioxidant capacity of the bud and leaf extracts was almost 100%, so a tenfold dilution was made, and the measurements were repeated.

The inhibition percentage in the diluted bud extracts (*Figure 1*) appears to be higher in samples collected in February, but only to a very small extent compared to the results of the buds collected in April. As expected, based on literature data, the buds at rest had a higher DPPH radical scavenging activity than the already swollen, popping buds. Analysing the measurement data, it can be established that the DPPH radical scavenging activity of the samples collected from the Ruben cultivars in February did not differ significantly from the ones collected in April ($p > 0.05$).

The comparison of the efficiency of the solvents used for extraction led to the conclusion that the use of acetone-containing solutions is better than the alcoholic ones. This fact was also supported by the significance analysis too since the calculated *p*-value in this case was 0.05. However, comparing the efficiencies of solvents containing 50% (v/v) acetone and 70% (v/v) acetone, it was found that there was no significant difference between the two extraction solvents.

The DPPH assay results in the case of blackcurrant leaf extracts are presented in *Figure 2*. Notable differences were not observed for leaves as compared to buds; the inhibition % values were similar to those obtained for buds collected at different times despite the fact that the average values continue to decrease as the buds develop into leaves (from February to June).

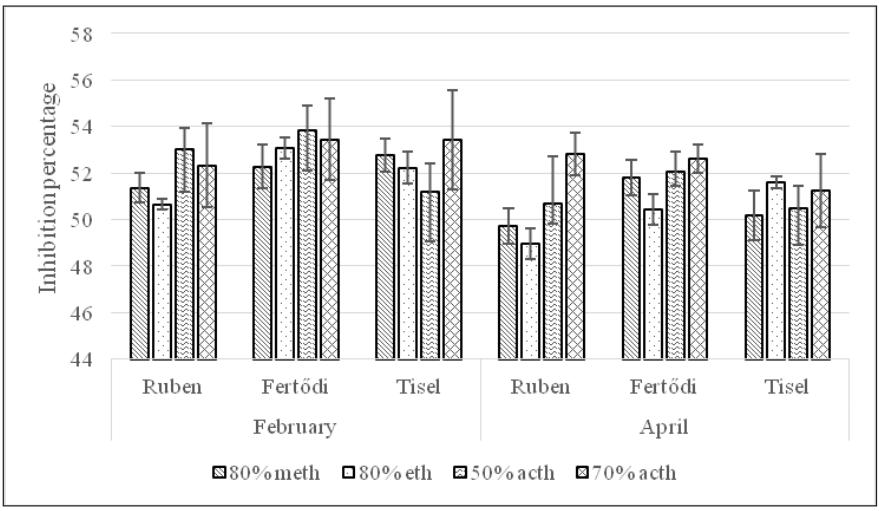

Figure 1. DPPH inhibition percentage in tenfold-diluted blackcurrant bud extracts

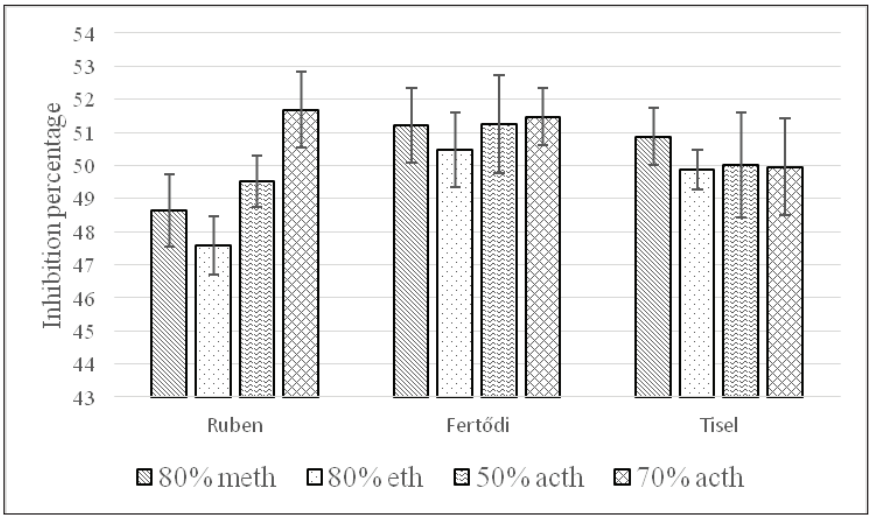

Figure 2. DPPH inhibition percentage in tenfold-diluted blackcurrant leaf extracts

In this case, the significance analysis ($p > 0.05$) showed that the method of extraction (i.e. the quality of the solvent used) did not affect the results of the DPPH assay.

In conclusion, the DPPH inhibition percentage results obtained for leaves and buds were similar to the ones reported previously (*Bryan-Thomas*, 2016; *Krzepilko et al.*, 2018).

3.2. Antioxidant-reducing power (FRAP assay) of the extracts

The results of the FRAP assay led to the conclusion that a higher antioxidant capacity characterized the buds collected in February as compared to the buds collected in April (*Figure 3*). An 8.1% difference can be observed in the average antioxidant capacity in the case of Ruben, 16.4% in Fertődi, and 18.2% in Tisel.

Comparing the cultivars' data, the highest antioxidant capacity was measured from the Fertődi samples. Furthermore, the acetone-containing extraction mixture had a 30% higher efficiency than the alcohol-based mixture, of which the mixture of 50% acetone and 2% acetic acid was found to be the most effective by 32%.

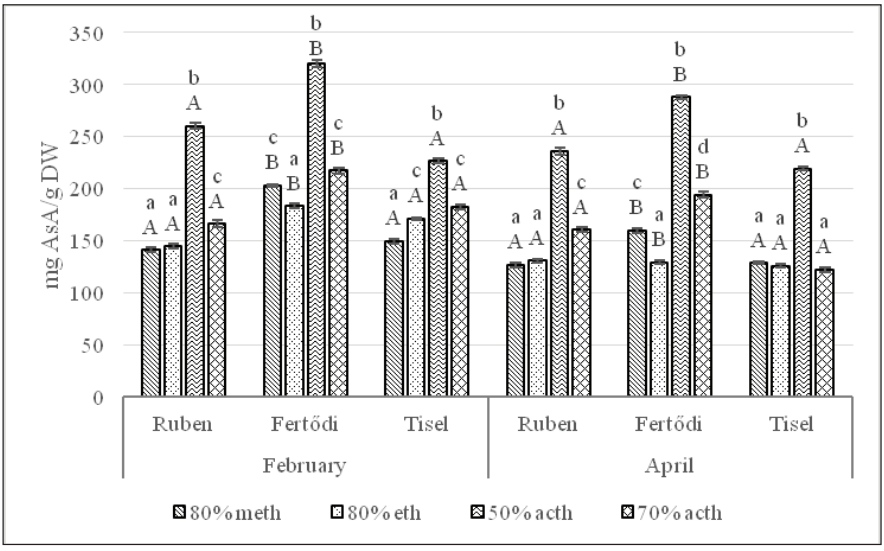

Notes: a–c significantly different between extraction solvents within cultivars; A–C significantly different between cultivars.

Figure 3. FRAP assay of blackcurrant bud extract in mg AsA/g DW

Fertődi shows the highest antioxidant capacity for leaves too (141–278 mg AsA/g DW), while the Ruben and Tisel samples show similar results (132–240 mg AsA/g DW) (*Figure 4*). Despite the difference, statistical analysis shows no significance in these values ($p > 0.05$).

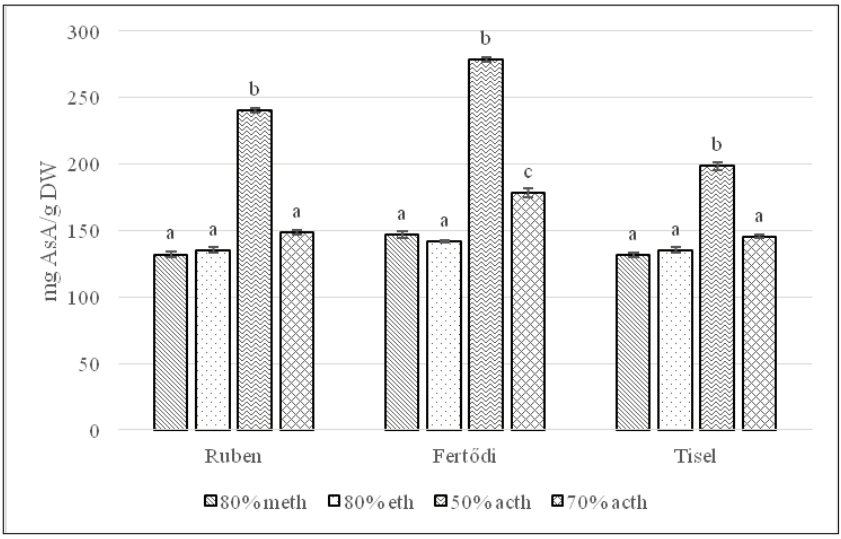

Notes: a–c significantly different between extraction solvents within cultivars.

Figure 4. FRAP assay of blackcurrant leaves in mg AsA/g DW

A study published in 2007, which also tested the antioxidant capacity of blackcurrant leaves, found that leaves harvested in June had the highest antioxidant capacity. This is due to the development of the leaves (*Tabart et al.*, 2007).

3.3. Total phenolic content

The polyphenolic components are responsible for the most significant antioxidant capacity (*Staszowszka-Karkut & Materska*, 2020). These components can be determined spectrophotometrically with the Folin–Ciocâlteu reagent, which is also an antioxidant capacity measurement with electron transfer (*Munteanu & Apetrei*, 2021; *Tabart et al.*, 2009). Various methods were tested to select the best extraction procedure expressed as total phenolics (TP) in buds and leaves. High yields of phenolic compounds were obtained from both buds and leaves with a solvent containing 50% (v/v) ethanol as compared to 30% (v/v) and 70% (v/v) ethanol and an extraction time of 15 min together with an ultrasonic bath. It was also observed that the TP content was higher in the leaves (89–97 mg GAE/g DW), with no significant difference ($p > 0.05$) between the treatments, than in the buds (45–56 mg GAE/g DW), with significant difference ($p < 0.05$) between the treatments (*Vagiri et al.*, 2012). *Tabart et al.* (2007) analysed the blackcurrant cultivar 'Noir de Bourgogne' and measured the total polyphenol content of 46.0 mg/g and 45.1 mg/g chlorogenic acid-equivalent (CAE) fresh weight (FW) in leaves and buds, respectively, using acetone/acetic acid/water (70:28:2) solvent. Previous

work has shown that the best extraction of phenolic compounds from blackcurrant buds and leaves is achieved with the acetone/acetic acid/water mixture.

In contrast, a higher total phenol content in buds was measured as compared to leaves, and the obtained TP values were higher with alcohols than with acetone/acetic acid/water solvents (*Figures 5–6*).

Phytochemical research shows that blackcurrant leaves and buds are a valuable source of polyphenols. The polyphenol content of leaves and buds can be up to five times higher than the polyphenol content of the fruit (*Tabart et al.*, 2006). The composition of the blackcurrant leaves has been described by several authors such as *Cortez & Gonzales de Mejia* (2019), *Ferlemi & Lamari* (2016). They identified mainly flavones and phenolic acids. Depending on the extraction conditions (pH, solvent type), the polyphenol content of the leaves was estimated to be between 4,000 and 20,000 mg/100 g DW (*Tabart et al.*, 2007). The values obtained in this study are situated in the middle of this range.

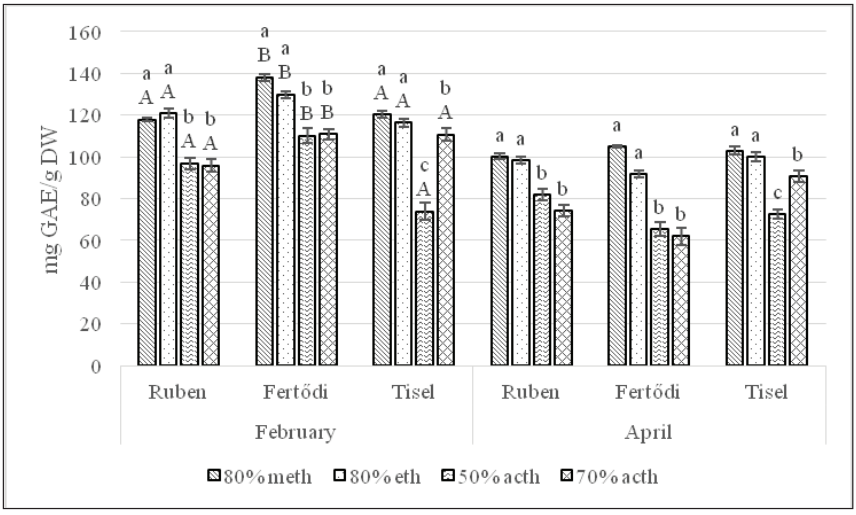

Notes: a–c significantly different between extraction solvents within cultivars; A–B significantly different between cultivars.

Figure 5. The total phenolic content of *R. nigrum* buds in mg GAE/g DW

Significant difference was observed in the total polyphenol content measured in Fertődi cultivars collected in February. No significant differences were noted in total polyphenol content measured in the buds of the different cultivars, collected in April. Nonetheless, a significantly ($p < 0.05$) – 33.7% – higher TP content was measured in the buds collected in February as compared to the ones collected in April in the case of Fertődi cultivars. Among the three blackcurrant cultivars, Fertődi buds had the highest total polyphenol content, with 110–138 mg GAE/g

DW polyphenol content measured in buds collected in February, depending on the solvent. Similar to the FRAP antioxidant capacity, the total polyphenol content of the buds was lower in samples collected in April.

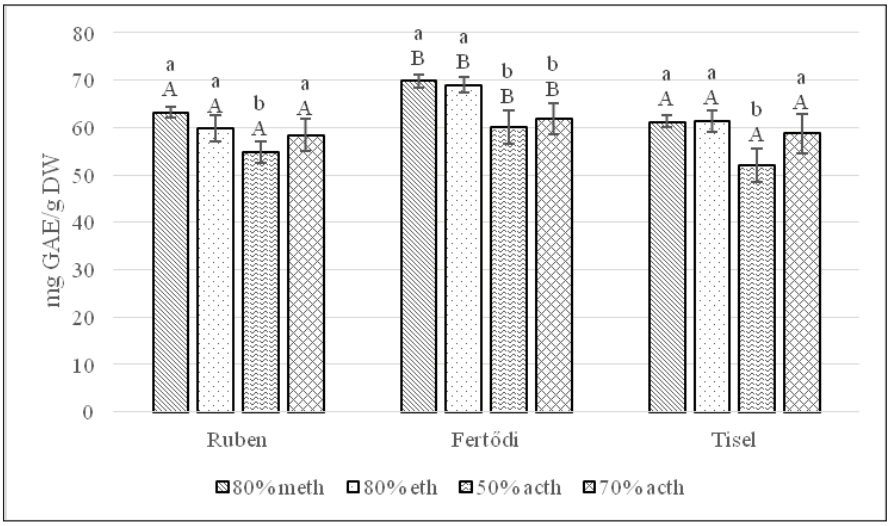

Notes: a–b significantly different between extraction solvents within cultivars; A–B significantly different between cultivars.

Figure 6. The total phenolic content of *R. nigrum* leaves in mg GAE/g DW

The results of the leaf extracts also showed that the total polyphenol content was higher in Fertődi, which is in agreement with the values reported in the literature (*Koczka et al.*, 2018). Furthermore, the alcohol-containing solvent had a significantly higher (26% in buds and 10% in leaves; $p < 0.05$ and $p < 0.05$ respectively) result in the extraction than in the acetone-containing solvent.

Besides the nature of the solvent, phenolic content depends on other extraction parameters too such as pH, temperature, solvent to solid ratio, particle size, and shape of the sample (*Tabart et al.*, 2007).

4. Conclusions

As the previously reported data shows, little attention has been given to research on the biologically active substances of leaves and buds of different *Ribes nigrum* cultivars, which were the research material in this study.

Volatile solvents affect the accuracy of the measurements, as the standard deviation was the highest for acetone in all tests due to its volatility. The correlation study shows that polyphenols contribute significantly to the binding of the DPPH radical

and the reduction of Fe^{3+} ions. The values obtained are in agreement with literature data, and it can be concluded that blackcurrant buds and leaves are an excellent source of antioxidants. It can also be concluded that not only the blackcurrant fruit but also the buds and leaves contain beneficial phenolic compounds and can be utilized to produce functional, health-protective products. The results show that in order to obtain the optimal content of the desired bioactive compounds, it is important to take into account the genotype, the place of cultivation, the time of harvest, the stage of bud development, and the position of the leaves. Of the different solvents, the acetone (50%)/water/acetic acid (2%) mixture proved to be the best for obtaining extracts with higher antioxidant capacities in blackcurrant leaves and buds. For extracting phenolic compounds, we recommend solutions containing 80% ethanol or methanol. In terms of harvesting time, February proved to be better for buds. Although there were significant differences in phenolic compound content and antioxidant activity between the cultivars studied, the pattern of change during the growing season was quite similar.

Therefore, these natural substances could be added to products in order to prevent or delay their deterioration by action of oxygen in the air.

References

[1] Benzie, I. F. F., Strain, J. J., The ferric reducing ability of plasma (FRAP) as a measure of antioxidant power: The FRAP assay. *Analytical Biochemistry,* 239. 1. (1996) 70–76.

[2] Bryan-Thomas, J., A comparative study of the antioxidant activity (DPPH), total flavonoid, total tannin, total polyphenol levels in plant extracts of the *Annona muricata*, *Ribes nigrum* and *Manilkara zapota*. *International Journal of Scientific and Research Publications*, 6. 9. (2016) 490–494.

[3] Cao, L., Park, Y., Lee, S., Kim, D.-O., Extraction, identification, and health benefits of anthocyanins in blackcurrants (*Ribes nigrum* L.). *Applied Sciences*, 11. (2021) 1863.

[4] Chişe, E., *Studiul comparativ al unor specii de Ribes în vederea valorificării lor ca şi plante medicinale.* PhD thesis, IOSUD – Universitatea de Vest Vasile Goldiş din Arad, Şcoala Doctorală de Biologie. (2018).

[5] Cortez, R. E., Gonzalez de Mejia, E., Blackcurrants (*Ribes nigrum*): A review on chemistry, processing, and health benefits. *Journal of Food Science*, 84. (2019) 2387–2401.

[6] Ferlemi, A. V., Lamari, F. N., Berry Leaves: An alternative source of bioactive natural products of nutritional and medicinal value. *Antioxidants (Basel)*, 5. 2. (2016) 17.

[7] Koczka, N., Stefanovits-Bányai, É., Prokaj, E., Element composition, total phenolics and antioxidant activity of wild and cultivated blackberry (*Rubus fruticosus* L.) fruits and leaves during the harvest time. *Notulae Botanicae Horti Agrobotanici Cluj-Napoca*, 46. 2. (2018) 563–569.

[8] Kowalski, R., de Mejia, E. G., Phenolic composition, antioxidant capacity and physical characterization of ten blackcurrant (*Ribes nigrum*) cultivars, their juices, and the inhibition of type 2 diabetes and inflammation biochemical markers. *Food Chemistry*, 359. (2021) 129889.

[9] Krzepiłko, A., Prazak, R., Skwaryło-Bednarz, B., Święciło, A., Buds, leaves, and seeds of blackcurrant—Source of bioactive substances with pro-health properties. *Food Science. Technology. Quality*, 2. (2018) 24–33.

[10] Munteanu, I. G., Apetrei, C., Analytical methods used in determining antioxidant activity: A review. *International Journal of Molecular Sciences*, 22. (2021) 3380.

[11] Nour, V., Trandafir, I., Cosmulescu, S., Antioxidant capacity, phenolic compounds and minerals content of blackcurrant (*Ribes nigrum* L.) leaves as influenced by harvesting date and extraction method. *Industrial Crops and Products*, 53. (2014) 133–139.

[12] Nowak, A., Czyzowska, A., Efenberger, M., Krala, L., Polyphenolic extracts of cherry (*Prunus cerasus* L.) and blackcurrant (*Ribes nigrum* L.) leaves as natural preservatives in meat products. *Food Microbiology*, 59. (2016) 142–149.

[13] Orav, A., Kailas, T., Müürisepp, M., Composition of blackcurrant aroma isolated from leaves, buds, and berries of *Ribes nigrum* L. *Proceedings of the Estonian Academy of Sciences. Chemistry*, 51. 4. (2002) 225–234.

[14] Piotrowski, W., Oszmiański, J., Wojdyło, A., Łabanowska, B. H., Changing the content of phenolic compounds as the response of blackcurrant (*Ribes nigrum* L.) leaves after blackcurrant leaf midge (*Dasineura tetensi* Rübs.) infestation. *Plant Physiology and Biochemistry*, 106. (2016) 146–158.

[15] Singleton, V. L., Rossi, J. A., Colorimetry of total phenolics with phosphomolybdic-phosphotungstic acid reagents. *American Journal of Enology and Viticulture*, 16. 3. (1965) 144–158.

[16] Staszowska-Karkut, M., Materska, M., Phenolic composition, mineral content, and beneficial bioactivities of leaf extracts from black currant (*Ribes nigrum* L.), raspberry (*Rubus idaeus*), and aronia (*Aronia melanocarpa*). *Nutrients*, 12. 2. (2020) 463.

[17] Stevic, T., Savikin, K., Ristic, M., Zdunic, G., Jankovic, D., Krivokuca-Dokic, D., Vulic, T., Composition and antimicrobial activity of the essential oil of the leaves of black currant (*Ribes nigrum* L.) cultivar Cacanska crna. *Journal of the Serbian Chemical Society*, 75. 1. (2010) 35–43.

[18] Tabart, J., Kevers, C., Pincemail, J., Defraigne, J.-O., Dommes, J., Antioxidant capacity of black currant varies with organ, season, and cultivar. *Journal of Agriculture and Food Chemistry*, 54. 17. (2006) 6271–6276.

[19] Tabart, J., Kevers, C., Pincemail, J., Defraigne, J.-O., Dommes, J., Comparative antioxidant capacities of phenolic compounds measured by various tests. *Food Chemistry*, 113. (2009) 1226–1233.

[20] Tabart, J., Kevers, C., Sipel, A., Pincemail, J., Defraigne, J.-O., Dommes, J., Optimisation of extraction of phenolics and antioxidants from black currant leaves and buds and of stability during storage. *Food Chemistry*, 105. (2007) 1268–1275.

[21] Teleszko, M., Wojdylo, A., Comparison of phenolic compounds and antioxidant potential between selected edible fruits and their leaves. *Journal of functional foods*, 14. (2015) 736–746.

[22] Vagiri, M., Ekholm, A., Andersson, S. C., Johansson, E., Rumpunen, K., An optimized method for analysis of phenolic compounds in buds, leaves, and fruits of black currant (*Ribes nigrum* L.). *Journal of Agricultural and Food Chemistry*, 60. 42. (2012) 10501–10510.

[23] Ziemlewska, A., Zagórska-Dziok, M., Nizioł-Łukaszewska, Z., Assessment of cytotoxicity and antioxidant properties of berry leaves as by-products with potential application in cosmetic and pharmaceutical products. *Scientific Reports*, 11. (2021) 3240.

Acta Univ. Sapientiae, Alimentaria, **14** (2021) 130–156

DOI: 10.2478/ausal-2021-0008

Some aspects of plate number estimation of plate heat exchangers (PHEs). A case study

A. Szép
e-mail: alszep@uni.sapientia.ro

Cs. D. András
e-mail: andrascsaba@uni.sapientia.ro

Sapientia Hungarian University of Transylvania, Cluj-Napoca,
Faculty of Economics, Socio-Human Sciences and Engineering,
Department of Food Science, RO-530104 Miercurea Ciuc, 1 Libertății Sq., Romania

Abstract. For the proper estimation of the plate number (N) of a plate heat exchanger (PHE) – in addition to the flow rates and thermophysical properties of fluids –, an appropriate correlation is needed for convective heat transfer coefficient (α) calculation. When one does not have a criterial equation for the corresponding plate shape, we propose a selecting method for α. With the suggested relationships from literature, we calculate the plate number of a geometrically known, similar heat duty PHE and choose those relationships that give the same plate number with the known heat exchanger. In our case study, the plate number determined by any of the screened equations for whole milk preheating has almost the same value ($n = 10 \pm 1$) regardless of the method used to solve the PHE model (plate efficiency and $N_{converg}$ or $K_{converg}$ convergence methods). For liquids' thermophysical property estimation, we recommend averaging the values given by equations from literature, followed by equation fitting.

Keywords and phrases: milk, thermophysical properties, plate heat exchangers, plate number estimation

1. Introduction

The main heat exchanger type in food industry is the plate heat exchanger (PHE), used for the heating or cooling of media with good rheological properties and with low solid content, to avoid solid deposition on the surface (usually Newtonian liquids as milk, various fruit juices, high-temperature cooking oils, cleaning and process waters, etc.) (*Mariott*, 1979; *Stoica et al.*, 2007; *Singh & Heldman*, 2013; *Kakaç et al.*, 2020). Hot water or steam (heating medium), chilled water, cooling water, brine or propylene glycol water solutions (cooling medium) are used as thermal agent (*Macovei*, 2001; *Kakaç & Liu*, 2002; *Heldman*, 2007; *Thulukkanam*, 2013). The PHE's operation is characterized by a continuous steady state (*Shah & Sekulić*, 2002; *Singh & Heldman*, 2013; *Roetzel et al.*, 2020), but it can also

be used for setting batch temperature (cooling/heating). Its widespread use is mainly due to its high heat transfer coefficient and the resulting low specific space requirements (*Stephan*, 2010; *Wang & Sunden*, 2007; *Thulukkanam*, 2013; *Neagu et al.,* 2014). An advantage of gasketed heat exchangers is cleanability (*Fonyó & Fábry*, 2004; *Neagu et al.*, 2014) and, perhaps more importantly, the variability of connection configurations (*Fonyó & Fábry*, 2004; *Macovei*, 2001) as: single-pass parallel switching (mainly countercurrent) (*Chisholm & Wanniarachchi*, 1999; *Singh & Heldman*, 2013), possible multipass-flow (serial switching) (*Macovei*, 2001), and, of course, multiple parallel and serial switching could be combined (*Maroulis & Saravacos*, 2003). The brazed exchangers have constant plate numbers, and the plates are joined by pressure or thermal welding, this type being used mainly in building central heating systems.

In the food industry, the almost exclusively (excepted high-pressure, e.g. water-air heaters) utilized PHE types are gasketed PHEs. Their advantage consists in their modular structure, wherefore the heat exchange surface could be easily increased, by supplementation of the plate number, and their cleaning is more simple and complete, in agreement with food industry requirements. Furthermore, this structure made suitable the compact assembly of plate pasteurizer, with heat recovery zones, as required in dairy and fruit industries. In the interstices between the plates, the flow is usually turbulent since the interstices are tight (usually 2–5 mm), and the plate surfaces are corrugated to assure the breaking of current lines, to increase the surface area, and to improve the plate's mechanical strength. The geometry, number, angle, and size of the corrugation are determinant for flow direction and local velocity (*Focke et al.*, 1985; *Heavner et al.*, 1993; *Muley & Manglik*, 1999; *Gut et al.*, 2004; *Kakaç et al.*, 2020). Therefore, the use of dimensionless number relations (criterial equations) to determine heat transfer requires great attention as their validity is restricted to the particular plate type. Nevertheless, in the literature, we can find criterial equations considered generally applicable, independent from plate type (*Kumar*, 1984; *Fonyó & Fábry*, 2004; *Macovei*, 2001; *Kakaç & Liu*, 2002; *Stoica et al.* 2007). The main goal of this article is to examine the general validity of these relations; as a case study, a milk pasteurizer pre-heating zone was chosen.

The engineering tasks related to the PHEs can be divided into several groups (*Stoica et al.*, 2007):

a) Assigning the appropriate heat exchanger type and size to a given heat power duty, sizing design, i.e. determination of the heat exchanger surface;
b) Checking the suitability of the heat exchanger for a certain duty, when the heat transfer surface area is given, and the flow parameters that assure the outlet temperature of the target fluid need to be determined;
c) Estimation of the outlet temperature of a medium with given flow characteristics and known inlet temperature in a heat exchanger of a defined configuration.

To achieve this goal, some basic knowledge is required (*Haslego & Polley*, 2002; *Faulkner*, 2013; *Dvorak & Vit*, 2017; *Ezgi*, 2017), namely:

a) The properties of the heat exchange media, influencing the impulse and heat transfer (density, dynamic or kinematic viscosity, thermal conductivity, and specific heat capacity). It is recommended to know the temperature dependence of the thermophysical properties;
b) The proper mathematical model of the heat exchanger;
c) The values of the geometric size of the plate and the thermal conductivity of the structural material of the plates;
d) The effect on heat transfer rate of the interaction between the flowing media and the structural material of the heat exchanger (fouling or deposition effect).

Moreover, it is important to know specific solving methods of the heat exchanger model because the model is usually underdetermined as it contains more variables than relationships (*Maroulis & Saravacos*, 2003; *Shah & Sekulić*, 2002; *Stoica et al.*, 2007; *Mota et al.*, 2015).

2. Materials and methods

In order to select the proper criterial equations from the literature and to determine the appropriate thermophysical properties required for using them in the design process, we used the method described below.

The thermophysical properties were plotted as a function of temperature (from the tabular data or fitted functions), excluding those that did not show the same trend as the majority, and then the average was calculated taking into account the remaining values; finally, a function was fitted on the average values. The fitted function was the same form as given in the literature for the specific thermophysical property (e.g. polynomial or exponential type relations).

To select the appropriate criterial equation for the heat transfer modelling of the PHE, the plate number required to perform the given thermal duty was determined using three resolution methods: plate number convergence ($N_{converg}$), overall heat transfer convergence ($K_{converg}$), or thermal efficiency (NTU-ε) – for a PHE of known size and thermal duty. Criterial correlations that result in plate number values equal to or close to the real heat exchanger were considered suitable for the proposed design task, namely for the determination of the plate number of the milk pre-heater PHE.

For modelling purposes, Excel software (Microsoft) and for graphical representation Statistica 8.0 (Statsoft, Inc) was used.

Estimation of the thermophysical properties of media involved in the heat exchange

The properties of the various heating and cooling media (water, water-ethylene glycol, water-propylene-glycol, steam) can be found quite accurately in the literature, but mostly in tabulated form (not as a correlation). From this tabular data, by means of different commercial software, it is usually easy to establish good correlations, which will be suitable in mathematical models.

In the case of liquid foods, it is a little more difficult to find the right correlations given the multitude of ingredients and interactions between them, which modify the thermo- and hydrodynamic (thermophysical) properties (*Rohm et al.*, 1996; *Minim et al.*, 2002; *Lewis*, 2006; *Heldman*, 2007; *Munir et al.*, 2016). Besides the widely utilized and accepted method of Choi and Okos (1986) based on the weighted average of the six food component properties (carbohydrate, protein, fat, mineral salt, fibre, and water), there is a great deal of other literature data on specific liquid foods as milk and other liquid dairy products. Furthermore, the Choi–Okos equations do not include viscosity, which property is crucial for heat transfer. Thermophysical property functions have a great variety as they do not always take into account all the constituents. The properties are expressed in function of different main component (fat, protein, total non-fat solid, or total solid content) molar or mass concentrations and temperature (*Gavrilă et al.*, 2002; *Apetrei et al.*, 2002; *Madoumier et al.*, 2015). Regardless of the chosen equation, it is always highly recommended to validate them by measurements or to compare the calculated results with reliable data. In every case when we start to estimate the properties from a very wide variety of regression equations with variable precision and validity range, a question arises: which one should be applied in the model?

To resolve this uncertainty, we propose an approximation method that assumes the following steps: we plotted the data from the correlations (as a function of temperature) found in literature (see *tables 1a–d*) and excluded the equation(s) showing markedly different values, whereafter we fitted a curve on the average value of the property. The method is presented only for whole milk, but the calculation was made also for other liquid milk varieties by using supplementary relations (*Hu et al.*, 2009) such as skim and standardized milk (data not shown). *Tables 1a–d* contain the relations from literature for the thermophysical properties (density, dynamic viscosity, heat capacity, thermal conductivity) of whole milk.

Table 1a. Equations for milk density estimation

No.	ρ (kg · m^{-3})	References
1.	$\rho = 1040.51 - 0.2665\,t - 2.307 \cdot 10^{-3}\,t^2 - -(F\%) \cdot (0.967 + 9.69 \cdot 10^{-3}\,t - 4.781 \cdot 10^{-5}\,t^2)$	*Kessler*, 2002 *Bertsch & Cerf*, 1983
2.	$\rho = 1185.64 - 0.341(t + 273.15) - 58.239\,X_w - 58.107\,X_F$	*Minim et al.*, 2002
3.	$\rho_f = 925.56 - 0.41757\,t$ $\rho_p = 1329.0 - 0.5184\,t$ $\rho_c = 1599.1 - 0.31046\,t$ $\rho_m = 2423.8 - 0.28063\,t$ $\rho_w = 1\,000.0791 + 0.008380\,t - 0.00561612\,t^2 + 0.0000135933\,t^3$ $\rho_{milk} = \frac{1}{\frac{X_f}{\rho_f} + \frac{X_p}{\rho_p} + \frac{X_c}{\rho_c} + \frac{X_m}{\rho_m} + \frac{X_w}{\rho_w}}$, x_i – mass fractions of: fat (f), protein (p), carbohydrate (c), minerals (m), and water (w) $\rho_{milk} = \sum_{i=1}^{5} \rho_i y_i$. *where*: $y_i = \frac{\frac{X_i}{\rho_i}}{\sum_1^5 \frac{X_i}{\rho_i}}$. y_i – volumetric fraction.	Engineering Toolbox Database
4.	$\rho = 1042.01 - 0.37\,t - 3.6 \cdot 10^{-4}\,t^2$, for whole milk	*Bon et al.*, 2010 *Munir et al.*, 2016
5.	$\rho = 1035 - 0.358\,t + 0.0049\,t^2 - 0.00010\,t^3$	*Rao et al.*, 2005
6.	$\rho = 1028.9 - 0.195\,t + 1.432\,X_F$ Fat content: 3…6%	*Watson & Tittsler*, 1961
7.	$\rho = 1038.2 - 0.17\,t - 0.003\,t^2 + \left(133.7 - \frac{475.5}{t}\right) \cdot X_F$	*Phipps*, 1969
8.	$\rho_{20\,°C} = \frac{1000}{0.123 \cdot X_F + 0.9665}$	*McCarthy & Singh*, 1990
9.	$DM\,(\%) = 400 \cdot (d - 1) + 1.21 \cdot (\%F) + 0.72$ DM(%) – dry matter, %, $\%F$ – fat content, $d = \frac{\rho_{milk}}{\rho_{water}}$	*Lewis*, 2006

Table 1b. Equations for milk viscosity estimation

No.	η (mPa · s)	References, temperature interval
1.	$\eta = Exp[(3.03 \cdot 10^{-5}\, t^2 - 0.01813\, t + 0.609) + (2.3 \cdot 10^{-4}\, t^2 + 5.49 \cdot 10^{-2}\, t + 0.206) \cdot X_F + (2.5 \cdot 10^{-3}\, t^2 + 0.629\, t + 5.42) \cdot {X_F}^2]$	*Kessler*, 2002
2.	$ln\eta = (3.92 \cdot 10^{-5}\, t^2 - 1.951 \cdot 10^{-2}\, t + 0.666) + (-9.53 \cdot 10^{-4}\, t^2 + 0.1674\, t - 4.37) \cdot X_F + (9.75 \cdot 10^{-3}\, t^2 - 1.739\, t + 98.3) \cdot {X_F}^2$	*Bertsch & Cerf*, 1983; 70… 135 °C
3.	$\eta = (0.9565 - 1.3004 \cdot 10^{-3}\, t + 1.958 \cdot 10^{-4}\, t^2) + (47.66 - 1.144 \cdot t + 7.2642 \cdot 10^{-3}\, t^2) \cdot X_F$	*Munir et al.*, 2016
4.	$ln\eta = (A_o + A_1 \cdot t + A_2 \cdot t^2) + (B_o + B_1 \cdot t + B_2 \cdot t^2) \cdot (\%F) + (C_o + C_1 \cdot t + C_2 \cdot t^2) \cdot (\%DM)^2$ i: 0 — A_i: 0.249 — B_i: 0.02549 — C_i: 0.000543 i: 1 — A_i: -0.013 — B_i: -0.000098 — C_i: -0.0000139 i: 2 — A_i: 0.000052 — B_i: 0.0000004 — C_i: 0.000000117	*Fernandez-Martin*, 1972; 0… 80 °C
5.	$A_F = 3.46 - 0.025\, t + 1.6 \cdot 10^{-4}\, t^2$ $A_P = 15.367 - 0.175\, t + 0.0017\, t^2$ $A_C = 3.35 - 0.0238\, t + 1.25 \cdot 10^{-4}\, t^2$ $\eta_{milk} = \eta_{water} \cdot Exp\left(\frac{\sum_1^3 A_i X_i}{X_{H_2O}}\right)$	*Morison et al.*, 2013
6.	$ln\eta = \frac{2721.5}{273 + t} + 0.1\,(\%F) - 8.9$	*Bakshi & Smith*, 1984; 0…. 30 °C
7.	$lg\eta = (1.2876 + 11.0710^{-4}\, t) \cdot \left(X_F + X_F^{5/3}\right) + 0.7687 \frac{1000}{273 + t} - 2.437$	*Phipps*, 1969; 40… 80 °C
8.	$\eta = \frac{6.45}{t^{0.85}} \cdot exp(0.05 + 0.08 \cdot (\%\, DM))$	*Ganea & Cojoc*, 2011
9.	$\eta = 2.82 - 4.58 \cdot 10^{-2}\, t + 2.83 \times 10^{-4}\, t^2$, for whole milk	*Bon et al.*, 2010
10.	$\eta = 0.96 + 0.058(\%F) + 0.156(\%P)$	*Rohm et al.*, 1996; at 25 °C

Table 1c. Equations for specific heat capacity estimation

No.	c_p $(J \cdot kg^{-1} \cdot K^{-1})$	References
1.	$c_p = 3744.48 + 1.15\,t + 0.00393\,t^2$	*Bon et al.*, 2010 *Munir et al.*, 2016
2.	$c_p = 1401.7 + 2.1 \cdot (t + 273.15) + 2181.6 \cdot X_w - 1.743 \cdot X_F$	*Minim et al.*, 2002
3.	$c_{p\,(P)} = 2008.2 + 1.2089\,t - 1.3129 \cdot 10^{-3}\,t^2$ $c_{p\,(F)} = 1984.2 + 1.4733\,t - 4.8008 \cdot 10^{-3}\,t^2$ $c_{p\,(C)} = 1548.8 + 1.9625\,t - 5.9399 \cdot 10^{-3}\,t^2$ $c_{p\,(M)} = 1092.6 + 1.8896\,t - 3.6187 \cdot 10^{-3}\,t^2$ $c_{p\,(H_2O)} = 4176.2 - 0.0980864\,t + 5.4731 \cdot 10^{-3}\,t^2$ $c_{p\,milk} = \sum_{1}^{5} c_{p(i)} \cdot X_i$	*Choi* & *Okos*,1986
4a.	$c_p = 1424\,X_c + 1549\,X_P + 1675\,X_F + 4187\,X_w$	*Heldman* & *Singh*, 1981
4b.	$c_p = 4187 \cdot X_w + (1373 + 11.3\,t) \cdot (1 - X_w)$	*Hwang* & *Gunasekaran*, 2003
5.	$c_p = 3692 + 2.976\,t$	*McCarthy* & *Singh*, 1990
6.	$c_p = 41.88 \cdot (\%H_2O) + (13.71 + 0.1129 \cdot t) \cdot (\%DM)$	*Fernandez-Martin*, 1972
7.	$c_p = 4190 - 2765\,X_C - 125\,X_P - 335\,X_F$	*Ganea* & *Cojoc*, 2011

Table 1d. Equations for heat conductivity estimation

No.	λ $(W \cdot m^{-1} \cdot K^{-1})$	References
1.	$\lambda = (5.9 \cdot 10^{-1} + 1.2 \cdot 10^{-3}\,t)(1 - 7.8 \cdot 10^{-3}\,X_{DM})$	*More & Prasad*, 1988
2.	$\lambda = (326.58 + 1.0112\,t - 3.37 \cdot 10^{-3}\,t^2) \cdot (0.46 + 0.54\,X_w) \cdot 0.00173$	*Riedel*, 1949
3a. 3b. 3c.	$\lambda = -0.2145 + 0.0014 \cdot (t + 273.15) + 0.4171\,X_w - 0.092\,X_F$ $\lambda = 0.0163 + 1.4 \cdot 10^{-3} \cdot (t + 273.15) + 0.2\,X_w + 0.04\,X_F$ $\lambda = 0.5279 + 0.00213\,t - 7.32 \cdot 10^{-6}\,t^2 \cdot (1 - 0.843\,X_F + 0.0019\,t)$	*Minim et al.*, 2002, *Munir et al.*, 2016 (from Minim data)
4.	$\lambda = 0.49 + 2.23 \times 10^{-3}\,t - 1.08 \times 10^{-5}\,t^2$ (whole milk)	*Bon et al.*, 2010
5.	$\lambda = (0.565 + 0.0018\,t - 0.0000058\,t^2) \cdot [1 - 0.005 \cdot (10 + 2 \cdot \%F) \cdot R]$ R- concentrating factor (DM in concentrate/DM in whole milk)	*McCarthy* & *Singh*, 1990

No.	$\lambda\ (\mathbf{W \cdot m^{-1} \cdot K^{-1}})$	References
6.	$\lambda_P = 0.17881 + 1.1958 \cdot 10^{-3}\, t - 2.7178 \cdot 10^{-6}\, t^2$	*Choi & Okos*, 1986
	$\lambda_f = 0.18071 - 2.7604 \cdot 10^{-4}\, t - 1.7749 \cdot 10^{-7}\, t^2$	
	$\lambda_c = 0.20141 + 1.3874 \cdot 10^{-3}\, t - 4.3312 \cdot 10^{-6}\, t^2$	
	$\lambda_m = 0.32962 + 1.4011 \cdot 10^{-3}\, t - 2.9069 \cdot 10^{-6}\, t^2$	
	$\lambda_w = 0.57109 + 1.7625 \cdot 10^{-3}\, t - 6.7036 \cdot 10^{-6}\, t^2$	
	$\lambda_{milk} = \sum_1^5 \lambda_i y_i.\ \ \lambda_{milk} = \frac{1}{\sum_i^5 \frac{y_i}{\lambda_i}}.\ \ y_i = \frac{\frac{X_i}{\rho_i}}{\sum_1^5 \frac{X_i}{\rho_i}}$	

The mathematical model of the heat exchangers

The mathematical model of PHE is based on the steady state heat transfer (*Fonyó* & *Fábry*, 2004; *Singh* & *Heldman*, 2013). Taking into account the heat transport for elementary surface, the fundamental equation of plate heat exchangers can be established:

$$\dot{Q} = K \cdot K \cdot A \cdot \Delta T_m, \text{ W} \tag{1}$$

The transferred heat flux ($\dot{Q}$) is determined by the surface (A), overall heat transfer coefficient (K), and the mean logarithmic temperature (ΔT_m).

$$\Delta T_m = \frac{(T_1^o - T_2) - (T_1 - T_2^o)}{ln\frac{T_1^o - T_2}{T_1 - T_2^o}} \tag{2}$$

The overall heat transfer coefficient (K) can be calculated in function of convective heat transfer coefficient, the heat conductivity of plate material (stainless steel), and the fouling heat resistance:

$$\frac{1}{K} = \frac{1}{\alpha_1} + r_1 + \frac{\delta}{\lambda} + r_2 + \frac{1}{\alpha_2}, \tag{3}$$

where: α_1, α_2 are convective heat transport coefficients, W/(m²·K), r_1, r_2 is the fouling resistance, and (m²·K/W), $\frac{\delta_p}{\lambda_p}$ is the heat resistance of the plate material, (m²·K/W).

For the estimation of convective heat transfer coefficient, the well-known relation can be used:

$$Nu = C \cdot Re^m Pr^n \Gamma^p, \tag{4}$$

where: C, m, n, p are coefficients depending on the flow characteristics of the two fluids and on the configuration of plates (see the appendices).

Empirical data are used to estimate the heat resistances of the fouling deposits. This is shown in *Table 2*.

Table 2. Heat resistance of deposits of different heat transfer agents (Fonyó & Fábry, 2004)

Heat transfer agent	r, m²·K/W	Heat transfer agent	r, m²·K/W
Dirty water	0.00009-0.00017	Clean water	0.000017-0.000043
Sugar juice	0.00013-0.00017	Fermented juice	0.000043
Brine	0.000086	Beer	0.00001-0.00003
River water	0.00004-0.00009	Milk	0.00001-0.00003

In order to determine the convective heat transfer coefficients, in addition to the liquid properties, it is necessary to know the nature of the flow regime, which is in fact determined by the geometry of the plates (plate corrugation and width, channel width) as well as the mass flow rates. The mathematical model of the PHE is shown in *Table 3.*

Table 3. Mathematical model for the PHEs' plate number calculation

Plate length, m	L
Plate width, m	W
Plate distances (gap width), m	δ
Plate surface, m²	$A_{plate} = L \cdot W \cdot \varphi; \quad \varphi = 1.15 - 1.2$
Interplate flow section area, m²	$S = W \cdot \delta$
Hydraulic diameter, m	$d_e = \frac{2 \cdot \delta}{\varphi}$
Released heat flow, W	$\dot{Q}_1 = m_{\tau 1} \cdot c_{p1} \cdot (T_1^o - T_1)$
Received heat flow, W	$\dot{Q}_2 = -m_{\tau 2} \cdot c_{p2} \cdot (T_2^o - T_2)$
Transferred heat, W	$\dot{Q} = K \cdot A \cdot \Delta T_m$ $A = N \cdot A_{plate} \cdot \varphi = N \cdot W \cdot L \cdot A_{plate} \cdot \varphi$
Flow velocities, m/s	$w_1 = \frac{m_{\tau 1}/\rho_1}{n_g - k \cdot A_k}$, $w_2 = \frac{m_{\tau 2}/\rho_2}{n_g - k \cdot A_k}$, n_g – gap number for one fluid

Reynolds numbers	$Re_1 = \frac{\rho_1 \cdot w_1 \cdot d_e}{\eta_1}, Re_2 = \frac{\rho_2 \cdot w_2 \cdot d_e}{\eta_2}$
Nusselt numbers	$Nu_1 = C \cdot Re_1^m Pr_1^n, Nu_2 = C \cdot Re_2^m Pr_2^n$
Convective heat transfer coefficients, W/(m²·K)	$\alpha_1 = \frac{Nu_1 \cdot \lambda_1}{d_e}, \alpha_2 = \frac{Nu_2 \cdot \lambda_2}{d_e}$
Overall heat transfer coefficients, W/(m²·K)	$K = \left(\frac{1}{\alpha_1} + r_1 + \frac{\delta}{\lambda} + r_2 + \frac{1}{\alpha_2}\right)^{-1}$
Calculated plate number from thermal relations	$N_t = \frac{\dot{Q}_{1/2}}{K \cdot \Delta T_m \cdot A_{plate}}$

The algorithms of several solution methods of the selected models (*Table 3*) for particular cases are presented below (*Jackson* & *Troupe*, 1966; *Okada*, 1972; *Kreith*, 1999; *Kakaç* & *Liu*, 2002; *Shah* & *Sekulić*, 2002; *Wright* & *Heggs*, 2002, *Wang et al.*, 2007; *Singh* & *Heldman*, 2013; *Thulukkanam*, 2013; *Faulkner*, 2013; *Dvorak* & *Vit*, 2017):

Plate number convergence ($N_{converg}$) steps:

1. Calculation of the thermal balance and the thermophysical parameters to determine the transferred heat and the outlet temperatures;
2. Calculation of the logarithmic mean temperature;
3. Giving an initial value for interplate gap number for a single fluid;
4. Determination of the flow velocities for both fluids, then calculation of the Reynolds numbers;
5. Determination of the values of thermophysical properties for the two fluids at their mean temperature followed by the calculation of the Nusselt numbers with the adopted criterial equation;
6. Calculation of the individual heat transfer coefficients for both fluids, using the Nusselt numbers, followed by the determination of the overall heat transfer coefficient for the PHE;
7. Calculation of heat transfer area followed by the determination of plate number (the fractional result needs rounding up);
8. Determination of channel numbers for each fluid. Impair plate number gives individual equal channel number for the two fluids;
9. Comparison of the resulted channel number with the initially chosen value in point 3. When these two values are equal, the real plate number is found; otherwise, the process will be restarted from point 3.

Overall heat transfer coefficient convergence ($K_{converg}$) steps:

1. Choosing the value for overall heat transfer coefficient (K value);
2. Calculation of the heat transfer area followed by the determination of plate number (the fractional result needs rounding up);
3. Determination of channel numbers for each fluid. For odd plate numbers, the number of channels for the two fluids will be equal, while for even plate numbers, the number of channels will differ by one unit;
4. Calculation in cascade of the fluid flow velocities, Re numbers, Nu numbers, and individual heat transfer coefficients;
5. Calculation of the value for K;
6. Comparison of the K value with the initially chosen K value in point 1. When these two values are equal, the real K value is found; otherwise, the process will be restarted from the beginning, setting the calculated K value as initial value, and the whole calculus will be repeated.

As the method converges, the final value of K will be obtained in several cycles.

Iterative calculation for thermal efficiency method (NTU-ε) with number of plate convergence

1. Determination of the changed heat:

$$\dot{Q}_{ch} = m_{\tau 1} \cdot \left(c_{p1}^{o} \cdot T_1^{o} - c_{p1} \cdot T_1\right) \text{ or: } \dot{Q}_{ch} = -m_{\tau 2} \cdot \left(c_{p2}^{o} \cdot T_2^{o} - c_{p2} \cdot T_2\right);$$

2. Calculation of the unknown temperatures (if any), the average temperatures, drawing the temperature profile, the temperature diagram, and, finally, determination of the logarithmic average temperature difference:

$$(\Delta T_m): \bar{T}_1 = 0.5 \cdot (T_1^{o} + T_1),\ \bar{T}_2 = 0.5 \cdot (T_2^{o} + T_2), \bar{T}_{wall} = 0.5 \cdot (\bar{T}_1 + \bar{T}_2);$$

3. Determination of the values of thermophysical (ρ, c_p, λ, η) properties for the two fluids at their mean temperature;
4. Calculation of the water equivalent of the two fluids: $C_1 = m_{\tau 1} c_{p1}$, $C_2 = m_{\tau 2} c_{p2}$;
5. Calculation of the ratio of the water equivalent of the two fluids: $R = \frac{C_{min}}{C_{Max}}$;
6. Calculation of the ratio of the thermal efficiency of the PHE:

$$\varepsilon = \frac{C_1(T_1^{o} - T_1)}{C_{min}(T_1^{o} - T_2^{o})} = -\frac{C_2(T_2^{o} - T_2)}{C_{min}(T_1^{o} - T_2^{o})};$$

7. Calculation of the number of transfer units (*NTU*): $NTU = \frac{ln\frac{1-\varepsilon R}{1-\varepsilon}}{1-R}$;
8. Choosing the value for plate number followed by calculation of the gap numbers for both fluids;

9. Calculation in cascade of the fluid flow velocities, Re numbers, Nu numbers, and individual heat transfer coefficients;
10. Calculation the value for overall heat transfer coefficient (K), taking into account the fouling resistance of both fluids;
11. Calculation of plate number: $N = \frac{\varepsilon \cdot C_{min}(T_1^o - T_2^o)}{K \cdot A_{plate} \cdot \Delta T_m} = \frac{NTU \cdot C_{min}}{K \cdot A_{plate} \cdot \varphi}$ and rounding up the value of N;
12. Comparison of the resulted plate number with the initially chosen value in point 8. When these two values are equal, the real plate number is found; otherwise, the process will be restarted from point 8, giving the calculated N for the chosen value.

The selection of the appropriate criterial equation for determination of the convective heat transfer coefficient from a large number of possibilities is quite a difficult task. We propose to extend the *Neagu et al.* (2014) method as follows:

a) we choose PHE with known geometry and appropriate/similar duty;
b) solving the model with the suggested criterial relations, determining the number of plates with all three convergence methods, and
c) selecting those relations that give close or equal plate number with the real one.

3. Results and discussions

The results of the average thermophysical property calculations

Whole milk density

Figure 1 shows the temperature dependence of the density of whole milk (fat content of 3.9%) based on the relations given in *Table 1a*; the average value is also shown.

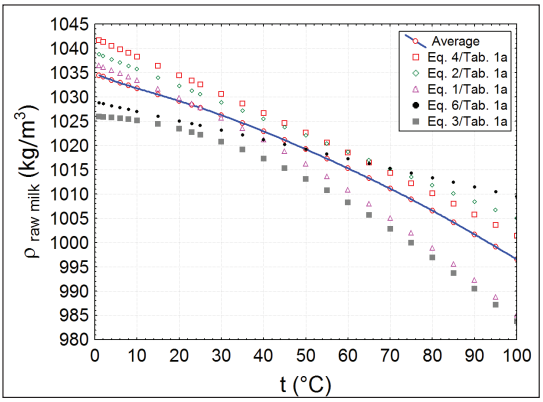

Figure 1. The temperature dependence of the density of whole milk (the curve number represents the equation in *Table 1a*)

The resulted fitted polynomial on the average value is:

$$\rho = 1034.4827 - 0.239955\, t - 0.00119775\, t^2 - 2.016 \cdot 10^{-6}\, t^3,\ \mathrm{kg/m^3},\ \mathrm{kg/m^3} \quad (5)$$

Whole milk dynamic viscosity

Figure 2 shows the temperature dependence of the dynamic viscosity of whole milk (fat content of 3.9%) based on the relations given in *Table 1b*; the average value is also shown. Correlation 8 (*Ganea & Cojoc*, 2011) was excluded as its results differed substantially from the rest of the values. As can be seen in *Figure 2*, the data are grouped in three distinct domains.

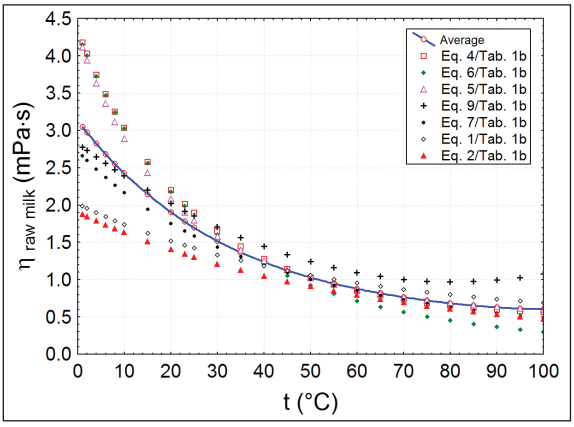

Figure 2. The temperature dependence of the dynamic viscosity of whole milk (the curve number represents the number of equation in *Table 1b*)

The resulted fitted function on the average value is:

$$\eta = 3.14926 \cdot e^{(1.08 \cdot 10^{-4}\, t^2 - 0{,}02765\, t)},\ \mathrm{mPa{\cdot}s} \quad (6)$$

It should be noted that at any temperature the value of the average viscosity is approximately twice as much as the water viscosity.

Whole-milk-specific heat capacity

Figure 3 shows the temperature dependence of the specific heat capacity of whole milk (fat content 3.9%), based on the relations given in *Table 1c*; the average value is also shown. It is to be mentioned that there exist substantial differences between the predicted values, mainly at lower temperatures, and also in the slope of the fitted line.

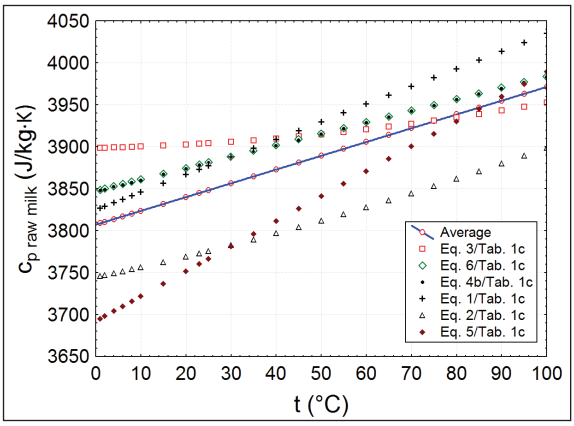

Figure 3. The temperature dependence of the specific heat capacity of whole milk (the curve number represents the number of equation in *Table 1c*)

The resulted fitted polynomial on the average value is:

$$c_p = 3808.7988 - 1.569827\,t,\ \mathrm{J/(kg{\cdot}K)} \tag{7}$$

Whole milk thermal conductivity

Figure 4 shows the temperature dependence of the heat capacity of whole milk (fat content 3.9%), based on the relations given in *Table 4*; the average value is also shown. Some relations were omitted since they did not fit into the trend or because they are lacking the data that would have specified the temperature range or fat content. There are substantial differences between the predicted values, mainly at lower temperatures.

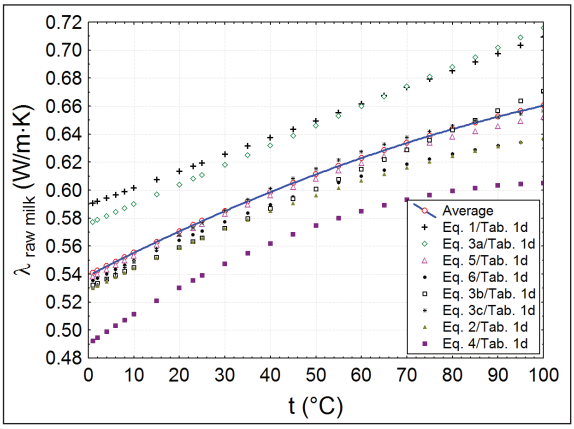

Figure 4. The temperature dependence of the thermal conductivity of whole milk (the curve number represents the number of equation in *Table 1d*)

The resulted fitted function on the average value is:

$$\lambda = 0.539 + 1.6674 \cdot 10^{-3} t - 4.3633 \cdot 10^{-6} t^2 - 1.7715 \cdot 10^{-9} t^3, \text{ W/(m·K)} \quad (8)$$

The selection of the appropriate criterial equations

To select the appropriate criterial equation, we have chosen the Singh and Heldman (2013) case study for PHEs, knowing not only the characteristics of the two fluids but also plate sizes and number. The two chosen heat duties of the PHE ($\dot{Q}$) are shown in *Table 4* and the main geometrical dimensions of the PHE in *Table 5.*

Table 4. The thermal duty of the reference PHE

Fluid	Mass flow, m_i, kg/s	t^0, °C	t, °C	t_m, °C	$\dot{Q}$, kW
Water	15 / 1.5	95	47	71	3008 / 300
Apple juice	10 / 1.0	15	87	51	3008 / 300

Table 5. The geometric dimensions of the reference PHE

L, m	W, m	δ, m	φ	S, m²	A_{plate}, m²	d_e, m	δ, m	λ, W/(m·K)
1.2	0.8	0.004	1.17	0.0032	1.12	0.0068	0.0006	15

The solutions of the model calculation performed with Excel flowsheets are presented in *Table 6*.

Table 6. The results of plate number calculated by several recommended criterial equations

$$Nu = C \cdot Re^m \cdot Pr^n \cdot \left(\frac{\eta}{\eta_{wall}}\right)^p$$

C	m	n	p	N for 3008 kW	N for 300 kW	References
0.4	0.64	0.4	0	50	6	*Singh* & *Heldman*, 2013
0.273	0.65	0.3/0.4	0	166	19	*Fonyó* & *Fábry*, 2004
0.352	0.536	0.3	0	266	27	*Maroulis* & *Saravacos*, 2003
0.023	0.8	0.33	0	No conv.	7100	*Maroulis* & *Saravacos*, 2003

C	m	n	p	N for 3008 kW	N for 300 kW	References
0.0366	0.8	0.3	0	No conv.	733	*Maroulis & Saravacos*, 2003
0.0188	0.889	0.292	0	No conv.	No conv.	*Gut et al.*, 2004
0.4	0.65	0.4	0	49	6	*Mariott*, 1979
0.374	0.66	0.33	0.15	47	6	*Macovei*, 2001; *Stoica* 1, 2007
0.314	0.666	0.333	0	56	6	*Stoica* 2, 2007
0.157	0.66	0.4	0	252	27	*Okada et al.*, 1972
0.348	0.64	0.33	0.17	63	6	*Kumar*, 1984
0.44	0.5	0.33	0.17	310	26	*Mulley et al.*, 1997/99

Because all three methods (plate number convergence, thermal efficiency, and heat transfer coefficient convergence) led to the same results, the plate convergence method was used for the selection of the criterial equations provided by the literature. Only five of the recommended correlations lead to a value close to reality, resulting 51 (for 3,008 kW) and 6 (for 300 kW) plate numbers. Thus, we continued to work only with the Kumar, Macovei, Stoica 1–2, Mariott, and Singh and Heldman correlations, as could be observed in *Table 6*.

Application of the selected relations to the milk preheater

The plate number for the preheater section of the pasteurizer installation was estimated. The heating was performed from the initial milk storage temperature (4 °C) to the optimal temperature for centrifugal separation (~44 °C) in the single-flow, countercurrent M6-type plate heat exchanger (Alfa Laval). The heat duty of the PHE is shown in *Table 7*, the calculated milk properties in *Table 8*, and the main geometrical dimensions of the M6 PHE in *Table 9*.

Table 7. The thermal duty of the milk preheater

Cold fluid	Mass flow, m_r, kg/s	t^0, °C	t, °C	t_m, °C	$\dot{Q}$, kW
Whole milk	1.7800	4	44	23	273760
Standardized milk	1.6756	68	26	47	273760

Table 8. Calculated thermophysical properties of milk

Milk type	t_m, °C	ρ kg/m³	η mPa·s	c_p	λ W/(m·K)	Pr
Whole milk	23	1028.32	1.7745	3844.94	0.575	11.85
Standardized milk	47	1020.00	1.057	3890	0.608	6.76

Table 9. The geometric dimension of the modelled PHE, type M6 (Alfa Laval)

L, mm	W, mm	δ, mm	φ	S, m²	A, m²	d_e, m	δ, m	λ_p, W/(m·K)
920	320	2.5	1.17	0.0007	0.288	0.004273	0.0008	15

The calculation results for the plate number required for preheating are shown in *Table 10*.

Table 10. The numbers of plates determined by the different design methods and the chosen formula for heat exchange coefficient

Name	Criterial equations	K W/(m²K)	Calculated plate number (N)		
			$N_{converg}$	NTU-e	$K_{converg}$
Kumar	$Nu = 0.348 \cdot Re^{0.640} Pr^{0.333} \left(\frac{\eta}{\eta_{wall}}\right)^{0.15}$	3706	11	11	11
Macovei, Stoica 1	$Nu = 0.374 \cdot Re^{0.666} Pr^{0.400} \left(\frac{\eta}{\eta_{wall}}\right)^{0.17}$	3986–4046	11	11	10
Stoica 2	$Nu = 0{,}314 \cdot Re^{0.666} Pr^{0.3/0.4}$	3680	11	11	11
Mariott	$Nu = 0.4 \cdot Re^{0.65} Pr^{0.4}$	4375	9	9	9
Singh & Heldman	$Nu = 0.4 \cdot Re^{0.64} Pr^{0.4}$	4188	10	10	10

It can be seen that the overall heat transfer coefficient values determined with different equations were situated in the range of K = 3680 – 4375 W/(m²·K), while the required number of plates take values between N = 9 and 11. It can also be seen that the convergence method gave almost the same plate number for each criterial equation. In engineering design, a safety factor is usually recommended, wherefore we propose to use the maximum value of the plate number (N = 11).

4. Conclusions

A key premise for a reliable and realistic computer-aided engineering model solution is the proper selection of the input data; for food engineering purposes, these are mainly the thermophysical properties of the fluids. For modelling purposes,

using continuous functions are more adequate than tabular data. Therefore, mainly polynomial or exponential functions are used for the determination of the value of temperature-dependent thermophysical property of the two exchanger fluids. The proposed data estimation method could be used for both tabular and correlation-based data selection and processing. By averaging the literature data from multiple sources describing the thermophysical properties of milk, equations were fitted, enabling the estimation of a property of adequate accuracy within a given range of temperature, and even beyond, using prudent extrapolation. In order to estimate the plate numbers of a PHE, in addition to the properties, it is necessary to know the criterial equations established between the corresponding dimensionless numbers. When we do not have a relation corresponding to the geometry of the plate (this is the case for most design tasks), it is necessary to select the appropriate one from the many relations recommended by the literature. For this purpose, we propose a useful methodology – somehow with reverse engineering philosophy – by recalculating the plate numbers of a known heat exchanger with the available relations. Based on the obtained results, those criterial equations are worth choosing which give close results to the real plate numbers. Using the selected criterial equation(s), the plate number required to perform the given thermal duty can be determined with good accuracy, using either the plate number convergence ($N_{converg}$), the overall heat transfer convergence ($K_{converg}$), or the thermal efficiency (NTU-ε) for resolving the PHE model. In future PHE design, we recommend the presented method for criterial equation selection.

References

[1] Apetrei, I., Ciocan, M. E., Simion, A. I., Gavrilă, L., Modelling of the thermophysical properties of milk II. Thermal capacity and thermal conductivity. *Annals of DAAAM for 2002 & Proceedings of the 13th International DAAAM Symposium "Intelligent Manufacturing & Automatisation: Learning From Nature" Conference*. 23–26 October 2002, Vienna, Austria. (2002) 15–16.

[2] Bakshi, A. S., Smith, D. E., Effect of fat content and temperature on viscosity in relation of pumping requirements of fluid milk products. *Journal of Dairy Science*, 67. (1984) 1157–1160.

[3] Bertsch, A. J., Cerf, O., Dynamic viscosities of milk and cream from 70 to 135 °C. *Journal of Dairy Research*, 50. (1983) 193–200.

[4] Bon, J., Clemente, G., Vaquiro, H., Mulet, A., Simulation and optimization of milk pasteurization processes using a general process simulator (ProSimPlus). *Computers and Chemical Engineering*, 34. (2010) 414–420.

[5] Buonopane, R. A., Troupe, R. A., Morgan, A., Heat transfer design method for plate heat exchangers. *Chemical Engineering Progress*, 59. (1963) 57–61.

[6] Chisholm, D., Wanniarachchi, A. S., Maldistribution in single-pass mixed-channel plate heat exchangers. *Compact Heat Exchangers for Power and Process Industries. HTD ASME*, 201. (1999) 95–99.

[7] Choi, Y., Okos, M., Effects of temperature and composition on the thermal properties of foods. *Food Engineering Process Applications*, 1. (1986) 93–101.

[8] Dvorák, V., Vit, T., CAE methods for plate heat exchanger design. *Energie Procedia*, 134. (2017) 234–243.

[9] Ezgi, C., Basic design methods of heat exchangers. In: Murshed Sohel, M. S., Lopes, M. M. (eds.), *Heat exchangers design, experiments and simulation*. IntechOpen. (2017).

[10] Fernandez-Martin, F., Influence of temperature and composition on some physical properties of milk and milk concentrates. I. Heat capacity. *Journal of Dairy Research*, 39. 1. (1972) 65–73.

[11] Fernández-Martín, F., Influence of temperature and composition on some physical properties of milk and milk concentrates II. Viscosity. *Journal of Dairy Research*, 39. 1. (1972) 75–82.

[12] Focke, W. W., Zachariades, J., Olivier, I., The effect of corrugation inclination angle on the thermohydraulic performance of heat plate exchangers. *International Journal of Heat and Mass Transfer*, 28. 8. (1985) 1469–1479.

[13] Fonyó Zs., Fábry Z., *Vegyipari művelettani alapismeretek*. Budapest: Nemzeti Tankönyvkiadó. (2004) 404.

[14] Ganea, G., Cojoc, D., *Utilaj tehnologic în industria alimentară*. Chisinău, Editura Tehnică. (2011) 6–11.

[15] Gavrilă, L., Simion, A., Apetre, I., Modelling of the thermophysical properties of milk I. Density and viscosity. *Annals of DAAAM for 2002 & Proceedings of the 13th International DAAAM Symposium "Intelligent Manufacturing & Automatisation: Learning From Nature" Conference*, 23–26 October 2002, Vienna, Austria. 179–180.

[16] Gulenoglu, G., Akturk, F., Aradag, S., Sezer, N., Kakaç, S., Experimental comparison of performances of three different plates for gasketed plate heat exchangers. *International Journal of Thermal Sciences*, 75. (2014) 249–256.

[17] Gut, J. A. W., Fernandes, R., Pinto, J. M., Tadini, C. C., Thermal model validation of plate heat exchanger with generalized configuration. *Chemical Engineering Science*, 59. (2004) 4591–4600.

[18] Haslego, C., Polley, G., Designing plate-and-frame heat exchangers. *Chemical Engineering Progress*, 9. (2002) 32–37.

[19] Heavner, R. L., Kumar, H., Wanniarachchi, A. S., Performance of an industrial plate heat exchanger: Effect of chevron angle. *AICHE Symposium Series*, 89. (1993) 262–267, 295.

[20] Heldman, R. D., *Fundamentals of Food Process Engineering*. 3rd ed., New York, Springer Science. (2007) 223–238.

[21] Heldman, R. D., Singh, R. P., *Food Process Engineering*. 2nd ed., Westport, AVI Publishing. (1981).

[22] Hu, J., Sari, O., Eicher, S., Rakotozanakajy, R. A., Determination of specific heat of milk at different fat content between 1 and 59 °C using micro DSC. *Journal of Food Engineering*, 90. (2009) 395–399.

[23] Hwang, C. H., Gunasekaran, S., Specific heat capacity. In: Heldman, D. R., Moraru, Carmen I. (eds.), *Encyclopedia of Agricultural, Food, and Biological Engineering*. New York, Marcel Dekker. (2003) 1572–1580.

[24] Jackson, B. W., Troupe, R. A., Plate heat exchanger design by ε-NTU method. *Chemical Engineering Progress Symposium Series*, 62. (1966) 185–190.

[25] Kakaç, S., Hongtan, L., Pramuanjaroenkij, A., *Heat exchangers: Selection, rating and thermal design*, 4th ed. Boca Raton, CRC Press. (2020).

[26] Kakaç, S., Liu, H. *Heat exchangers: Selection, rating and thermal design*. 2nd ed. Boca Raton, CRC Press. (2002) 394.

[27] Kessler, H. G., *Food and bio process engineering: Dairy technology*. Münich, Verlag Kessler. (2002).

[28] Kreith, F. *Mechanical engineering handbook*. Boca Raton, CRC Press. (1999).

[29] Kumar, H., The plate heat exchanger: Construction and design. *1st UK National Conference of Heat Transfer*, 86. (1984) 1275–1286.

[30] Lewis, M. J., *Physical properties of foods and food processing systems.* Cambridge, Woodhead Publishing. (2006).

[31] Macovei, V., *Calcule de operații* şi *utilaje pentru precesarea termică* şi *biochimică* în *biotehnologie*. Galați, Editura Alma. (2001) 59.

[32] Madoumier, M., Azzaro-Pantel, C., Tanguy, G., Gésan-Guiziou, G., Modelling the properties of liquid foods for use of process flowsheeting simulators: Application to milk concentration. *Journal of Food Engineering*, 164. (2015) 70–89.

[33] Mariott, J., Where and how to use plate heat exchangers. *Chemical Engineering*, 78. 8. (1971) 127–133.

[34] Maroulis, Z. B., Saravacos, G. D., *Food process design*. New York, Marcel Dekker. (2003).

[35] McCarthy, O. J., Singh, H., Physico-chemical properties of milk. In: McSweeney, P., Fox, P. (eds.), *Advanced dairy chemistry. Volume 3: Lactose, water, salts, and minor constituents*. New York, Springer. (1980) 707–758.

[36] Minim, L. A., Coimbra, J. S. R., Minim, V. P. R., Telis-Romero, J., Influence of temperature and water and fat contents on the thermophysical properties of milk. *Journal of Chemical Engineering Data*, 47. (2002) 1488–1491.

[37] More, G. R., Prasad, S., Thermal conductivity of concentrated whole milk. *Journal of Food Process Engineering*, 10. 2. (1988) 105–112.

[38] Morison, K. R., Phelan, J. P., Bloore, C. G., Viscosity and non-Newtonian behavior of concentrated milk and cream. *International Journal of Food Properties*, 16. (2013) 882–894.,

[39] Mota, F. A. S., Carvalho, E. P., Ravagnani, M. A. S. S., Modeling and design of plate heat exchanger. In: Kazi, S. N. (ed.), *Heat transfer studies and applications.* IntechOpen. (2015) 165–199.

[40] Muley, A., Manglik, R. M., Enhanced heat transfer characteristics of single-phase flows in a plate heat exchanger with mixed Chevron plates. *Journal of Enhanced Heat Transfer*, 4. 3. (1997) 187–201.

[41] Muley, A., Manglik, R. M., Experimental study of turbulent flow heat transfer and pressure drop in a plate heat exchanger with chevron plates. *Journal of Heat Transfer*, 121. (1999) 110–117.

[42] Munir, M. T., Yu, Z., Wilson, D. I., Young, B. R., Virtual milk for modelling and simulation of dairy processes. *Journal Dairy Science*, 99. (2016) 3380–3395.

[43] Neagu, A. A., Koncsag, C., Bărbulescu, A., Botez, E., Calculation methods for gasket plate heat exchangers used in vegetable oil manufacture. *Revista de Chimie*, 66. 9. (2014) 1503–1509.

[44] Okada, K. Ono, M., Tominura, T., Konno, H., Ohtani, S., Design and heat transfer characteristics of new plate heat exchanger. *Heat Transfer – Japanese Research*, 1. 1. (1972) 90–95.

[45] Phipps, L. W., The interrelationship of the viscosity, fat content and temperature of cream between 40 and 80 °C. *Journal of Dairy Research*, 36. (1969) 417–426.

[46] Rao, M. A., Rizvi, S. S. H., Datta, A. K., *Engineering properties of foods*. Boca Raton, CRC Press. (2005).

[47] Riedel, L., Thermal conductivity measurements on sugar solution, fruit juice and milk. *Chemie Ingenieur Technik*, 21. 17. (1949) 340–341.

[48] Roetzel, W., Luo, X., Chen, D. *Design and operation of heat exchangers and their networks*. London, Elsevier Academic Press. (2020).

[49] Rohm, H., Müller, A., Hend-Milnera, I., Effect of composition of raw milk viscosity. *Milchwissenschaft*, 51. (1996) 259–261.

[50] Shah, R. K., Sekulić, D. P., *Fundamentals of heat exchanger design*. Hoboken, Wiley. (2002).

[51] Singh, P. R., Heldman, D. R., *Introduction to Food Engineering*. 5th ed. Amsterdam, Elsevier-Academic Press. (2013).

[52] Stephan, P. (ed.), *VDI Heat Atlas*. Berlin–Heidelberg, Springer-Verlag. (2010).

[53] Stoica, A., Stroescu, M., Dobre, T., Floarea, O., *Operații termice in industria alimentară.* Bucharest: Politehnica Press. (2007) 184.

[54] Thulukkanam, K., Heat exchanger thermal design. In: Thulukkanam, K., *Heat exchanger design handbook*, 2nd ed. Boca Raton, CRC Press. (2013) 117–144.

[55] Thulukkanam, K., Plate heat exchangers and spiral plate heat exchangers. In: Thulukkanam, K., *Heat exchanger design handbook*. 2nd ed. Boca Raton, CRC Press. (2013) 393–432.

[56] Wang, L., Sunden, B., Manglik, R. M., *Plate heat exchangers: Design, applications and performance*. Southampton–Boston, WIT Press. (2007).

[57] Watson, P. D., Tittsler, R .P., Densité du lait aux bases températures. *Journal of Dairy Science*, 44. 416–424. (1961).

[58] Wright, A. D., Heggs, P. J., Calculation of new plate heat exchanger effectiveness and pressure drop using existing performance data. *Chemical Engineering Research and Design*, 4. (2002) 1–9.

Appendices

Appendix 1. Criterial equations suitable for estimating heat transfer coefficient for PHEs

No.	Equations	References
1.	$Nu = 0.273 \cdot Re^{0.65} Pr^{m} \cdot \left(\frac{\delta}{L}\right)^{0.35}$ m= 0.3 ↓ / 0.4 ↑	*Fonyó* & *Fábry*, 2004
2.	$Nu = 0.4 \cdot Re^{0.64} Pr^{0.4}$	*Singh* & *Heldman*, 2013
3.	$Nu = a \cdot Re^{m} Pr^{1/3}$ $Re > 5 \;\; a = 0.352; \; m = 0.539$	Maroulis & Saravacos, 2003
4.	$Nu = 0.023 \cdot Re^{0.8} Pr^{1/3}$	
5.	$Nu = 0.664 \cdot Re^{0.5} Pr^{1/3}$; Laminar	
6.	$Nu = 0.0366 \cdot Re^{0.8} Pr^{1/3}$; Turbulent	
7.	$Nu = 0.0188 \cdot Re^{0.889} Pr^{0.292}$ $10 < Re < 1000$	*Gut et al.*, 2004
8.	$Nu = 0.273 \cdot Pr^{1/3}$ $10 < Re < 1000$	
9.	$Nu = 0.273 \cdot Re^{0.65} Pr^{0.4} (W/L)^{0.36}$	*Kreith et al.*, 1999
10.	$Nu = 0.0169 \cdot Re^{0.897} Pr^{0.3} (W/L)^{0.36}$	
11.	$Nu = C \cdot Re^{x} Pr^{y} \left(\frac{\eta}{\eta_{wall}}\right)^{z}$ $Laminar: Re < 400 \;\; Turbulent \; Re > 400$ $C = 0.15 \ldots 0.4; x = 0.65 \ldots 0.85; y = 0.3 \ldots 0.45;$ $z = 0.05 \ldots 0.2$	*Mariott*, 1971
12.	$Nu = 0.0645 \cdot Re^{0.78} Pr^{0.46}$	*Macovei*, 2001
13.	$Nu = 0.374 \cdot Re^{0.666} Pr^{0.333} \cdot \left(\frac{\eta}{\eta_{wall}}\right)^{0.15} \; Re > 400$	*Macovei*, 2001 *Stoica et al.*, 2007
14.	$Nu = 0.314 \cdot Re^{0.666} Pr^{y} \quad y = 0.3 \;\; \downarrow and \;\; y = 0.4 \;\uparrow$	
15.	$Nu = 0.718 \cdot Re^{0.349} Pr^{0.33}; \; \beta = 30°$	*Mota et al.*, 2015
16.	$Nu = 0.157 \cdot Re^{0.666} Pr^{0.4}; \;\; \beta = 30°$	*Okada et al.*, 1972
17.	$Nu = 0.249 \cdot Re^{0.64} Pr^{0.4}; \;\; \beta = 45°$	

No.	Equations	References
18.	$Nu = 0.327 \cdot Re^{0.65} Pr^{0.4}$; $\beta = 60°$	*Okada et al.*, 1972
19.	$Nu = 0.478 \cdot Re^{0.62} Pr^{0.4}$; $\beta = 75°$	
20.	$Nu = 1.89 \cdot Re^{0.46} Pr^{0.5}$; $\beta = 60°$ and $20 < Re < 150$	*Focke et al.*, 1985
21.	$Nu = 0.57 \cdot Re^{0.7} Pr^{0.5}$; $\beta = 60°$ and $150 < Re < 600$	
22.	$Nu = 1.12 \cdot Re^{0.6} Pr^{0.5}$; $\beta = 60°$ and $600 < Re < 16000$	
23.	$Nu = 1.67 \cdot Re^{0.44} Pr^{0.5}$; $\beta = 45°$ and $45 < Re < 300$	
24.	$Nu = 0.405 \cdot Re^{0.7} \cdot Pr^{0.5}$; $\beta = 45°$ and $300 < Re < 2000$	
25.	$Nu = 0.84 \cdot Re^{0.6} Pr^{0.5}$; $\beta = 45°$and $2000 < Re < 20000$	
26.	$Nu = 0.77 \cdot Re^{0.54} Pr^{0.5}$; $\beta = 30°$ and $120 < Re < 1000$	
27.	$Nu = 0.44 \cdot Re^{0.64} Pr^{0.5}$; $\beta = 30°$ and $1000 < Re < 42000$	
28.	$Nu = 0.72 \cdot Re^{0.59} Pr^{0.4} \phi^{0.41} \left(\frac{\beta}{30}\right)^{0.66}$; $30° < \beta < 80°$ and $1000 < Re < 4000$	*Chisholm et al.*, 1999
29.	$Nu = 0.471 \cdot Re^{0.5} Pr^{0.33} \left(\frac{\eta}{\eta_{wall}}\right)^{0.14}$; $\beta = 30° \ldots 60°$ and $20 < Re < 400$	*Muley et al.*, 1997
30.	$Nu = 0.1 \cdot Re^{0.76} Pr^{0.33} \left(\frac{\eta}{\eta_{wall}}\right)^{0.14}$; $\beta = 30° \ldots 60°$ and $Re > 1000$	
31.	$Nu = 1.6774 \cdot \left(\frac{d_e}{L}\right)^{0.333} \left(\frac{\beta}{30°}\right)^{0.38} Re^{0.5} Pr^{0.33} \left(\frac{\eta}{\eta_{wall}}\right)^{0.14}$; $\beta = 30° \ldots 60°$ and $30 \leq Re < 400$	
32.	$Nu = 0.278 \cdot \varphi^{0.317} Re^{0.683} Pr^{0.33} \left(\frac{\eta}{\eta_{wall}}\right)^{0.17}$; $\beta = 45°/90°$ and $400 < \frac{Re}{\phi} < 10000$	*Heavner*, 1993
33.	$Nu = 0.308 \cdot \varphi^{0.333} Re^{0.667} Pr^{0.33} \left(\frac{\eta}{\eta_{wall}}\right)^{0.17}$; $\beta = 23°/90°$ and $400 < \frac{Re}{\phi} < 10000$	
34.	$Nu = 0.195 \cdot \varphi^{0.308} Re^{0.692} Pr^{0.33} \left(\frac{\eta}{\eta_{wall}}\right)^{0.17}$; $\beta = 45°/45°$ and $400 < \frac{Re}{\phi} < 10000$	
35.	$Nu = 0.118 \cdot \varphi^{0.280} Re^{0.720} Pr^{0.33} \left(\frac{\eta}{\eta_{wall}}\right)^{0.17}$; $\beta = 23°/45°$ and $400 < \frac{Re}{\phi} < 10000$	

No.	Equations	References
36.	$Nu = 0.089 \cdot \varphi^{0.282} Re^{0.718} Pr^{0.33} \left(\frac{\eta}{\eta_{wall}}\right)^{0.17}$; $\beta = 23°/23°$ and $400 < \frac{Re}{\phi} < 10000$	*Heavner*, 1993
37.	$Nu = 0.023 \cdot Re^{0.8} Pr^{0.33} \left(\frac{\eta}{\eta_{wall}}\right)^{0.14}$; $\beta = 30°/30° - 30°/45° \ldots 60°/60°$ and $Re > 4000$	*Wang et al.*, 2007
38.	$Nu = 0.348 \cdot Re^{0.64} Pr^{0.4} \left(\frac{\eta}{\eta_{wall}}\right)^{0.17}$; $\beta = 30°$	Kumar equation *Neagu et al.*, 2014
39.	$Nu = 0.44 \cdot \left(\frac{\beta}{30}\right)^{0.38} Re^{0.5} Pr^{0.33} \left(\frac{\eta}{\eta_{wall}}\right)^{0.17}$	Mulley equation *Kakaç* & *Liu*, 2002
40.	$Nu = 0.329 \cdot Re^{0.529} Pr^{0.33} \left(\frac{\eta}{\eta_{wall}}\right)^{0.17}$; $\beta = 30°$	Bond equation *Gulenoglu et al.*, 2014
41.	$Nu = 0.45 \cdot \left(RePr\frac{d_h}{L_v}\right)^{0.333} \left(\frac{\eta}{\eta_{wall}}\right)^{0.17}$; $\beta = 30°$	Buonopane–Troupe equation, *Thulukkanam*, 2013
42.	$Nu = 0.263 \cdot Re^{0.65} Pr^{0.4}$	*Buonopane et al.*, 1963
43.	$Nu = C \cdot Re^m Pr^n \Gamma$ C, Γ and m, n are presented in *Appendix 2*.	*Muley*, 1999

Appendix 2. The C coefficient and m, n exponents of the proposed relation (*Mulley*, 1999), as a function of the angle of inclination of the folds

Angle	C	m	n	Γ	Re
V shape 30 °	0.718	0.349	1/3	$\left(\frac{\eta}{\eta_{wall}}\right)^{0.17}$	*<10*
	0.348	0.64	1/3		*10… 100*
	0.329	0.529	1/3		
	$0.44\left(\frac{6\beta}{\pi}\right)^{0.36}$	0.5	1/3		
V shape 45 °	0.718	0.349	1/3		*< 10*
	0.4	0.598	1/3		*10…100*
	0.3	0.663	1/3		*> 100*

Angle	C	m	n	Γ	Re
V shape 50 °	0.63	0.333	1/3	$\left(\frac{\eta}{\eta_{wall}}\right)^{0.17}$	*< 20*
	0.291	0.591	1/3		*20…300*
	0.13	0.732	1/3		*> 300*
V shape 60 °	0.562	0.326	1/3		*< 20*
	0.306	0.529	1/3		*20…400*
	0.108	0.703	1/3		*> 400*
V shape 65 °	0.562	0.326	1/3		*< 20*
	0.331	0.503	1/3		*20…500*
	0.087	0.718	1/3		*> 500*

Acta Universitatis Sapientiae

The scientific journal of Sapientia Hungarian University of Transylvania
(Cluj-Napoca, Romania) publishes original papers and
surveys in several areas of sciences written in English.
Information about each series can be found at:
http://www.acta.sapientia.ro.

Acta Universitatis Sapientiae, Alimentaria

Contact address and subscription:
Acta Universitatis Sapientiae, Alimentaria
RO 400112 Cluj-Napoca, Romania
Str. Matei Corvin nr. 4.
E-mail: acta-alim@acta.sapientia.ro

This volume contains one issue.

Sapientia University

sciendo

Scientia Publishing House

ISSN 1844-7449
http://www.acta.sapientia.ro

Information for authors

Acta Universitatis Sapientiae, Alimentaria publishes original papers and surveys in all field of Food Science. All papers are peer-reviewed.

Papers published in current and previous volumes can be found in Portable Document Format (PDF) form at the address: http://www.acta.sapientia.ro.

The submitted papers should not be considered for publication by other journals.

The corresponding author is responsible for obtaining the permission of co-authors and of the authorities of institutes, if needed, for publication. The Editorial Board is disclaiming any responsibility.

Submission must be made by e-mail (acta-alim@acta.sapientia.ro) using the Word and PDF format. The submitted PDF document will be used as a reference.

The manuscript must have the following subheadings: Abstract, Keywords, Introduction, Material and methods, Results and discussions, Conclusions, Acknowledgements, References.

For more details use the instructions for authors from

http://www.acta.sapientia.ro/acta-alim/alimentaria-main.htm.

One printed copy is provided free of charge to all authors. No reprints are available.

Printed by F&F INTERNATIONAL
Director: Enikő Ambrus

Supported by: